ROLE OF MICRORNAS IN

LUNG-ASSOCIATED DISEASES

By

LI ZHANG

Master of Science in Microbiology
Sichuan University
Chengdu, Sichuan, China
2007

Master of Science in
Biochemistry and Molecular Biology
Oklahoma State University
Stillwater, OK
2010

Submitted to the Faculty of the
Graduate College of the
Oklahoma State University
in partial fulfillment of
the requirements for
the Degree of
DOCTOR OF PHILOSOPHY
May, 2015

ROLE OF MICRORNAS IN

LUNG-ASSOCIATED DISEASES

Dissertation Approved:

Dr. Lin Liu

Dissertation Adviser

Dr. Pamela Lloyd

Dr. Myron Hinsdale

Dr. Ramanjulu Sunkar

ACKNOWLEDGEMENTS

I would like to take this opportunity to express my deeply sincere gratitude to my advisor, Dr. Lin Liu to letting me fulfill my dream of Ph.D. His critical suggestions and his ability to bring out best of me that had a significant influence on me. I greatly appreciate that he provides us such a wonderful platform in the form of lab environment and technical help.

I would also like to convey my gratitude to Dr. Pamela Lloyd, Dr. Myron Hinsdale and Dr. Ramanjulu Sunkar for serving on the committee. Their suggestions, expertise and critique had let me to answer the biological phenomenon under investigation in a better way and improved the quality of research.

I would like to specially thank Dr. Teluguakula Narasaraju who had helped me in a great way during my research career. I owe my deep sense of gratitude to him for imparting me a sense of appreciation of one's work.

I thank my colleagues Dr. Chaoqun Huang, Dr. Sunil More, Dr. Pulavendran Sivisami, Dr. Qiao Zhang, Dr. Ye Yang, Dr. Chunling Zhao, Lakmini Kumari Senavirathna, Gayan Bamunuarachchi and Xuxu Gou for their help and suggestions.

I also want to thank the Center of Veterinary Health Sciences for providing me three student seed grants which enabled me to improve the quality of my research work and grant writing experience.

I am lucky to have wonderful parents, Wencheng Zhang & Jianfen Luo who always

encourages me to perform better and be a better person. Without them, I don't think it would be possible for me to finish my study.

Last but not the least, I owe my deeply sincere gratitude to my sister, Xiaowei Lin; aunts and uncles, Wenqun Zhang & Bin Lin, Kangming Ma & Yimei Luo; grandma, Peiying Luo; my dear friends, Shuiyi Lu, Jia Hu, Na Li and Weiwei Ren. With their love, encouragement and understanding, I am able to complete the present work and push me farther than I thought I could go.

Name: LI ZHANG

Date of Degree: MAY, 2015

Title of Study: ROLE OF MICRORNAS IN LUNG-ASSOCIATED DISEASES

Major Field: PHYSIOLOGICAL SCIENCES

Abstract:

MicroRNAs (miRNAs) are small non-coding RNAs that can repress protein synthesis by translational repression and mRNA decay to regulate signaling pathways. miRNAs play important roles in various cellular processes including cell inflammatory response and differentiation.

NF-κB is one of the best-characterized transcription factors providing the link between early membrane-proximal signaling events and changes in gene expression, and regulates the expression of many genes that play a role in inflammation. Here, we evaluated the *in vitro* effect of lipopolysaccharide (LPS) on cultured bovine alveolar macrophages and report that miR-26b, a LPS - responsive miRNA, repressed the phosphatase and tensin homolog (PTEN) involved in the activation of the NF-κB signaling pathway in bovine alveolar macrophages. LPS stimulation up-regulated miR-26b after 1 h and down-regulated miR-26b after 6 and 36 h. Furthermore, miR-26b enhanced the LPS-induced TNF-α, IL-8, IL-1β, IL-10 and nitric oxide production and directly inhibited that of IL-6. In addition, miR-26b promoted LPS-induced NF-κB signaling pathway. Moreover, miR-26b directly leads to PTEN silencing in bovine alveolar macrophages. PTEN silencing enhanced the LPS-induced mRNA expression of TNF-α, IL-8, IL-1β, IL-10 and IL-6, and up-regulated the NF-κB pathway. Taken together, we conclude that miR-26b participates in the inflammatory response of LPS-stimulated bovine alveolar macrophages by modulating the NF-κB pathway through targeting PTEN.

The efficacy of the current protocols to differentiate mouse induced pluripotent stem cells (iPSCs) and Mesenchymal Stem Cells (MSCs) into alveolar epithelial type II (AEC II) cells is low. And, whether miRNAs are involved in the differentiation of iPSCs and MSCs into lung epithelial cells is unknown. We aimed to identify specific miRNAs that can efficiently promote the differentiation of iPSCs and MSC into AEC II cells. Through miRNA microarray analysis, we identified that miR-29a was highly enriched in AEC II cells. miR-29a induced the differentiation of iPSCs and MSCs into AEC II cells under the stimulation of proper growth factors and growing on appropriate matrix. We show here that miR-29a suppressed the Dual-Specificity Phosphatase 2 (DUSP2) involved in the activation of the mitogen-activated protein kinase (MAPK) signaling pathway to promote the differentiation of iPSCs and MSCs into AEC II cells. In addition, dexamethasone, 8-bromoadenosine 3, 5-cyclic monophosphate (cAMP), and isobutylmethylxanthine (IBMX) (DCI) further facilitated the miR-29a-mediated differentiation process. Moreover, we found that AEC II cells derived from iPSCs and MSCs secreted pulmonary surfactant and trans-differentiated into alveolar epithelial type I (AEC I) cells. Furthermore, miR-29a engineered MSC-AEC II cells attenuated lung injury induced by elastase. In addition, our studies may contribute to the cell-based therapy for COPD.

TABLE OF CONTENTS

Chapter Page

LIST OF TABLES

LIST OF FIGURES

Figure Page

CHAPTER I

INTRODUCTION

I-1: MicroRNAs

MiRNAs are a class of evolutionarily conserved small non-coding RNAs (~21–23 nucleotides) (1, 2). miRNAs regulate the target gene expression at post-transcriptional level by imperfect base pairing specifity between sequences in the 3′-untranslated region (3′-UTR), and the miRNA 5′-proximal 'seed' region (positions 2–8) (3, 4). The interaction between miRNA and its mRNA target typically leads to protein synthesis inhibition by translational repression and mRNA decay (5). In rare cases, miRNAs can activate translation (6, 7). miRNAs have important roles in various critical cellular processes such as apoptosis, proliferation, and differentiation (8-10).

It is also known that miRNAs are potential regulators to immune responses in immunoactive cells including alveolar macrophage cells (11). Numerous investigations have supported that miRNAs are new regulators of inflammatory and immune responses (12, 13). NF-κB pathway plays an important role in inflammatory and immune responses. While it has been reported that miR-146 is an NF-κB transactivational target and is involved in a negative feedback loop by down regulation of IRAK1 and TRAF6 (14). miR-155 has also been indicated to be an NF-κB transactivational target and negatively regulates IKKs and other genes, constituting a negative feedback loop (14). miR-181b works as a key player in a positive feedback loop linking NF-κB (NF-κB - IL-6 - STAT3 - miR-181b-CYLD-NF-κB) and promotes cell transformation through

participating in an exclusive epigenetic circuit (14). Unlike miR-181b, miR-21 has recently been identified to be involved in the inflammation-transformation positive feedback loop to elevate NF-κB activity through repressing PTEN expression (14). miR-301a increases NF-κB activity down-regulating NKRF, which in turn, promotes miR-301a transcription (14). Collectively, all these data strongly suggest that miRNAs play an important role as central regulators of the NF-κB pathway. However, currently, the target genes and the biological function of miRNAs in NF-κB pathway of bovine alveolar macrophages (bAMs) related to bovine lung disease is still poorly characterized.

MiRNAs have been used to generate iPSCs from fibroblast and the miR-302 / 367 cluster has been reported to reprogram mouse and human somatic cells to iPSCs without exogenous transcription factors (15) . Down-regulation of miR-21 and miR-29a enhances embryonic fibroblasts (MEFs) reprogramming efficiency into iPSCs through ERK1/2 phosphorylation (16). In another study, miR-130, miR-301 and miR-721 were shown to enhance iPSC generation via targeting the homeobox transcription factor Meox2 (also known as Gax) (17). Thus, it is reasonable to speculate that certain miRNAs may increase the efficiency of differentiation of iPSCs into lung epithelial cells based on the modulation and fine-tuning of transcriptional networks under proper conditions. However, few studies have been made on miRNAs and differentiation of iPSCs into AEC II *in vitro*.

MiRNAs have been identified to act in functional networks linked to MSC differentiation as well. MiR-29a has been reported to suppress FOXA3A and to decrease chondrogenic differentiation from human MSCs (18). MiR-128, which is enriched in brain, has been found to regulate rat bone marrow MSC differentiation into neuron-like cells through Wnt signaling (19) MiR-204 has been determined to target RUNX2 and promotes adipocyte differentiation from human MSCs (20) Recently, human decidua-derived MSCs have been reported to be able to differentiate into functional AEC II cells that synthesize and secrete pulmonary surfactant

complex (21) However, the role of miRNAs in regulating MSC differentiation into AEC II cells is not well understood. The focus of this study is to highlight the regulation of AEC II differentiation from MSCs by miRNA.

I-2: Bovine Respiratory Disease (BRD)

Bovine respiratory disease (BRD) complex, also known as shipping fever, is one of the biggest health obstacles and causes great economic losses in the global cattle industry (22). Stressful management practices, environmental factors, and a variety of microorganisms are believed to contribute to the pathogenesis of BRD. *Mannheimia haemolytica*, formally known as *Pasteurella haemolytica*, is a small gram-negative, facultatively anaerobic bacterium and is the primary bacterial agent responsible for the clinical disease and pathophysiological events characterized by acute lobar fibrinonecrotizing pneumonia (23). *M. haemolytica* alone can cause fibrinous pneumonia when directly delivered into the lungs in sufficient numbers (>5 $X10^9$ colony-forming units in non-immune calves) (24). *M. haemolytica* produces various potential virulence factors. One of them is the endotoxin, lipopolysaccharide (LPS) that causes acute inflammation, hemorrhage, edema and hypoxemia (25).

Among these main products of *M. haemolytica*, LPS is one of the toxins involved in BRD complex. LPS is a component of the outer membrane of Gram-negative bacteria such as *M. haemolytica* and *Escherichia coli* which stimulates the innate immune system and is one of the most important pathological initiating factors during severe bovine inflammatory disease (26). *M. haemolytica* LPS is a well-characterized virulence factor because of its pathogenic role in shipping fever (27, 28). In addition, LPS stimulation of macrophages enhances acetylation of histone H4 lysine residues that are believed to be responsible for neutrophil recruitment (29). The inflammatory response which is associated with lung injury due to bacterial infection is an important aspect of BRD. It has been demonstrated that LPS from *E.coli* (O55: B5) causes the intensive enzymatic and oxidative response of bovine neutrophils *in vitro* during the course of

BRD (26). The ensuing inflammatory response to LPS and the associated lung injury and sepsis are pivotal in BRD (26). However, the pathogenesis of BRD is still not completely understood.

I-3: Chronic Obstructive Pulmonary Disease (COPD)

Chronic obstructive pulmonary disease (COPD) is a worldwide health problem and a major cause of chronic morbidity and mortality throughout the world. COPD is predicted to become the third leading cause of death by 2030. The causes of COPD are cigarette smoking, indoor air pollution (such as biomass fuel used for cooking and heating), outdoor air pollution, occupational dusts and chemicals (vapors, irritants, and fumes) or alpha1-antitrypsin deficiency. Cigarette smoking is the major risk factor. To attenuate and eventually limit this increasing COPD trend, a unified international effort is required.

COPD is characterized by progressive and chronic inflammation of the lungs, breathlessness, and fatigue and reduced daily activity. These symptoms worsen acutely at exacerbations of chronic bronchitis. The airflow limitation in COPD that is associated with chronic inflammation is also progressive and not fully reversible. Patients who have symptoms of cough, sputum production, or dyspnea, and / or a history of exposure to risk factors for COPD should be considered for a diagnosis of COPD. The presence of FEV1< 80% and a combination of FEV1/ FVC<70% indicates that it is not fully reversible of the airflow limitation.

The central airways, peripheral airways and pulmonary vasculature all have pathologic changes in COPD. Inflammatory cells infiltrate the surface epithelium of trachea, bronchi, and bronchioles with internal diameter greater than 2 to 4 mm (30-32). Mucus hyper secretion leads to enlarged mucus-secreting glands and increasing numbers of goblet cells. For small bronchi and bronchioles with an internal diameter of less than 2 mm, chronic inflammation results in repeat cycles of airway wall injury and repair (33) that causes airway wall structural remodeling. In those remodeled airways, collagen content and scar tissue that narrows the lumen increase (34). Eventually, fixed airway obstruction is produced(34) .

Pulmonary vasculature also changes in COPD. It is characterized by thickening of the vessel walls in the beginning of COPD. Intimal thickening occursin the beginning followed by increasing smooth muscle proliferation and inflammatory cell infiltration of the vessel wall (35, 36). As COPD worsens, mucus hypersecretion, ciliary dysfunction, airflow limitation, pulmonary hyperinflation, gas exchange abnormalities, pulmonary hypertension and cor pulmonale will develop. These will lead to symptoms including chronic cough, sputum production, and destruction of alveolar structure. In advanced COPD, the lung's capacity for gas exchange decreases due to peripheral airway obstruction, parenchymal destruction, and pulmonary vascular abnormalities, producing hypoxemia and hypercapnia. Cardiovascular complications of COPD develop as well, such as high blood pressure (37).

Lung transplantation is a possible treatment for patients who have end stage lung diseases including chronic obstructive pulmonary disease, idiopathic pulmonary fibrosis, cystic fibrosis, alpha1-antitrypsin disease, and primary pulmonary hypertension. However, it is limited because of the low availability of donor lungs, immune rejection and complications. Due to these limitations, lung stem and progenitor cells or alveolar cell transplantation is an attractive alternative therapy (38). However, the limitation of this approach is the scarcity of alveolar epithelial cells and the difficulty of expanding these cells *in vitro*. One potential future treatment for severe lung diseases including COPD is to find a reliable source of functional lung epithelial cells for use in lung-related therapies. Induced pluripotent stem cells (iPSC) and adult mesenchymal stem cells (MSC) are two possible cell sources for cell-based treatments.

I-4: Stem Cells

Stem cells are cells in the body that share 3 main characteristics including unlimited self-renew through cell division, differentiation to form different structures and tissues as the need arises, and continual division and differentiation after they are transplanted into another organism**.** In general, stem cells are a continual source of cells throughout the individual life-span.

Stem cells are typically classified into embryonic stem cells and adult stem cells. Embryonic stem cells are derived from the inner mass of the blastocyst. Embryonic stem cells are referred to as totipotent since they are able to regenerate all three germ layers of an organism. Adult stem cells that are able to differentiate to one or several mature cells types are considered uni- or multipotent (39, 40).

Stem cell-based therapy has successfully demonstrated beneficial therapeutic effects in a variety of diseases including heart disease, bone disease, cancer, hepatic disease, and lung disease (41-45). In recent years, there is increasing interest in exploiting the potential therapeutic properties of stem cells for the treatment of lung diseases, and stem cells have been extensively investigated as a potential source of alveolar epithelial cells (21). It has been reported that stem cells have therapeutic effects on COPD characterized by emphysema and chronic bronchitis (46-48).

iPSCs are embryonic-like cells reprogrammed from mouse and human adult somatic cells through retroviral transduction of defined factors, and possess various properties of embryonic stem cells(49). Thus, iPSCs offer the possibility to generate gene-corrected and patient-specific lung progenitor cells for individuals with genetic diseases (50). iPSCs became one of the most promising applications for patient-specific regenerative medicine due to their self-renewal capacity and potential for differentiation (51). Current clinical strategies are not effective for progressive chronic lung disease. Therefore, cell-based therapies have become an important new frontier in lung research and disease treatment (52). Particularly, for these lung diseases caused by developmental deficiencies or chronic depletion of endogenous stem cell pools such as COPD, exogenous stem cell therapies may represent a better approach (53). Recent studies have reported that mesenchymal stem cells (MSCs) and endothelial progenitor cells (EPCs) are candidates for cell therapy of COPD (49, 54, 55). Currently, investigations have begun to examine the possibility of generating lung progenitor epithelial cells from somatic cells since iPSCs can be

created from dermal skin fibroblasts and patient specific iPSCs could avoid the immune rejection problems that might occur if heterologous sources of embryonic stem cells were employed (50). Deciphering the regulation mechanisms of efficient differentiation to target cells would unveil the pathophysiology of diseases and provide a potential therapeutic strategy for specific diseases (56, 57). There is increasing interest in exploiting the regenerative potential of stem cells or progenitor cells for the treatment of chronic lung diseases like COPD. Cell transplantation becomes an alternative to whole – organ transplantation (38). However, this approach requires generating large quantities of pure AEC II cells in vitro and conditions for directing iPSCs to differentiate along an alveolar epithelial lineage with homogeneity are not yet fully defined. Recent studies have shown that human iPSC- derived AEC II cells adhered to and proliferated within the acellular lung matrices of rats and humans, and displayed markers of differentiated pulmonary epithelium (58). Previous studies have revealed that both endothelial progenitor cells activated by hepatocyte growth factor (HGF) and autologous stem cells (ASCs) have benefited lung damage in an elastase-induced emphysema model (59, 60). Based on these findings, we sought to investigate the regenerative potential of miRNA engineered iPSCs – AEC II cells in the context of an elastase induced mouse emphysema model.

MSCs are cells that can be collected from mesenchyme or stroma of several tissues such as bone marrow and adipose tissue (61-63) and able to differentiate into derivatives of the mesodermal lineage including adipocytes, osteocytes, chondrocytes, and myocytes. MSCs have been assessed in a large number of clinical trials since MSCs are able to home to sites of injury and inflammation, differentiate into cells of the mesodermal lineage, and secrete trophic factors to promote proliferation and differentiation of local progenitor cells (64). In a recent study, bone marrow (BM)-derived stem cells transplanted to the lungs were shown to benefit regeneration after elastase-induced pulmonary emphysema (59). Another study revealed that adipose stem cell treatment in mice attenuated lung and systemic injury induced by cigarette smoking (65).

However, the effect and potential therapeutic treatment of miRNA- engineered MSCs in COPD is still unclear.

I-5: Alveolar Epithelial Type II (AEC II) Cells

Gas exchange in the lung occurs within alveoli, alveolar epithelium, and capillaries. Efficient gas exchange and host defense rely on the integrity of the alveolar epithelium. The alveolar epithelium is composed of alveolar epithelial type I (AEC I) and type II cells (AEC II). AEC II cells play a vital role in maintaining alveolar homeostasis and are considered to be the progenitor cells of the alveolar epithelium, which are critical for lung repair after injury. AEC II cells secrete surfactant (66, 67) and proliferate when AEC I cells in the alveolar epithelium are damaged by a variety of disease conditions to renew the alveolar epithelium (68-70). AEC II cells are also phagocytic, activate macrophages, and secrete soluble mediators associated with immune responses such as responding to signals of neighboring cells or circulating immune cells, migrating and spreading in response to injury (71-74). The repair capacity of endogenous lung epithelial progenitor cells is often insufficient and diminishes with increasing age. Incomplete repair of alveolar epithelium is one of the major factors leading to chronic lung diseases including chronic obstructive pulmonary diseases. Therefore, maintaining a sufficient supply of AEC II cells is of considerable practical and therapeutic interest.

Each alveolus contains AEC I cells and cuboidal AEC II cells secreting high levels of surfactant protein C (SP-C). In COPD and idiopathic pulmonary fibrosis (IPF), the delicate architecture of the alveoli is lost (75) . Several studies have indicated that in COPD these pathologies are induced in part by defects in the alveolar epithelium, increased apoptosis and senescence (76, 77) .

A recent study has shown that intratracheal instillation of AEC II cells reduces the severity of bleomycin-induced pulmonary fibrosis and that AEC II cells can be derived from human and mouse embryonic stem cells (78, 79). However, the efficacy of differentiation is very low and to

date, none of the studies has explored the role of miRNA in the differentiation of iPSCs and MSCs into AEC II cells.

CHAPTER II

MATERIALS AND METHODOLOGY

II-1: MicroRNA-26b modulates the NF-κB pathway in bovine alveolar macrophages by regulating PTEN

i. Bovine alveolar macrophage isolation and LPS stimulation

Bovine lungs (Ralph's Packing Company, Perkins, Oklahoma) were infused by gravity (30 cm height) with cold Hanks' balanced salt solution (pH 7.4) without Ca^{2+} or Mg^{2+} ($HBSS^{-}$). The infused fluid was gauze-filtered. bAMs were collected by centrifugation (200 x g, 10 min at 4°C). After being washed twice in $HBSS^{-}$, bAMs were resuspended in Dulbecco's Modified Eagle's medium (DMEM) (ATCC, Manassas, VA) with 10% fetal bovine serum (FBS) (Atlanta Biologicals, Atlanta, GA) and seeded into 6- well cell culture plates at a density of 4 million cells per well. bAMs were allowed to adhere for 4 h and then stimulated with 1 μg/ml of *Escherichia coli* LPS (055:B5; Sigma-Aldrich, St Louis, MO) for 1-48 h. Viable cell counts were performed by trypan blue dye exclusion assay. The purity of bAMs was determined by immunocytochemistry with monoclonal anti-CD68 (EBM11). bAMs were maintained in DMEM containing 10% FBS, 100 U/ml penicillin and 100 mg/ml streptomycin.

ii. Immunocytochemistry

Freshly isolated bAMs were seeded in 24-well cell culture plates and allowed to adhere for 4h. Then cells were twice with phosphate buffered saline (PBS) (pH 7.4) and fixed with 4%

paraformaldehyde in PBS for 30 min, followed by permeabilization with 0.1% Triton X-100 for 15 min and blocking with 1% bovine serum albumin (BSA) for 1 h. Cells were incubated with mouse monoclonal anti-CD68 (EBM11) (1:100) (Dako, Carpenteria, CA) at 4°C overnight. Cells were then washed and incubated with Alexa-Fluor-488-conjugated anti-(mouse IgG) secondary antibodies (1:500) (Bio-Rad, Hercules, CA). The negative controls were treated as described above except the omission of the primary antibody. 4', 6-Diamidino-2-phenylindole dihydrochloride (DAPI) (2.5 mg/ml) (Sigma-Aldrich, St Louis, MO) staining was performed for counting cells. Cells were viewed on a Nikon Eclipse TE 2000 U inverted fluorescence microscope or Nikon Eclipse E600 fluorescence microscope.

iii. MicroRNA microarray printing, hybridization and data analysis

The microRNA microarray was in-house printed using miRCURY LNA™ ready-to-spot probe set 11.0 (Exiqon, Vedbaek, Denmark). Capture probes were complementary to mature microRNAs for all microRNAs in human, mouse, rat and their related viruses registered in miRBase Release Version 11.0. The in-house printed miRNA microarray used a miRCURY LNA oligo set that contained 317 bovine miRNAs.

Four hundred ng of total RNA from control (without LPS stimulation) samples from all time points (0, 1, 6 and 36 h) was used as a common reference control labeled with Hy3 or Hy5 and co-hybridized with the same amount of total RNAs of LPS stimulated cells from the corresponding time points labeled with the other dye, Hy5 or Hy3. Dye swaps was performed to eliminate the bias. The hybridized slides were scanned with ScanArray Express (PerkinElmer Life and Analytical Sciences, Boston, MA) and the images were analyzed with GenePix 5.0 pro (Axon Instruments, Union City, CA). The data were calculated, normalized, and qualified as described previously (80). For data analysis, the weak and bad spots were eliminated using RealSpot software according to the assigned QI. LOWESS normalization was performed for the remained spots. The miRNA signals from control and LPS samples were compared using a two-

tailed student's t-test, and those with a p-value of less than 0.05 were considered significantly different.

iv. RNA isolation and quantitative real-time PCR

Total RNA was extracted from bAM cells using TRI Reagent (Molecular Research Center, Inc., Cincinnati, OH). Residual DNA was removed using DNA-free DNase (Ambion, Austin, TX). RNA was reverse-transcribed into cDNA using M-MLV reverse transcriptase (Invitrogen, Carslbad, CA). Quantitative RT-PCR (qRT-PCR) was performed in triplicate on an ABI 7500 system (Applied Biosystems, Foster City, CA) using SYBR Green I detection and gene-specific primers (Table 1). The fluorescent signal was only detected in the amplification step for each cycle. A melt curve was generated to check the specificity of the amplification at the dissociation stage. 18S rRNA was used as an internal control. The relative amount of each mRNA relative to 18S rRNA was calculated with the equation $2^{-(CtmRNA - Ct18S)}$.

For quantification of miRNA, 5 μg of total RNA was poly (A)-tailed using A-Plus™ Poly (A) Polymerase tailing kit (Epicentre Biotechnologies, Madison, WI). 1.5 μg of poly (A)-tailed RNA was reversed-transcribed into cDNA using oligo dT primers and M-MLV reverse transcriptase. qRT-PCR was performed using the target mature miRNA sequence as the forward PCR primer (Table 1) and a universal primer (5'- GCGAGCACAGAATTAATACGACTCAC-3') as the reverse primer. U6 snRNA was used as an internal control. The relative amount of each miRNA to U6 snRNA was calculated by the comparative Ct method using the equation $2^{-(CtmiRNA - CtU6)}$.

v. Cytokine measurement in culture medium

Immediately after collection, culture medium was centrifuged at 1,000 rpm for 5 min at 4°C to remove residual cells. The supernatant was harvested and stored at -80°C for subsequent analysis. Concentrations of TNF-α, IL-8, IL-1β, IL-10 and IL-6 in culture medium were assayed using a bovine TNF-α ELISA kit (Raybiotech, Norcross, GA); a bovine IL-8 ELISA kit

(MyBiosource, San Diego, CA); a bovine IL-1β ELISA kit (Thermo Scientific, Waltham, MA); a bovine IL-10 ELISA kit (MyBiosource) and a bovine IL-6 ELISA kit (Thermo Scientific), following manufacturers' instructions. All samples were assayed in duplicate. Cytokine concentrations were determined by relevant standard curves and expressed as pg/ml.

vi. Construction of lentiviral vectors

We constructed a lentiviral miR-26b expression vector as previously described (81). The lentiviral control vector (miR-con) contains a non-relevant sequence as a negative control. For PTEN silencing lentiviral vector, shRNA of PTEN (Table 1) was cloned into pSIH1-H1-copGFP Vector (System Biosciences, Mountain View, California, USA). The control shRNA vector was purchased from System Biosciences. The lentiviruses were generated in HEK 293T cells using Lenti-X HTX Packaging Mix (Clontech, Mountain View, CA), then titered and stored at -80°C until use.

vii. Target gene and pathway analysis of miR-26b

Web-based Pictar (URL: http://pictar.mdc-berlin.de/) and TargetScan (URL: http://www.targetscan.org/mmu_50/) software was used to predict the pathways and targets of miR-26b. Commonly used algorithms give variable weight to: (i) complementarity to the miRNA seed region; (82) evolutionary conservation of the miRNA recognition elements (MREs); (iii) free energy of the miRNA-mRNA heteroduplex; and (iv) mRNA sequence features outside the target site. TargetScan and PicTar focus on the seed region in miRNA targeting (83, 84). TargetScan requires an exact match to ≥7 bases of the seed sequence (83). PicTar imposes a stringent free energy cutoff for imperfect matches (84). Both TargetScan and PicTar improve their predictions because of evolutionary conservation. Furthermore, TargetScan improves predictions for non-conserved sequences and adds a ‘context score’ considering features in the surrounding mRNA which include local A-U content and location (near either end of the 3′-UTR

is preferred) (85). mRNAs that have a high context score or multiple predicted MREs are more likely to be true targets.

viii. Construction of 3'-UTR luciferase reporter vectors

We divided the three binding sites of PTEN into 2 segments for cloning due to the sequence length. PTEN1 contained two binding sites (43-49 and 1278-1285), and PTEN2 contained one binding site (2618-2625). PTEN1 and PTEN2 were PCR-amplified from bovine genomic DNA and cloned into the pmirGLO vector (Promega, Madison, WI) downstream of a firefly luciferase reporter gene using the Nhel I and Sal I restriction sites. We used over-lapping PCR to construct the luciferase reporters with mutant PTEN 3'-UTR of miR-26b binding sites. We first amplified PTEN1 or PTEN2 as two fragments with overlapping mutation sites using two primer sets. The annealing two fragments were then used as a template to amplify the mutant PTEN1 or 2. The primer sequences are listed in Table 1.

Table 1: Primers designed for PCR amplification

	Forward primer	Reverse primer
18S	CTGTTGCTCTCTTGGCAGCTT	GGTGGAAAGGTGTGGAATGTG
TNF α	TGATGCTGATTTGGTGACTGATT	TTATTTCTCGCCACTGACCAGTAG
IL-6	CCAGAGAAAACCGAAGCTCTCA	TCCTTGCTGCTTTCACACTCA
IL-8	CTGTTGCTCTCTTGGCAGCTT	GGTGGAAAGGTGTGGAATGTG
IL-10	TGCATAGCTCAGCACTACTCTGTTG	GCTGGTTGGCAAGTGGATACA
miR-26b	ACCCAGTTCAAGTAATTCAGGA	GCGAGCACAGAATTAATACGACTCACTATAGGTTTTTTTTTTTTAACCT
U6	AGGCTCTGAAAGACCGAGTG	GCGAGCACAGAATTAATACGACTCACTATAGGTTTTTTTTTTTTVN
PTEN	GTGGTGGAACTTGCAATCCT	AGGTTTCCTCTGGTCCTGGT
PTEN-1 3'-UTR-WT (PTEN1-WT)	CATGCTAGCCACCACTGACTCTGATCCAGAG	TCCGTCGACCATATGCAGTCTGGGCATATCA
PTEN-1 3'-UTR-Mutant-1 (PTEN1-M1)	ACACCATGAAAACAACTATCTATAAACTGAA	TTCAGTTTATTCAAGTTTGTTTTCATGGTGT
PTEN-1 3'-UTR-Mutant-2 (PTEN1-M2)	TAACTGTTAGGGAATTTTCTATCTATATTGAATACATAT	ATATGTATTCAATATAGATAGAAAATTCCCTAACAGTTA
PTEN-2 3'-UTR-WT (PTEN2-WT)	TAAGCTAGCGGAATGTGAAGGTCTGAATGA	ATGTCGACGCAACCACAGCCATCGTTAT
PTEN-2 3'-UTR-Mutant (PTEN2-M3)	CTTACTTGTCTGAAGTTCGTAGACGGCATCACT	AGTGATGCCGTCTACGAACTTCAGACAAGTAAG
PTEN shRNA	GATCCGCTGAAAGACATTATGATACCTTCAAGAGAGGTATCATAATGTCTTTCAGCTTTTTG	AATTCAAAAAGCTGAAAGACATTATGATACCTCTCTTGAAGGTATCATAATGTCTTTCAGCG

ix. Dual luciferase reporter assay

Raw 246.7 cells were seeded in a 96-well plate (2 x10^4 cells / well). After being in culture for 24 h, the cells were co-transfected with 5 ng of wild-type or mutant PTEN 3'-UTR luciferase

reporter construct and 100 ng of miR-26b expression plasmid using Lipofectamine 2000 (Invitrogen, Carlsbad, CA). The empty pmirGLO vector was used as a control. 24 h after transfection, cells were harvested and dual luciferase activities were measured. Data were normalized by dividing firefly luciferase activity by *Renilla* luciferase activity.

For the pathway activity, Raw 246.7 cells were seeded in a 96 well plate at a density of 2 $x10^4$ cells /well. After being in culture for 24 h, the cells were transfected with 50 ng of miR-26b and 100 ng of NF-κB pathway-luciferase-reporter construct (SABiosciences, Frederick, MD). miR-con was used as a control. 24 h after transfection, LPS (1 μg/ml) was added. After 18 h stimulation, the cells were harvested. NF-κB transcriptional activity was measured with the Dual Luciferase Reporter Assay System. Data were expressed as a ratio of firefly luciferase activity to *Renilla* luciferase activity.

x. Western blotting

bAMs were stimulated with LPS (1 μg/ml) for 0, 1, 6 and 36 h. Controls were bAMs without LPS stimulation. Then, cells were lysed in in lysis buffer (Thermo Scientific, Rockford, IL). D_C protein assay kit (Bio-Rad, Hercules, CA) was used to determine the protein concentration. Twenty μg of protein extracts were separated by 10% SDS-PAGE and then transferred onto nitrocellulose membranes. Proper transfer was ensured by staining the membrane with Ponceau S. Membranes were blocked overnight with 5% dried skimmed milk powder in 100 mM TBST. Then, the membranes were incubated at 4°C overnight with primary antibodies: anti-PTEN (1:500 dilution, Bioss, Woburn, MA) and anti-β actin (1:500 dilution, Sigma-Aldrich) as the loading control. After being washed with TBST three times, the membranes were incubated with horseradish peroxidase-conjugated secondary antibodies (Bio-Rad, Hercules, CA) for 1 h. Blots were washed again and target proteins were visualized using the enhanced chemiluminescence detection system. All experiments were repeated three times.

For miR-26b overexpression, we infected bAMs with miR-26b lentivirus at a multiplicity of infection (MOI) of 50 and then stimulated the cells with LPS (1 μg/ml) for 5 - 60 min. The lentivirus containing miR-con was used as a virus control (VC). At the end of incubation, the cells were lysed in lysis buffer (Thermo Scientific) and used for Western blotting as above. The membranes were incubated at 4°C overnight with primary antibodies: anti-PTEN (1:500 dilution, Bioss, Woburn, MA), anti-Akt (1:500 dilution, Bioss), anti-phospho-Akt (1:1000, Millipore, Bellerica, MA), anti-IKKb (1:1000, Cell Signaling Technologies, Beverly, MA), anti-IKKa (1:1000, Cell Signaling Technologies), anti-phospho-IKKa/b (1:1000, Cell Signaling Technologies, Beverly, MA), anti-IκBα (1:1000, Cell Signaling Technologies, Beverly, MA), anti-phospho-IκBα (1:1000, Cell Signaling Technologies, Beverly, MA),anti-NF-κB p65 (1:1000, Abcam, Cambridge, MA), anti-phospho-NF-κB p65 (1:500 dilution, Bioss), anti–GAPDH (1:500 dilution, Sigma-Aldrich) and anti-β actin (1:500 dilution, Sigma-Aldrich). All experiments were repeated three times. Each target was run a separate gel to avoid the results may come from the previous blot antibodies.

xi. Nitric oxide measurement

The level of nitric oxide production was monitored by measuring nitrite and nitrate concentration in the cultured medium. bAM culture media was collected and centrifuged at 4°C for 5 min to remove residual cells. The amount of nitric oxide in the supernatant was measured by mixing the medium with the same volume of Griess reagent (100 μl) in a 96- well plate. The plate was incubated for 15 min at room temperature and read at 570 nm by a spectrophotometer (86).

xii. Statistics

For comparisons across more than 2 groups, statistical analysis was performed using one-way ANOVA followed by Tukey's post hoc test. For comparisons of 2 groups, statistical analysis was performed using student t-test considering unequal variance. Statistical difference was accepted at $p < 0.05$.

II-2: MicroRNA-29a Efficiently Promotes the Differentiation of Mouse Induced Pluripotent Stem Cells and Mesenchymal Stem Cells into Alveolar Epithelial Type II Cells

i. Culture of mouse iPSCs

Mouse iPSCs (iPS-MEF-Ng-492B-4) (Cell Bank, RIKEN BioResource Center, Japan) were propagated on mouse embryo fibroblasts (MEFs) (ATCC, Manassas, VA). MEFs were seeded in 25 cm^2 flasks and cultured in Dulbecco's Modified Eagle's Medium (DMEM) (ATCC) supplemented by 10% fetal bovine serum (FBS) (Atlanta Biologicals, Atlanta, GA), 50 U/ml penicillin and 50 mg/ml streptomycin (15140-163, Life Technologies, Gaithersburg, MD). The cells were treated with mitomycin C (Sigma-Aldrich, St Louis, MO) at a final concentration of 8 μg/ml and incubated at 37°C with 5% CO_2 to halt cell division so that they could be used to condition the medium for iPSCs. After a 3-hr incubation at 37°C, mitomycin C-containing medium was aspirated and the cells were trypsinized. A single cell suspension (5×10^5) was seeded on a gelatin (Sigma-Aldrich, St Louis, MO) coated 25 cm^2 flask. The next day, MEF medium was removed and 5 ml of mouse iPSC medium was added. The iPSC medium consisted of DMEM (high glucose, without sodium pyruvate) (GIBCO), 15% FBS, 0.1 mM nonessential amino acids (Sigma-Aldrich), 0.1 mM 2-mercaptoethanol (Sigma-Aldrich), 1000 U/ml mouse LIF (Millipore, Bellerica, MA), 50 U/ml penicillin, and 50 mg/ml streptomycin. iPSCs were plated on the MEF feeder cells and cultured at 37°C, 5% CO_2 and 90-95% humidity, with medium changed every day. Undifferentiated iPSCs were passaged every 4-5 days onto fresh feeder cells.

ii. Removal of contaminating MEFs from iPSCs

iPSC medium was discarded and 1 ml per 25 cm^2 flask of 0.25% trypsin-EDTA (Sigma-Aldrich) was added. After a 5-min incubation, 5 ml of mouse iPSC medium was added to break up the cell clumps. The cells were transferred into a conical tube and centrifuged at 200 g for 5 min. Then, the cell pellet was resuspended in 5 ml mouse iPSC medium and added to a 25 cm^2

flask without gelatin coating. The cells were incubated at 37°C with 5% CO_2 for 1 h. Most MEF cells attached to the bottom of the flask. The supernatant containing iPSCs was collected and centrifuged at 200 g for 5 min to obtain the purified iPSCs.

iii. Isolation of mouse BM-MSCs

The femur and tibia were removed from C57BL/6 mice and the bones were kept in storage buffer (2% fetal bovine serum, 2% penicillin/streptomycin and PBS) on ice. After all the bones were collected, the bones were put in a p100 petri dish and washed with 20 ml of storage buffer once or twice so that hairs were washed away. The ends of bones were cut and the marrow was flushed thoroughly with the MSC culture medium (DMEM-high glucose without glutamine, 15% FBS, 1x L-glutamine, 10 mM 2-mercaptoethanol, 5 mM N-acetyl cysteine, 800 µM N-tert-butyl-alpha-phenylnitrone, 50 U/mL penicillin and 50 mg/mL streptomycin) using a 3 ml syringe until the bone become pale (reddish to white). After finishing all bones, the marrow was pipetted up and down into a single cell level. Cell suspension was centrifuged and the supernatant was removed. After that, 10 ml of fresh degassed culture medium was added. Cells were cultured in a 5% O2 hypoxia chamber (Billus-Rothebery, CA) and incubated at 37°C with 5% CO2.

When the cells reached 80% confluence, the culture medium was removed and 1 ml of 0.25% trypsin-EDTA was added and incubated for 5 min at room temperature. Then, 5 ml MSC medium was added to break up the cells to a single cell suspension. After that, the CD11b population was depleted first, and then the CD45 population was depleted using specific antibodies [anti-mouse CD11b microbeads (130-049-601) and anti-mouse cd45 microbeads (130-052-301)] as per the manufactures' instruction (Miltenyi Biotec). After depletion, these cells were plated into two p100 dishes (P1) (1:2 split) with 10 ml of degassed medium and were incubated in a hypoxic (5% CO_2, 5% O_2 and 90% N_2) chamber at 37°C. Once the culture reached 80-90% confluence, the cells were ready for use (P2). The purity of the attached MSCs was assessed by flow cytometry.

iv. Isolation of mouse primary AEC II cells

Mouse AEC II were isolated from male C57BL/6 mice (8-10 weeks of age) according to the previously reported procedure, with some modification (48, 49). Mice were anesthetized with ketamine (80 mg/kg of body weight) and xylazine (10 mg/kg of body weight). The abdominal cavity was opened, exsanguinated and cannulated with a 20-gauge luer stub adapter through the intratracheal route. Lungs were perfused with solution II which is prepared with 10 mM HEPES, pH 7.4, 0.9% NaCl, 0.1% glucose, 5 mM KCl, 1.3 mM $MgSO_4$, 1.7 mM $CaCl_2$, 0.1 mg/ml streptomycin sulfate, 0.06 mg/ml penicillin G, 3 mM Na_2HPO_4 and 3 mM NaH_2PO_4, followed by instilling 1 ml of the digestion cocktail which contains solution II plus dispase (500 caseinolytic units/ml) directly through the trachea. Three lungs were isolated, pooled into a beaker containing ~17 ml of the digestion cocktail and incubated at 37°C for 45 minutes. After incubation, the lungs were chopped small. Lung tissues were further digested with the addition of DNase I (100 μg/ml) for 45 minutes at 37°C, with intermittent shaking. The digested lungs were filtered through 160-, 37- and 15-μm gauge nylon mesh sequentially. The filtrate was centrifuged at 250 g for 10 minutes. The cell pellet was resuspended in DMEM and incubated in a 100-mm-diameter Petri dish coated with mouse IgG (75 μg per dish) for 1 hour. The cells were spun down at 250 g for 10 minutes and resuspended in DMEM containing 10% FBS. The yield was ~8×10^6 cells per mouse and the cell viability was >95%.

v. *In vitro* differentiation of iPSCs into AEC II cells

We used a two-step differentiation protocol (5) to drive iPSCs into AEC II cells. The first step was endoderm induction for 6 days in differentiation medium plus Activin A (20 ng/ml). The differentiation medium consisted of 25% (v/v) Ham's F12 medium (Invitrogen, Carlsbad, CA), 75% (v/v) Iscove's modified Dulbecco's medium (Invitrogen) supplemented with 0.5X of N-2 Supplement and B-27 Supplement minus vitamin A (Invitrogen), 0.05% BSA, 2 mM glutamine (Invitrogen), 0.5 mM ascorbic acid (Sigma), 0.45 mM 1-thioglycerol (Sigma-Aldrich),

50 U/ml penicillin and 50 mg/ml streptomycin (5). The second step was lung epithelial induction for 5 days in differentiation medium containing FGF-2 (50 ng /ml). Medium was changed daily.

vi. *In vitro* Differentiation of MSCs into AEC II cells

1 x 10^5 P2 MSCs were seeded on each well of collagen IV-coated 6-well plates and cultured in differentiation medium (small airway growth medium, SAGM) and MSC culture medium (Control) for 11 days. SAGM media is a previously established lung differentiation culture media (87-89).

For miR-29a derived MSC differentiation, MSCs were infected with miR-29a lentivirus at a MOI of 50. After culture for 24h, cells were serum starved for another 24h. Then, media wwas switched to SAGM with DCI and cells were cultured for 11 days.

vii. Immunocytochemistry

iPSCs were plated onto gelatin-coated 24-well cell tissue culture plates at a density of 1 x 10^6 cells per well. Immunostaining was carried out the next day. Cells were washed with phosphate-buffered saline (PBS), fixed with 4% paraformaldehyde in PBS for 30 min at room temperature, and permeabilized with 0.1% Triton X-100 for 15 min. The fixed cells were blocked with 1% bovine serum albumin (BSA) for 1 h and were then incubated with mouse monoclonal anti-Nanog (1:100, Sigma-Aldrich) or anit-SSEA-1 (1:100, Life Technology) at 4°C overnight. The cells were washed and incubated with Alexa-Fluor-488-conjugated anti-mouse IgG secondary antibodies (1:500) (Bio-Rad, Hercules, CA). 4', 6-Diamidino-2-phenylindole dihydrochloride (DAPI) (2.5 mg/ml) (Sigma-Aldrich) nuclear staining was performed for counting cells.

iPSC or MSC differentiated cells were plated onto 24-well cell tissue culture plates at a concentration of 1 x 10^6 cells per well. Immunostaining was carried out the next day. Cells were washed with PBS, fixed with 4% paraformaldehyde in PBS for 30 min at room temperature (RT) and permeabilized with 0.1% Triton X-100 for 15 min at RT. Cells were blocked with 1% bovine

serum albumin (BSA) for 1 h at RT. Cells were incubated with mouse monoclonal anti-SP-C (1:100, Santa Cruz Biotechnology, CA) or syrian hamster anti-T1 α (1:100, Developmental Studies Hybridoma Bank, Iowa City, IA) at 4°C overnight. The next day, cells were washed and incubated with Alexa-Fluor-546-conjugated anti-mouse IgG secondary antibodies (1:500) (Biolegend, San Diego, CA) or Alexa-Fluor-546-conjugated goat anti-hamster IgG secondary antibody (Life Technology). 4', 6-Diamidino-2-phenylindole dihydrochloride (DAPI) (2.5 mg/ml) (Sigma-Aldrich, St Louis, MO) nuclear staining was performed for counting cells.

Cells were viewed on a Nikon Eclipse TE 2000 U inverted fluorescence microscope or Nikon Eclipse E600 fluorescence microscope.

viii. Flow cytometry analysis of mesenchymal stem cell surface molecules

Mouse bone marrow MSCs were assessed by flow cytometry before and after differentiation. Cells were dissociated into a single-cell suspension by incubation with 0.25% trypsin-EDTA for 2 min at room temperature. Cells were then washed and resuspended in PBS containing 1% BSA at a density of 50,000 cells in 100 µl for each marker. Rat anti-mouse CD16/CD32 (#553141, BD Biosciences, San Jose, CA) was added first to block non-antigen-specific binding sites of immunoglobulins to Fc-receptors. Then, cells were washed, resuspended with PBS containg1% BSA (Fisher) and incubated on ice for 30 min in the dark with 1 µl conjugated antibodies against Sca-1 (eBioscience, San Diego, CA), CD9 (eBioscience), CD29 (eBioscience), CD44 (eBioscience), CD81 (eBioscience), CD11B (eBioscience), CD45 (eBioscience). In a parallel group, cells were also incubated on ice for 30 min in the dark with 1 µl related IgG including rat IgG2a K Isotype Control Alexa Fluor 488 (eBioscience), rat IgG2b K Isotype Control Alexa Fluor 488 (eBioscience), Armenian Hamster IgG Isotype Control PE (eBioscience), Mouse IgG1 K Isotype Control PE (eBioscience), anti-Mouse CD31 (PECAM-1) PE (eBioscience) and streptavidin PerCP-Cyanine5.5 (eBioscience). For CD81 which needed a secondary antibody for detection, cells were resuspended in 100 µl of PBS containing 1% BSA

with 1 µl streptavidin PerCP-Cyanine5.5 (eBioscience) for another 30 min on ice in the dark after the primary antibody was washed away. The control group was unstained cells. Cells were washed twice with PBS containing 1% BSA and analyzed by flow cytometry.

ix. RNA isolation and quantitative real-time PCR

Total RNA was extracted using TRI Reagent (Molecular Research Center, Inc., Cincinnati, OH). Residual DNA was removed using DNA-free DNase (Ambion, Austin, TX). First-strand cDNA was synthesized using M-MLV reverse transcriptase (Invitrogen). Quantitative RT-PCR (qRT-PCR) was performed on an ABI 7500 system (Applied Biosystems, Foster City, CA) using SYBR Green I detection and gene-specific primers. Each sample was run in triplicate. The fluorescent signal was only detected in the amplification step for each cycle. A melt curve was generated to check the specificity of the amplification at the dissociation stage. 18S rRNA was used as an internal control. The relative amount of each gene of interest was normalized against 18S rRNA from the same cDNA sample and calculated with the equation $2^{-\Delta Ct}$ and fold change of gene transcript levels between different samples was calculated with the equation $2^{-\Delta\Delta Ct}$, where $\Delta Ct = Ct_{18s} - Ct_{gene}$ and $\Delta\Delta Ct = \Delta Ct_{sampleA} - \Delta Ct_{sampleB}$. Primers are listed in Table 2.

For quantification of miRNAs, 5 µg of total RNA was poly A-tailed using A-Plus™ Poly A Polymerase tailing kit (Epicentre Biotechnologies, Madison, WI). 1.5 µg of poly A-tailed RNAs were reversed-transcribed into cDNA using oligo dT primers and M-MLV reverse transcriptase. qRT-PCR was performed using the target mature miRNA sequence as the forward PCR primer and a universal primer (5'- GCGAGCACAGAATTAATACGACTCAC-3') as the reverse primer. U6 snRNA was used as an internal control. The relative amount of each miRNA to U6 snRNA was calculated by the comparative Ct method using the equation 2- ($Ct_{miRNA} - Ct_{U6}$). Primers are listed in Table 3

Table 2 qRT-PCR Primers for mRNA

	Forward primer	Reverse primer
18S	CTGTTGCTCTCTTGGCAGCTT	GGTGGAAAGGTGTGGAATGTG
SP-C	CATCGTTGTGTATGACTACCA	CCTGGAAGTTCTGGAGTTTTCT
SP-B	CTTGGCACAGGTCATTAGCTC	CATCGTTGTGTATGACTACCA
ABCA3	CAGCTCACCCTCCTACTCTG	ACTGGATCTTCAAGCGAAGCC
T1-α	ACCGTGCCAGTGTTGTTCTG	AGCACCTGTGGTTGTTATTTTGT
AQP5	CCTTATCCATTGGCTTGTCGG	TCTGAGCTGTGGCAGTCGTTC
Nanog	CCTCATCAATGCCTGCAGTTT	CTCAGTAGCAGACCCTTGTAAGCA
Sox	TAGAGCTAGACTCCGGGCGATGA	TTGCCTTAAACAAGACCACGAAA
Oct4	TCTTTCCACCAGGCCCCCGGCTC	TGCGGGCGGACATGGGGAGATCC
cMyc	TGACCTAACTCGAGGAGGAGCTGGAATC	AAGTTTGAGGCAGTTAAAATTATGGCTGAAGC
Klf	GCGAACTCACACAGGCGAGAAACC	TCGCTTCCTCTTCCTCCGACACA
Dnmt3b	CTGTGAAGGTCAGAGGAAAACGT	TGATCTCCAGACCCACATGGT
TNF-α	CCGGGAGAAGAGGGATAGCTT	TCGGACAGTCACTCACCAAGT
IL-1β	GAAATGCCACCTTTTGACAGTG	CTGGATGCTCTCATCAGGACA
IL-6	TAGTCCTTCCTACCCCAATTTCC	TTGGTCCTTAGCCACTCCTTC
MCP-1	CCCAAGCAGAAGTGGGTTCA	GCTGCAGATTCTTGGGTTGTG

Table 3 qRT-PCR Primers for miRNA

	Forward primer	Reverse primer
U6	AGGCTCTGAAAGACCGAGTG	GCGAGCACAGAATTAATACGACTCACTATAGGTTTTTTTTTTTTVN
miR-19b	ATGGCTGTGCAAATCCATGCAAAACTGA	GCGAGCACAGAATTAATACGACTCACTATAGGTTTTTTTTTTTTCGGAAC
miR-30b	GGCGAGTGTAAACATCCTACACTCAGCT	GCGAGCACAGAATTAATACGACTCACTATAGGTTTTTTTTTTTTAACCAT
miR-451	GGCGAGAAACCGTTACCATTACTGAGTT	GCGAGCACAGAATTAATACGACTCACTATAGGTTTTTTTTTTTTGAGGCC
miR-142-3p	GGCGAGTGTAGTGTTTCCTACTTTATGGA	GCGAGCACAGAATTAATACGACTCACTATAGGTTTTTTTTTTTTGAGGTG
miR-142-5p	GTGGCCATAAAGTAGAAAGCACTACT	GCGAGCACAGAATTAATACGACTCACTATAGGTTTTTTTTTTTTAACCT
miR-22	GTGGCTTCAAGTAATTCAGGATAGGTT	GCGAGCACAGAATTAATACGACTCACTATAGGTTTTTTTTTTTTAACCT
miR23b	GGCGAGATCACATTGCCAGGGATTACC	GCGAGCACAGAATTAATACGACTCACTATAGGTTTTTTTTTTTTAACCAT
miR-24	TCGTCGTGCCTACTGAGCTGATATCAGT	GCGAGCACAGAATTAATACGACTCACTATAGGTTTTTTTTTTTTCGGAAC
miR-29a	TCGTCTAGCACCATCTGAAATCGGTTA	GCGAGCACAGAATTAATACGACTCACTATAGGTTTTTTTTTTTTAGTCAA
let-7f	GCTGGCTGAGGTAGTAGGTTGTGTGGTT	GCGAGCACAGAATTAATACGACTCACTATAGGTTTTTTTTTTTTGAGGTT

x. MicroRNA microarray printing, hybridization and data analysis

The microRNA microarray was in-house printed using miRCURY LNA™ ready-to-spot probe set 11.0 (Exiqon). Four hundred ng of total RNA from mouse iPSCs or ACE II were labeled with Hy3 or Hy5 using miRCURY LNA™ microRNA power labeling kit (Exiqon). Mouse iPSC RNAs labeled with Hy3 were paired and mixed with AEC II RNAs labeled with Hy5. To eliminate dye bias, dye swap was performed. Slides were hybridized with the mixed Hy3/Hy5 or Hy5/Hy3 labeled RNAs for 16 to 18 h at 56°C. After hybridization, the slides were stringently washed and dried. The hybridized slides were scanned with ScanArray Express (PerkinElmer Life and Analytical Sciences, Boston, MA). The images were imported into

GenePix 5.0 pro (Axon Instruments, Inc. Union City, CA) for data extraction. The image and exported raw data were imported into Realspot software developed by our laboratory for quality test and Lowess normalization (90). The miRNAs with an average quality of less than 1 were filtered. To identify differentially expressed miRNAs, a two-tailed Student's t-test assuming unequal variance was performed between iPSCs and ACE II groups. $P < 0.05$ was considered to be significant.

xi. Target genes and pathway analysis of miR-29a

The pathways and targets of miR-29a were predicted by the web-based software programs Pictar (http://pictar.mdc-berlin.de/) and TargetScan (URL: ttp://www.targetscan.org/mmu_50/).

xii. Vector construction

To construct microRNA expression vectors, pri-miRNA was amplified by PCR using specific primers and human genomic DNA. The fragments were inserted into a lentiviral vector (Clontech, San Jose, CA) at the XhoI and EcoR I sites (91). A similar size non-relevant genomic DNAsequence was used to construct a control vector (miR-con). The lentiviruses were generated in HEK 293T cells using Lenti-X HTX Packaging Mix (Clontech, Mountain View, CA), then titered and stored at -80°C until use.

xiii. Construction of 3'-UTR luciferase reporter vectors

We cloned the binding sites of target genes by PCR-amplification from mouse genomic DNA into the pmirGLO vector (Promega, Madison, WI) downstream of a firefly luciferase reporter gene using the Nhel I and Sal I restriction sites. We used over-lapping PCR to construct luciferase reporters with mutations in the 3'-UTR of genes with miR-29a binding sites. We first amplified the binding site of the target gene as two fragments with overlapping mutation sites using two primer sets. The annealing two fragments were then used as a template to amplify the mutant gene. Specific primers are listed in Table 4.

Table 4 Primers for vector construction

	Forward primer	Reverse primer
DUSP2 (DUSP2 3'-UTR-WT)	TACGCTAGCACAGCTCTGGCTTTGACTGA	ATAGTCGACAGCACCAATTACAGCGAGA
DUSP2-Mutant (DUSP2 3'-UTR- Mutant)	TGACGGCTGCTCTGATATCATGTACTTCTGAGGT	ACCTCAGAAGTACATGATATCAGAGCAGCCGTCA
Akt3 (Akt3 3'-UTR-WT)	TACGCTAGTGGTTAGAATCTGGCTAGAATCT	ATAGTCGACAGCCACTGCCAGCAGCGGCT
DUSP9 (DUSP9 3'-UTR-WT)	TACGCTAGAGCCGCATGGAGCTGATAGGCT	ATAGTCGAGGACAGGTATGGAGCCAAGA
Akt2 (Akt2 3'-UTR-WT)	TACGCTAGGCCGCCTGCCATTCTACAACC	ATAGTCGAGCCGAGCCTCTGCTTTGGGT

xiv. Dual luciferase reporter assay

For the 3'-UTR reporter assay, HEK 293T cells were seeded in a 96-well plate (2 x 10^4 cells/ well). After being in culture for 24 h, the cells were co-transfected with 5 ng of wild-type or mutant 3'-UTR luciferase reporter construct and 100 ng of miR-29a or let-7b expression plasmid using lipofectamine 2000 (Invitrogen). The empty pmirGLO vector was used as a negative control. Cells were harvested 24 h after transfection and dual luciferase activities were measured. Firefly luciferase activity was normalized against *Renilla* luciferase activity.

For studies of pathway activity in iPSCs, iPSCs were cultured in differentiation medium with Activin A (20 ng/mL) for 6 days and with FGF-2 (50 ng/mL) for 5 days. The cells were then seeded in a 96-well plate at a density of 2 x10^4 cells/well. After being in culture for 24 h, the cells were transfected with 50 ng of miR-29a, miR-22 or let-7b expression vector and 100 ng of ERK, JNK or Wnt/β-catenin pathway luciferase reporter construct (SABiosciences, Frederick, MD). miR-con was used as a vector control. 24 h after transfection, epidermal growth factor (EGF) (10 ng/well), phorbol 12-myristate 13-acetate (PMA) (1 ng/well) or Wnt3a conditioned medium (50% v/v) were added. After 18 h stimulation, the cells were harvested. ERK, JNK and Wnt/β-catenin transcriptional activities were measured using the Dual Luciferase Reporter Assay System. Data were expressed as a ratio of firefly luciferase activity to *Renilla* luciferase activity.

For studies of pathway activity in MSC, HEK293T cells were seeded in a 96-well plate at a density of 2 x10^4 cells /well. After being in culture for 24 h, the cells were transfected with 50 ng of miR-29a expression vector and 100 ng of ERK-MAPK or JNK-MAPK pathway-luciferase-reporter construct (SABiosciences, Frederick, MD). miR-con was used as a vector control. 24 h

after transfection, epidermal growth factor (EGF) (10 ng/well) or phorbol 12-myristate 13-acetate (PMA) (1 ng/well) were added. After 18 h stimulation, the cells were harvested. ERK-MAPK or JNK-MAPK transcriptional activities were measured using the Dual Luciferase Reporter Assay System. Data were expressed as a ratio of firefly luciferase activity to *Renilla* luciferase activity.

xv. Western blot

For studies of iPSCs, iPSCs were infected with miR-29a lentivirus at a multiplicity of infection (MOI) of 50. The lentivirus containing miR-con was used as a virus control (VC). After 48h, the cells were lysed in lysis buffer (Thermo Scientific, Rockford, IL). DC protein assay kit (Bio-Rad, Hercules,CA) was used to determine protein concentrations. Twenty µg of protein extracts were separated by 10% SDS-PAGE and then transferred onto nitrocellulose membranes. Proper transfer was ensured by staining the membrane with Ponceau S. Membranes were blocked overnight with 5% dried skimmed milk powder in 100 mM Tris-buffered saline plus 0.1% Tween 20 (TBST). Then, the membranes were incubated at 4°C overnight with primary antibodies: rabbit polyclonal anti-DUSP2 (1:500, Abcam, Cambridge, MA), rabbit polyclonal anti-DUSP9 (1:500, Abcam) or rabbit monoclonal anti-GAPDH (1:1000, Cell Signaling Technology, Beverly, MA). After being washed with TBST three times, the membranes were incubated with secondary antibodies (goat anti-rabbit antibody conjugated to horseradish peroxidase (HRP) (Bio-Rad, Hercules, CA) for 1 h. Blots were washed again and target proteins were visualized using the enhanced chemiluminescence detection system.

For studies of MSCs, MSCs were infected with miR-29a lentivirus at a multiplicity of infection (MOI) of 50. The lentivirus containing miR-con was used as a virus control (VC). After 48h, the cells were lysed in lysis buffer (Thermo Scientific, Rockford, IL). DC protein assay kit (Bio-Rad, Hercules, CA) was used to determine the protein concentration. Twenty µg of protein extracts were separated by 10% SDS-PAGE and then transferred onto nitrocellulose membranes. Proper transfer was ensured by staining the membrane with Ponceau S. Membranes were blocked

overnight with 5% dried skimmed milk powder in 100 mM Tris-buffered saline plus 0.1% Tween 20 (TBST). Then, the membranes were incubated at 4°C overnight with primary antibody: rabbit polyclonal to DUSP2 (1:500, Abcam, Cambridge, MA). After being washed with TBST three times, the membranes were incubated with horseradish-peroxidase-conjugated anti-(Rabbit-IgG) (1:2000) (Bio-Rad, Hercules, CA) for 1 h. Blots were washed again and the target protein was visualized using the enhanced chemiluminescence detection system. β-actin (Sigma) was used as a loading control.

xvi. Proliferation assay

The 5-bromo-2- deoxyuridine (BrdU) assay of iPSC-derived AEC II or MSC- derived AEC II was carried out to assess cell proliferation using a cell proliferation assay kit (Millipore, Temecula, CA) according to the manufacturer's instructions Absorbance, which reflects the incorporation of BrdU into the cell DNA and thus transition through the cell cycle, was read at 450 nm. Freshly isolated primary AEC II were used as a positive control.

xvii. Surfactant lipid secretion assay

Freshly isolated primary AEC II from wild-type C57BL/6 mice and cells derived from iPSCs or MSCs of the 11th day with miR-29a in the presence or absence of DCI were cultured in 96-well plates overnight. Cells were then washed twice by PBS and DMEM containing 10% FBS was added. The cells were incubated at 37°C for 30 min. Culture medium was removed as a zero time control (0 h) for one set of wells. Cells were stimulated with lung surfactant secretagogues (100 μM ATP, 0.1 μM PMA and 10 μM terbutaline; ATP+PMA+Terb) for 2 h at 37°C. Unstimulated cells in parallel cultures were used as controls. At the end of incubation, phosphatidylcholine in both medium and cell lysate was measured using a phosphatidylcholine assay kit (Abcam, Cambridge, MA) following the manufacturer's instructions. Surfactant secretion was expressed as a percentage [(nmol in medium/nmol in medium and cell lysate) x 100]. All of the secretion data were corrected by subtracting the value of 0 h.

xviii. ELISA for SP-C

ELISA was performed on cell culture medium collected before and after stimulation of iPSC-AEC II, MSC-AEC II or freshly isolated primary AEC II to quantify secreted SP-C using a SP-C ELISA kit (MyBiosource, San Diego, CA) according to the manufacturer's instructions. The stimulation method is as the same as that used in the surfactant lipid secretion assay. SP-C values were normalized to the total number of cells.

xix. Transmission electron microscopy

Differentiated cells were fixed in 4% paraformaldehyde for 1 hour. Cells were washed 3 times in 0.1M phosphate-buffered saline (PBS) pH 7.4 for 15 minutes each wash. After then, cells were dehydrated through an ethanol series (50%, 70%, 90%, 95% & three times in 100% ethanol) for 15 minutes each and were washed three times for 15 minutes each in propylene oxide. The cell pellet was placed in 1:1 propylene oxide and Poly/Bed overnight. The next day the vials were uncapped and left under the fume hood until most of the solvent had evaporated. 100% Poly/Bed was gently added to the cell pellet and the samples were placed in an oven at 60° C to polymerize for 48 hours. Embedded cells were sectioned and picked up on carbon film TEM grids. Grids were stained with Reynold's lead citrate stain followed by 2.5% uranyl acetate. Cells were imaged on a JEOL JEM-2100 transmission electron microscope.

xx. Induction of pulmonary emphysema and treatment

Lung emphysema was induced in mice (C57BL/6, female, 8 weeks) by intratracheal instillation of elastase (Sigma, St. Louis, MO) at a dose of 0.25 U per mouse. Two weeks after elastase administration, mice were randomly divided into 3 groups ($n>5$ each group) which were intratracheally administered 50 ul PBS only, 50 ul AEC II differentiated from miR-29a-engineered MSCs, or miR-con-engineered MSCs from male mice (500,000 cells per mouse). Mice were sacrificed after 1 week for analysis. Intratracheal instillation of PBS instead of elastase was used as blank control in a parallel group.

To determine whether the intratracheally instilled male cells stayed in the female lungs, lung tissue from each mouse was harvested 1 week after intratracheal injection of cells and genomic DNA was prepared using the Genomic DNA Purification Kit (Promega, Madison, WI). DNA from each mouse was analyzed by qRT-PCR as previously described (92). Cytokine mRNA levels were also analyzed by qRT-PCR as described in "Quantitative real-time PCR".

xxi. Morphological assessment

The mean linear intercept (MLI) was used to assess the morphology of mouse lungs. MLI was performed as a measure of interalveolar wall distance and determined by light microscopy at a magnification of 20X. The MLI was obtained by dividing the total length of a line drawn across the lung section by the total number of intercepts encountered in 50 lines per each lung.

xxii. Statistics

For comparisons across more than 2 groups, statistical analysis was performed using one-way ANOVA followed by Tukey's post hoc test. For comparisons of 2 groups, statistical analysis was performed using two-tailed student t-test assuming unequal variance. Statistical difference was set at $p < 0.05$.

CHAPTER III

FINDINGS

III-1: MicroRNA-26b modulates the NF-κB pathway in bovine alveolar macrophages by regulating PTEN

i. Viability and purity of bovine macrophages

The viability of the isolated bAMs were 72 ± 1.8 % and 92 ± 0.5% (mean ± SE, n=9) before and after attachment as revealed by trypan blue staining, respectively (Fig. 1A). The purity of the attached bAMs was determined by Wright's Giemsa staining and immunostaining for the surface antigen CD68, which is a cell surface marker for macrophages. The immunostaining showed that 96.1 ± 0.5% (means ± SE, n=9) cells were positive for CD68 (Fig. 1B). Only cell preparations containing bAMs with > 95% purity were used for our studies.

ii. LPS induces time-dependent cytokine mRNA expression and nitric oxide production in bAMs

LPS induces rapid production and release of inflammatory cytokines and chemokines known to be involved in lung inflammation and acute lung injury (93). To evaluate the role of LPS of *E.coli* (O55:B5) in pathogenesis of BRD, we investigated its *in vitro* effects on cultured bAMs. We incubated bAM monolayers with LPS for various time periods and assessed the

activation of bAMs by measuring cytokine mRNA expression. TNF-α and IL-6 mRNA expression peaked at 1 h after LPS stimulation of bAMs (Fig. 2A, B) while IL-1β and IL-10 mRNA expression peaked at 6 and 36 h post-LPS exposure, respectively, as compared to untreated bAMs (Fig. 2C, D).

It is well known that nitric oxide generated from LPS-stimulated bAMs causes cytotoxic injury to pulmonary cells (94). NO also plays an important role in numerous pathophysiological conditions including inflammation, and is induced in a nuclear factor (NF)-κB-dependent manner (95-97). To investigate the time course of LPS on NO production, bAMs were treated with LPS for 0, 1, 6 and 36 h. LPS markedly enhanced NO production as detected in the culture supernatant, reaching a maximum at 6 h post-LPS stimulation (Fig. 2E). Here, we demonstrated that *E. coli* LPS increased cytokine mRNA expression and nitric oxide production in bAMs. Based on cytokine expression and NO production, we chose 1, 6 and 36 h for further studies.

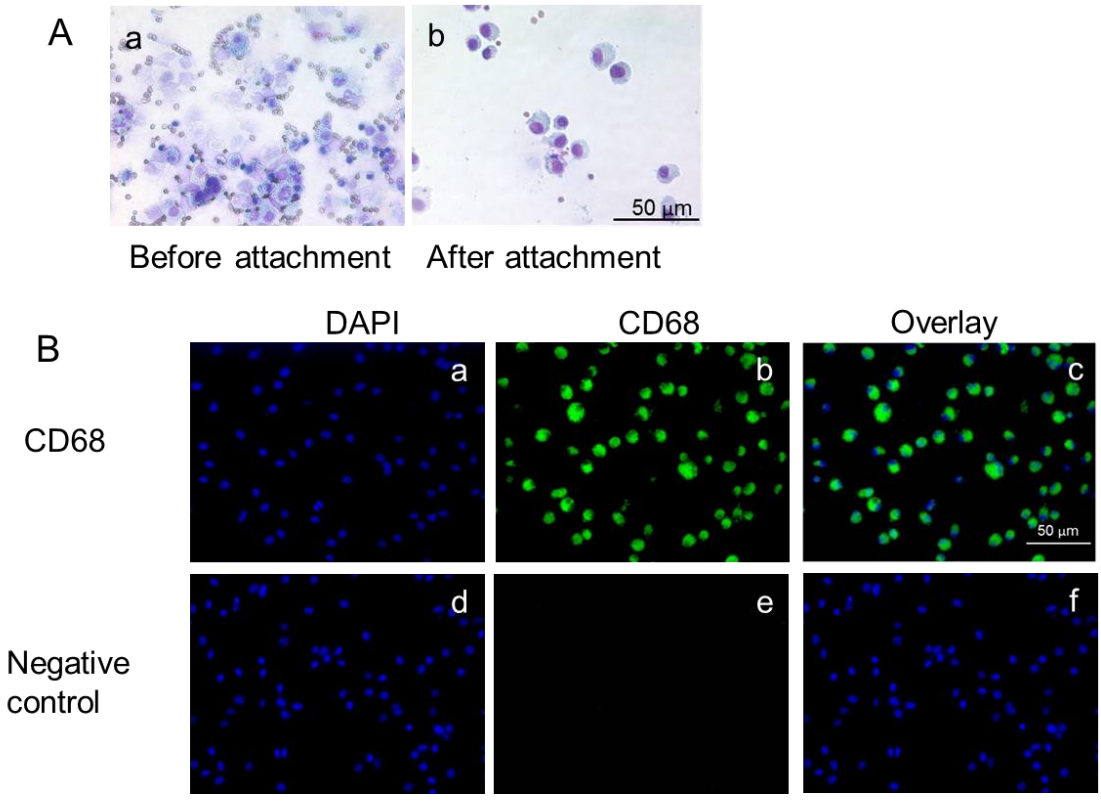

Fig. 1: Identification of bAMs by Wright's Giemsa and immunostaining. (A) Wright's Giemsa staining. bAMs were identified by their large, nonlobulated, and dark nuclei and large amounts of cytoplasm. (B) Immunostaining using antibodies against the cell surface antigen CD68 for macrophages. Upper panels, CD68 antibody; Lower panels: negative control without the primary antibody. Scale bar is 50 μm.

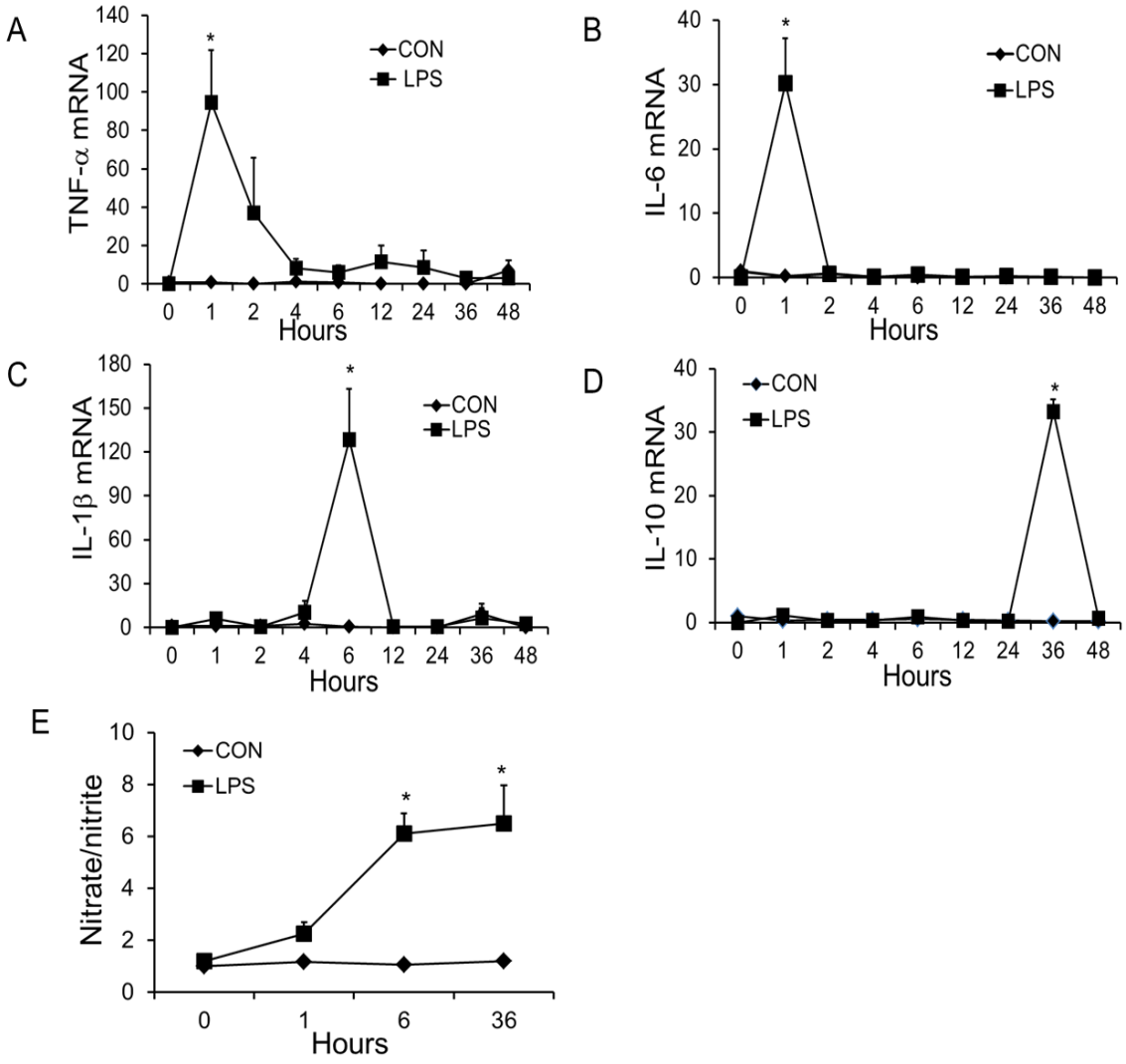

Fig. 2: LPS induces mRNA expression of cytokines and NO production from bAMs. bAMs were stimulated with LPS (1 μg/ml) for 0-48 h. Controls were bAMs without LPS stimulation. The mRNA expression of TNF-α (A), IL-6 (B), IL-1β (C), and IL-10 (D) was measured by real-

time PCR using 18S rRNA as an endogenous control. (E) NO production in the medium was determined using the Griess reagent in triplicate. Data were expressed as a fold change relative to 0 h control. Results are shown as means ± SE. *P<0.05 vs. 0 h (n=3 cell preparations).

iii. miR-26b is dynamically changed in bAMs after LPS stimulation

Based on our preliminary microRNA microarray studies, we found that miR-26b was a LPS-responsive miRNA in bAMs and confirmed the microarray data by qRT-PCR (Fig. 3). miR-26b expression in bAMs was increased in the early phase, but decreased in the later stages after LPS stimulation.

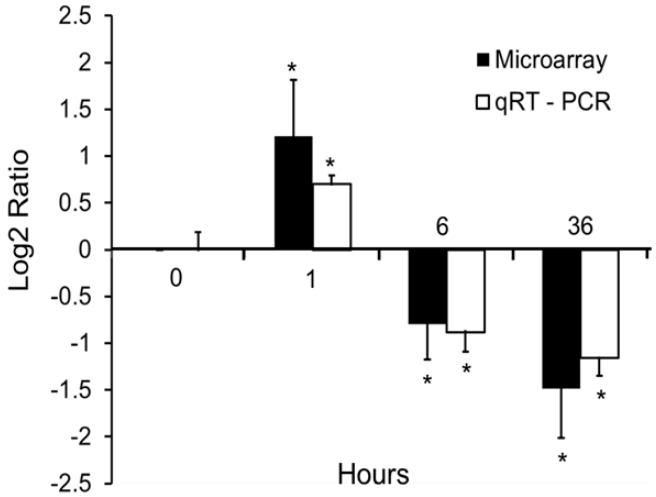

Fig. 3: miR-26b expression in LPS-stimulated bAMs. bAMs were treated with LPS (1 µg/ ml) for 0, 1, 6 and 36 h. miRNA expression level was determined by miRNA microarray and real-time PCR. Each expression ratio (LPS to common reference control) was log2 transformed. The miRNA signals obtained from the miRNA microarray from control and LPS treated samples were compared using a two-tailed Student's t-test. Results are expressed as means ± SE. * P< 0.05 vs common reference control (n=3 cell preparations).

iv. miR-26b enhances LPS-induced mRNA and protein expression of TNF-α, IL-8, IL-1β and IL-10 but represses that of IL-6

We further explored whether miR-26b regulates inflammatory cytokine mRNA levels in LPS-stimulated bAMs. We first determined the miR-26b expression level after infecting bAMs with different MOIs of miR-26 lentivirus or control lentivirus (VC). Maximal expression of miR-26b was achieved at a MOI of 50 (Fig. 4 A). We then infected bAMs with miR-26b lentivirus or VC at a MOI of 50 and challenged with LPS for 0, 1, 6 and 36 h. The blank control group (BC) was bAMs without virus infection. As seen in Fig. 4 B-F, the combination of miR-26b and LPS greatly augmented TNF-α, IL-8, IL-1β and IL-10 mRNA expression. However, miR-26b markedly reduced the level of IL-6 mRNA, consistent with the report that IL-6 is a direct target of miR-26b (98).

Cytokine protein production in culture supernatant of bAMs was quantified by ELISA. In cells doubly challenged with LPS and miR-26b, we detected a significant increase in TNF-α, IL-8, IL-1β and IL-10 and a decrease in IL-6 in the bAM supernatant at 6 h, as compared with the levels of these cytokines in VC treated with LPS (Fig. 4G-K). The trend is consistent with the change in mRNA levels.

v. miR-26b promotes LPS-induced NO production

Since NO is up-regulated by LPS and proinflammatory cytokines, we next examined NO production in miR-26b-challenged bAMs. NO production was increased after 6 h of LPS stimulation in lentiviral miR-26b-infected bAMs compared to VC-infected bAMs but this effect did not reach the significant level (Fig. 4L). These results suggest that miR-26b and LPS synergistically enhance TNF-α, IL-8, IL-1β and IL-10 but repress IL-6 expression at the mRNA level, resulting in enhanced TNF-α, IL-8, IL-1β andIL-10 but decreased IL-6 protein levels in the culture medium. miR-26b also enhanced NO production but not reach the significant level.

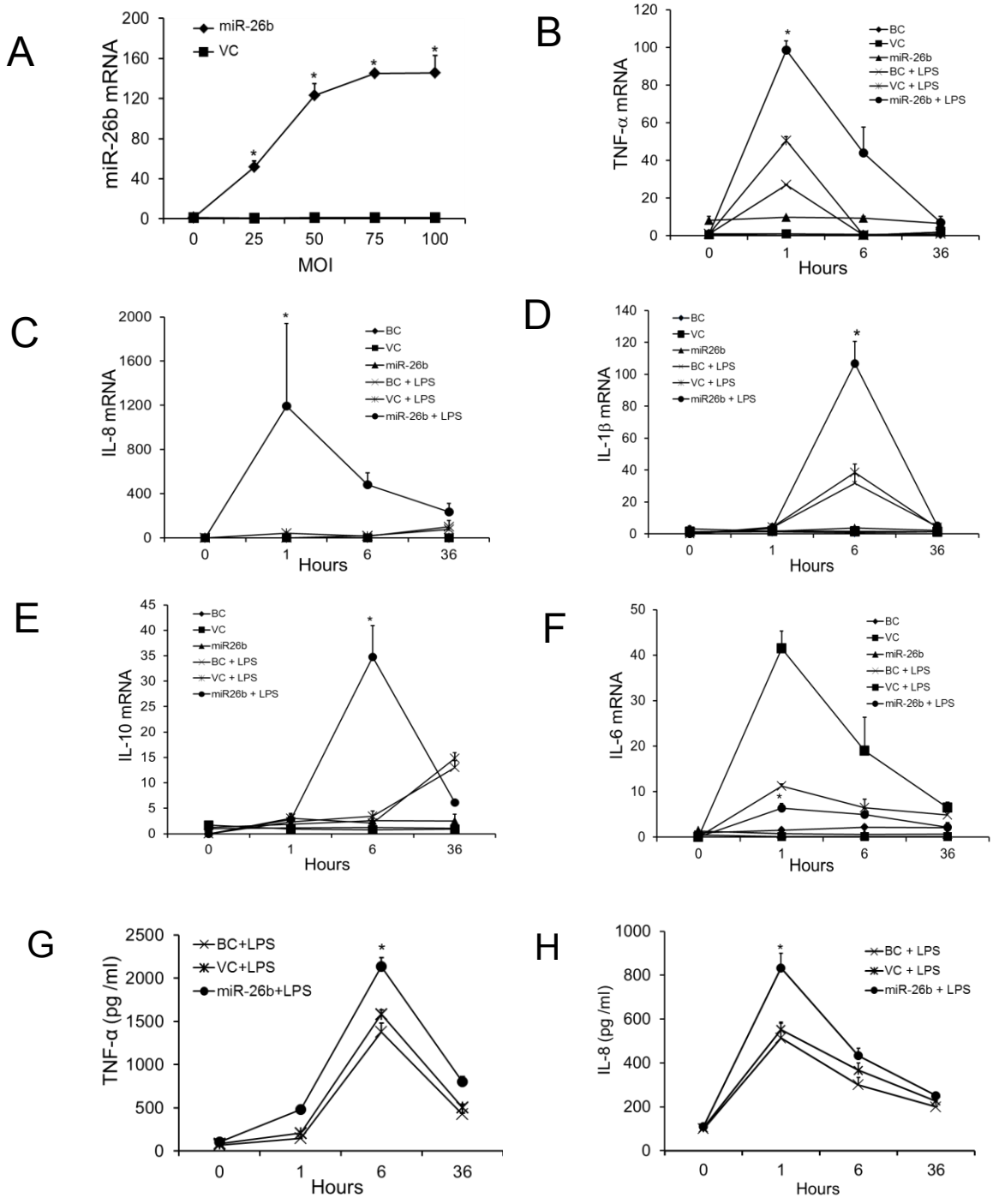
A
miR-26b mRNA
miR-26b
VC
MOI
B
TNF-α mRNA
BC
VC
miR-26b
BC + LPS
VC + LPS
miR-26b + LPS
Hours
C
IL-8 mRNA
Hours
D
IL-1β mRNA
miR26b
miR26b + LPS
Hours
E
IL-10 mRNA
Hours
F
IL-6 mRNA
Hours
G
TNF-α (pg /ml)
BC+LPS
VC+LPS
miR-26b+LPS
Hours
H
IL-8 (pg /ml)
Hours

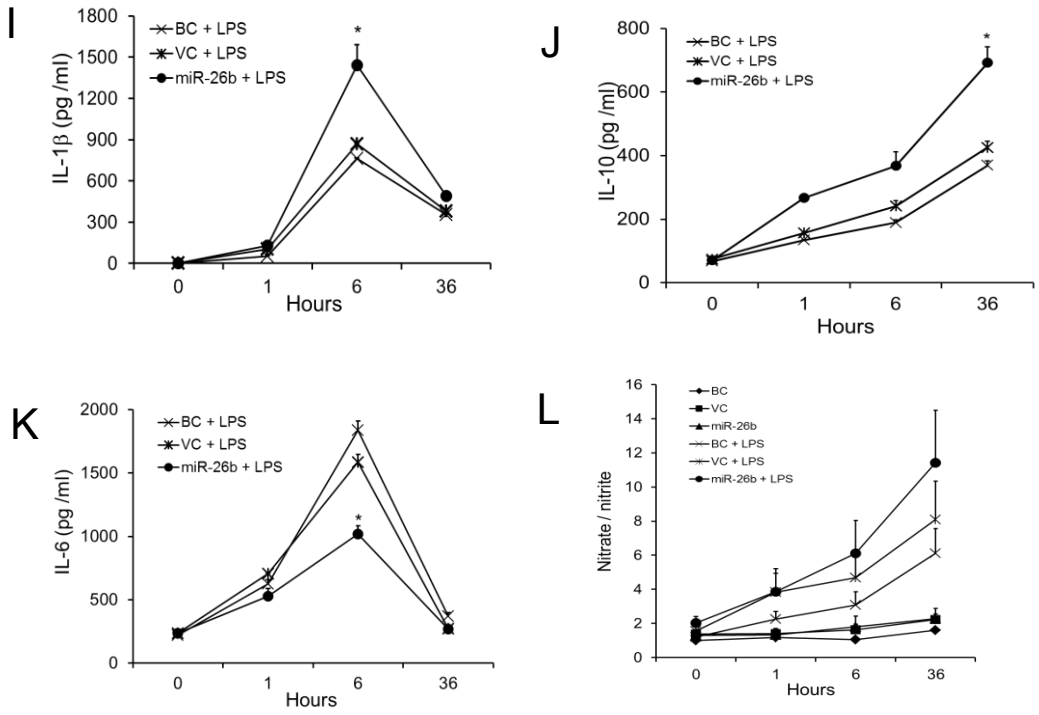

Fig. 4: miR-26b enhances LPS-induced TNF-α, IL-8, IL-1β and IL-10 mRNA and protein expression and NO production, but represses IL-6 mRNA and protein expression. bAMs were infected with various multiplicity of infection (MOI) of miR-26b lentivirus. (A) miR-26b expression level was determined by real-time PCR. Data was expressed as a fold change to 0 h VC. Results are expressed as means ± SE (n=3 cell preparations). bAMs were infected with lentiviruses expressing miR-26b or the lentiviral control vector (VC) at a MOI of 50. bAMs that were not infected with lentiviruses served as the blank control (BC). Then, bAMs were incubated with or without LPS (1 μg/ml) for 1, 6 and 36 h. The mRNA expression of TNF-α (B), IL-8 (C), IL-1β (D), IL-10 (E) and IL-6 (F) at indicated time points was analyzed by real-time PCR. The expression of each gene was normalized to the average of BC control samples at 0 h. TNF-α (G), IL-8 (H), IL-1β (I), IL-10 (J), IL-6 (K) and NO (L) in the culture supernatant were assayed with a specific ELISA kit or Griess reagent (for NO). Results are expressed as mean ± SE. *P<0.05 vs. VC+LPS (n=3 cell preparations).

vi. PTEN is suppressed by miR-26b

To decipher how miR-26b regulates LPS-induced cytokine expression, we used the bioinformatics tool, Targetscan, to predict target genes of miR-26b. Among these potential targets, there are 3 binding sites in the 3'-UTR of PTEN, which is highly conserved in mammals including cows, humans, mice and rats. Furthermore, PTEN inhibition activates Akt, which consequently activates IκB kinase (IKK), leading to degradation of IκB and nuclear translocation of the transcription factor NF-κB (99). Therefore, we chose PTEN for further analysis.

To verify whether PTEN is a potential target of miR-26b, Raw 247 cells were co-transfected with the PTEN 3'-UTR firefly luciferase reporter vector and miR-26b or the control vector, miR-Con. Due to the length of the PTEN 3'-UTR, we cloned binding sites 1 and 2 into one luciferase reporter vector (PTEN1-WT), and cloned binding site 3 into a second reporter vector (PTEN2-WT) (Fig. 5A). We found that miR-26b suppressed activities of both PTEN1 and PTEN2 (Fig. 5B). When we mutated the binding site 1 or 2 in PTEN1 (PTEN1-M1 or PTEN1-M2), the inhibition of the reporter activities by miR-26b was reduced compared to PTEN1-WT. Furthermore, the mutation of both binding sites PTEN1-M1+M2) completely abolished the miR-26b inhibition. Similarly, the mutation of the binding site 3 in PTEN2 (PTEN2-M3) also resulted in no inhibition of the reporter activity by miR-26b. These results suggest that the three binding sites in 3'-UTR of PTEN are all involved in the binding of miR-26b.

To further confirm the results, western blotting and qRT-PCR were used to determine the endogenous protein and mRNA expression levels of PTEN at different time points paralleled by the same time points of the miR-26b response to LPS. The results showed that PTEN protein and mRNA levels was reduced at 1 h after LPS stimulation and increased at 6 h and 36 h after LPS stimulation (Fig. 5C, D). However, PTEN protein and mRNA levels have no change in the control condition (Fig. 5C, D). The results support the functional correlation of miR-26b and PTEN. Additionally, western blotting was used to determine the endogenous PTEN protein

expression in miR-26b-overexpressing bAMs as well. The result showed that the PTEN protein level was reduced by miR-26b overexpression (Fig. 5E, F). We thus concluded that PTEN is a target of miR-26b in bAMs.

vii. miR-26b enhances LPS-induced NF-κB signaling pathway activity

PTEN is known to inhibit Akt phosphorylation and thus the NF-κB pathway (100, 101). Therefore, we next investigated whether miR-26b can activate NF-κB signaling. We first used a dual luciferase-reporter assay to assess the effect of miR-26b on the NF-κB pathway. We found that miR-26b up-regulated the activity of the NF-κB-luciferase reporter construct after LPS stimulation compared with the control vector, miR-Con (Fig. 6A). Then, we determined the effect of miR-26b on LPS-induced phosphorylation of Akt, IKK, IκBα and P65. miR-26b greatly enhanced the phosphorylation of Akt, IKK, IκBα and P65 after a 15-min LPS stimulation (Fig. 6B). Thus, these results show that miR-26b and LPS cooperatively up-regulate the NF-κB signaling pathway.

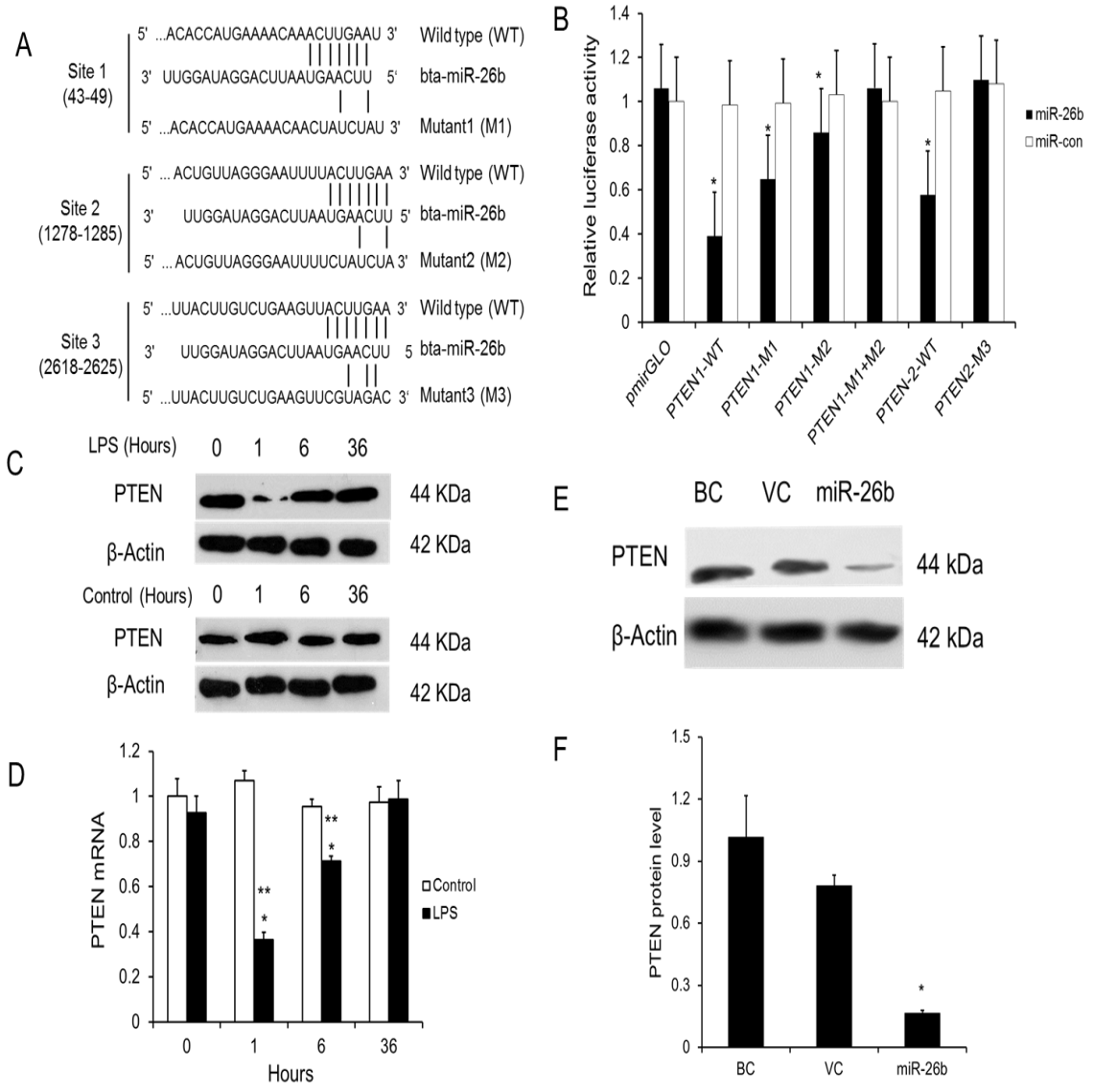

Fig. 5: PTEN is a target of miR-26b. (A) The potential interaction between miR-26b and the putative binding sites in the 3'-UTR of the bovine PTEN gene. Mutations of bta-miR-26b binding sites in the 3'-UTR of bovine PTEN are indicated. (B) 3'-UTR luciferase reporter assays. HEK293T cells were co-transfected with wild-type (WT) PTEN1, PTEN2 or their mutants (M1, M2, M1+M2 or M3) and miR-26b or miR-con for 24 h. Firefly luciferase activity was normalized to *Renilla* luciferase activity. The results were expressed a ratio of empty pmirGLO vector + miR-con (mean ± SE). *P<0.05 vs. miR-con (n=3 cell preparations). (C) bAMs were stimulated with LPS (1 μg/ml) for 0-36 h. Controls were bAMs without LPS stimulation. The protein

expression level of PTEN was measured by western blotting. (D) the mRNA levels of PTEN at the same time points of LPS stimulation were measured by real-time PCR using 18S rRNA as an endogenous control. *p<0.05 vs. miR-con at the same time point; **P<0.05 vs. miR-26b at 0 h stimulation (n=3 cell preparation). (E) Western blotting for PTEN in the infected bAMs without lentivirus (BC) or with lentivirus expressing miR-26b or the lentiviral control vector (VC). (F) The bands were quantified by ImageJ. The relative PTEN expression levels were normalized to β-actin. Results are expressed as mean ± SE. *P<0.05 vs. BC (n=3 cell preparations).

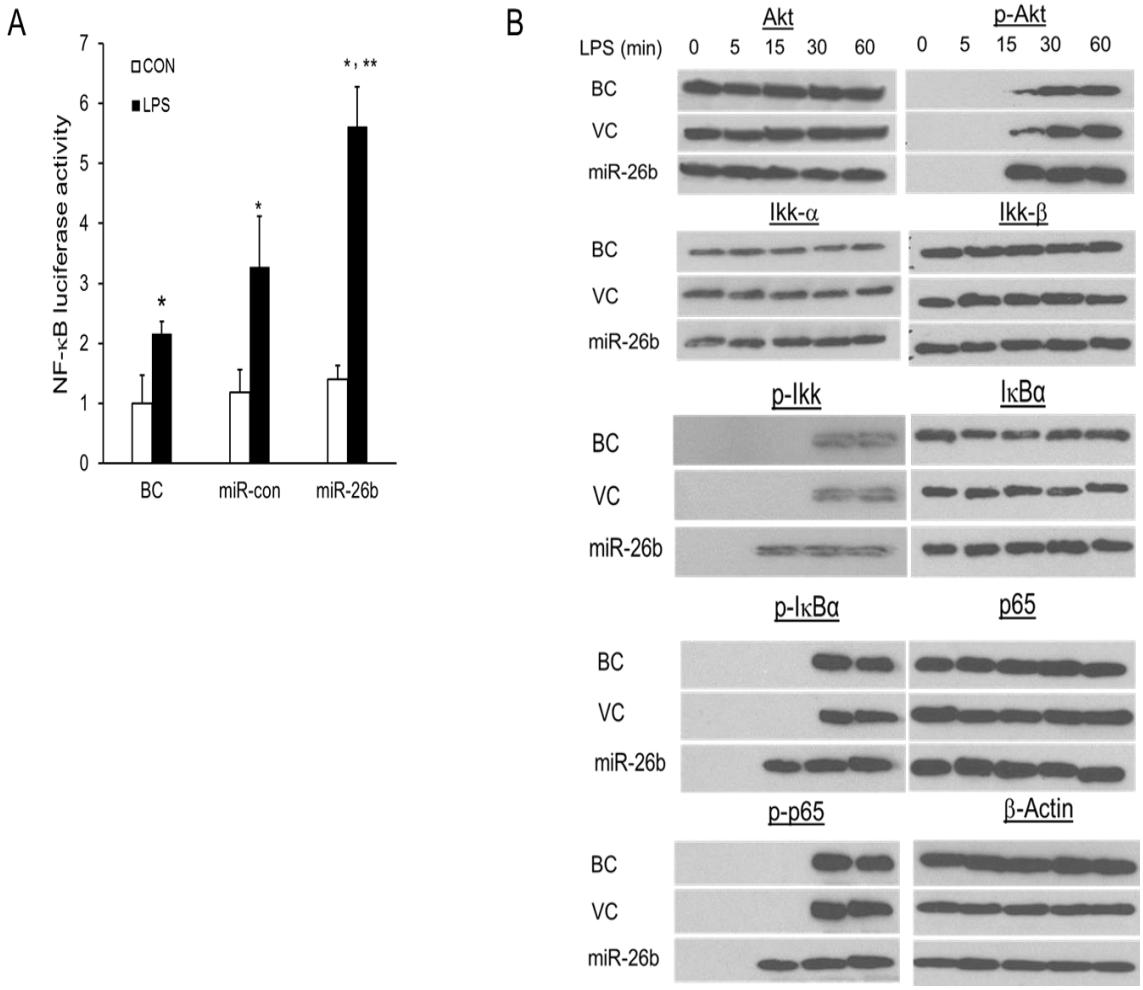

Fig. 6: miR-26b activates NF-κB signaling. (A) Raw 246.7 cells were co-transfected with a NF-κB luciferase-reporter construct and miR-26b or miR-Con. After 24 h culture, cells were

stimulated with or without LPS (CON). Blank Control (BC): Raw 246.7 cells transfected with only NF-κB luciferase-reporter construct. The firefly luciferase activity was normalized to *Renilla* luciferase activity. Results are expressed as fold change over blank control (BC). Results are expressed as mean ± SE. **P<0.05 vs. miR-Con with LPS, *P<0.05 vs. CON (n=3 cell preparations). (B) Western blot analysis of phosphorylated Akt, Ikk, IκBα and p65 in lysates from bAMs infected with miR-26b or control lentivirus (VC) at a MOI of 50 for 16 h, and then treated for 0 – 60 min (above lanes) with LPS. Blank control (BC): bAMs without virus infection.

viii. PTEN silencing enhances LPS-induced cytokine expression and activates the NF-κB signaling pathway

In order to assess the role of PTEN in the LPS-induced NF-κB signaling pathway and in inflammatory responses in bAMs, we silenced PTEN using a PTEN shRNA lentivirus to see whether the cytokine mRNA expression and NF-κB signaling pathway were affected. PTEN shRNA significantly reduced the expression of PTEN protein in bAMs (Fig. 7A).

To determine whether silencing PTEN causes the same cytokine responses as miR-26b in LPS-induced bAMs, bAMs were infected with PTEN shRNA lentivirus or the control lentivirus (Con-shRNA) at a MOI of 50 and then treated with LPS for 0, 1, 6 and 36 h after infection. Similar to miR-26b, PTEN silencing markedly increased the mRNA expression of TNF-α and IL-1β at 1 and 6 h, respectively (Fig. 7B, D). However, PTEN silencing enhanced IL-8 and IL-10 mRNA expression at 36 h rather than at 1 or 6 h as for the case of miR-26b (Fig. 7C, E). In contrast to miR-26b, which decreased the mRNA expression of IL-6 (Fig. 4F), PTEN silencing increased IL-6 mRNA level (Fig. 7F). This is consistent with the observation that IL-6 is a direct target of miR-26b (98).

To investigate the molecular mechanism by which PTEN silencing influences the LPS-induced NF-κB pathway in bAMs, we determined the phosphorylation of the components

involved in the pathway by western blotting (Fig. 8). The phosphorylation of Akt, IKK, IκBα, and p65 was enhanced by PTEN silencing after 15 min of LPS stimulation in bAMs, which is the same pattern as for miR-26b (Fig. 6B).

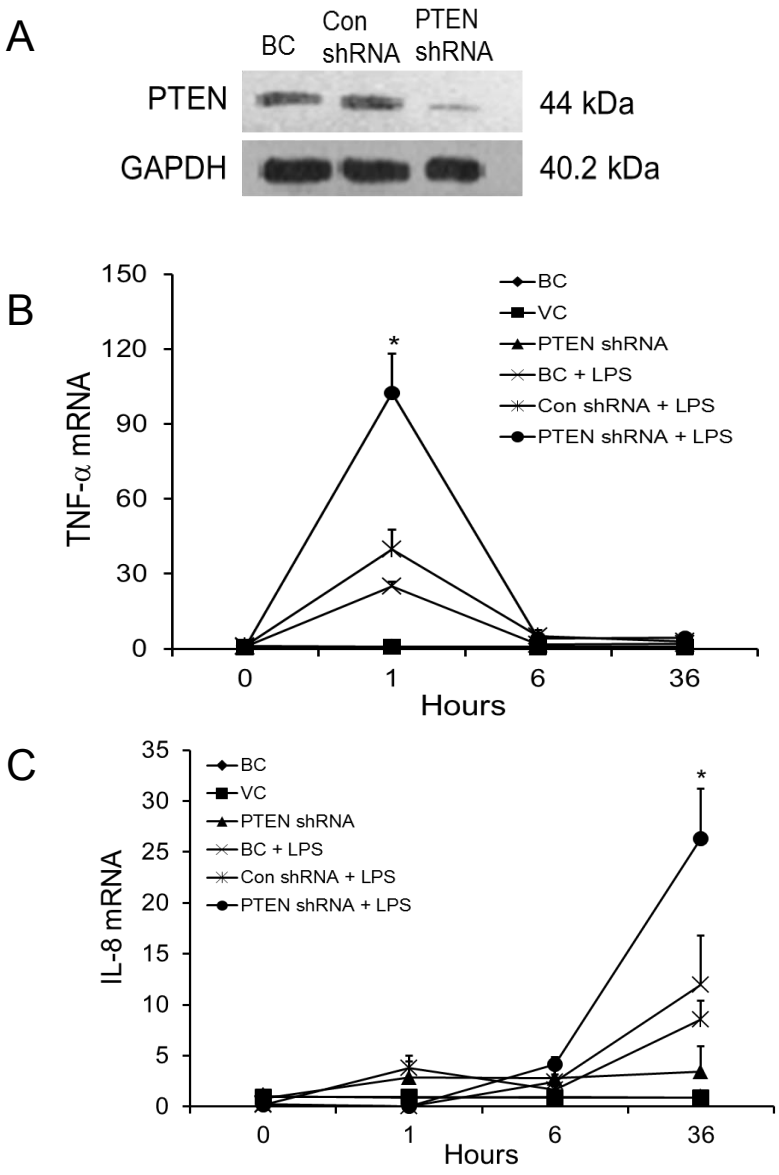

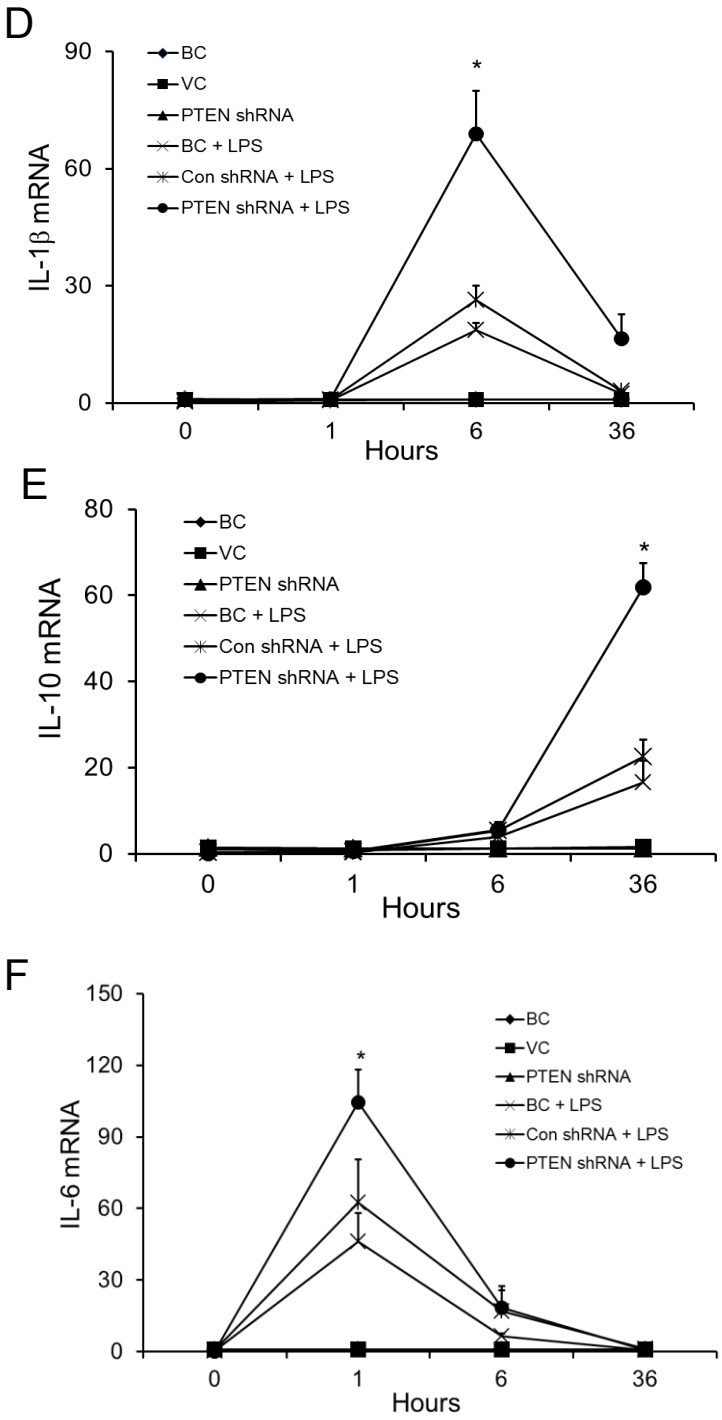
D
90
60
30
0
IL-1β mRNA
BC
VC
PTEN shRNA
BC + LPS
Con shRNA + LPS
PTEN shRNA + LPS
*
0
1
6
36
Hours
E
80
60
40
20
0
IL-10 mRNA
BC
VC
PTEN shRNA
BC + LPS
Con shRNA + LPS
PTEN shRNA + LPS
*
0
1
6
36
Hours
F
150
120
90
60
30
0
IL-6 mRNA
BC
VC
PTEN shRNA
BC + LPS
Con shRNA + LPS
PTEN shRNA + LPS
*
0
1
6
36
Hours

Fig. 7: PTEN silencing promotes LPS-induced TNF-α, IL-8, IL-1β, IL-10 and IL-6 mRNA expression. bAMs were infected with PTEN silencing lentivirus (PTEN shRNA) or virus control (Con shRNA) and cultured for 24 h. Blank control (BC): bAMs without virus infection. (A) Western blot analysis was performed to determine PTEN expression. (B-F) infected or un-infected bAMs were stimulated with or without LPS (1 μg/ml) for 1, 6 and 36 h. The mRNA expression of TNF-α (B), IL-1β (C), IL-8 (D), IL-10 (E) and IL-6 (F) at indicated time points was analyzed by real-time PCR. The expression of each gene was normalized to the average of BC control samples at 0 h. Results are expressed as mean ± SE. *P<0.05 vs. Con shRNA + LPS (n=3 cell preparations).

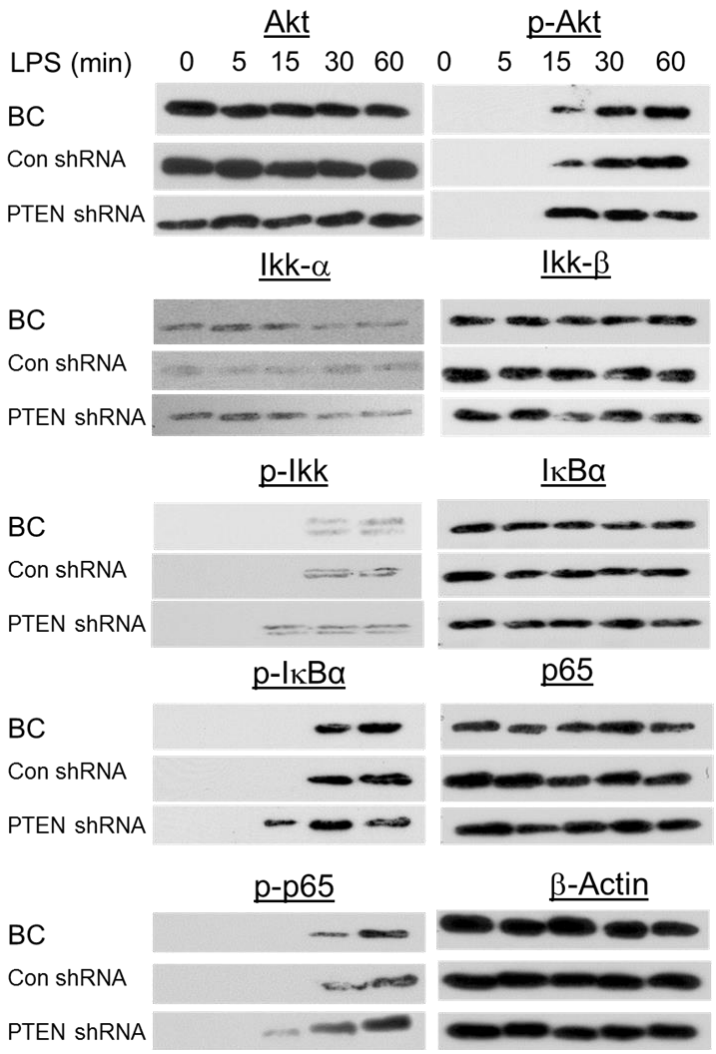

Fig. 8: PTEN silencing activates NF-κB signaling in bAMs. Western blot analysis of phosphorylated Akt, Ikk, IκBα and p65 in lysates of bAMs infected with lentiviruses expressing PTEN shRNA or vector control (Con shRNA) at MOI=50 for 16 h, and then treated for 0 – 60 min (above lanes) with LPS. Blank control (BC): bAMs without virus infection.

III-2: MicroRNA-29a Efficiently Promotes the Differentiation of Mouse Induced Pluripotent Stem Cells and Mesenchymal Stem Cells into Alveolar Epithelial Type II cells

III-2-1: iPSCs

i. Characterization of iPSCs

We first characterized iPSCs using immunostaining and qRT- PCR. The iPSCs expressed the pluripotent markers, NANOG and SSEA-4 as revealed by immunostaining (Fig 9A). qRT-PCR analysis showed that iPSCs had a high level of mRNA expression of pluripotent markers, Sox2, Oct4, Nanog, and Dnmt3b. These markers were absent in MEF feeder cells except Dnmt3b with a low expression (Fig 9B). NANOG-positive cells were 65 ± 0.67% and 95 ± 1.34% (mean ± SE, n=4 cell preparations) before and after removing MEF contamination (Fig 9C, D).

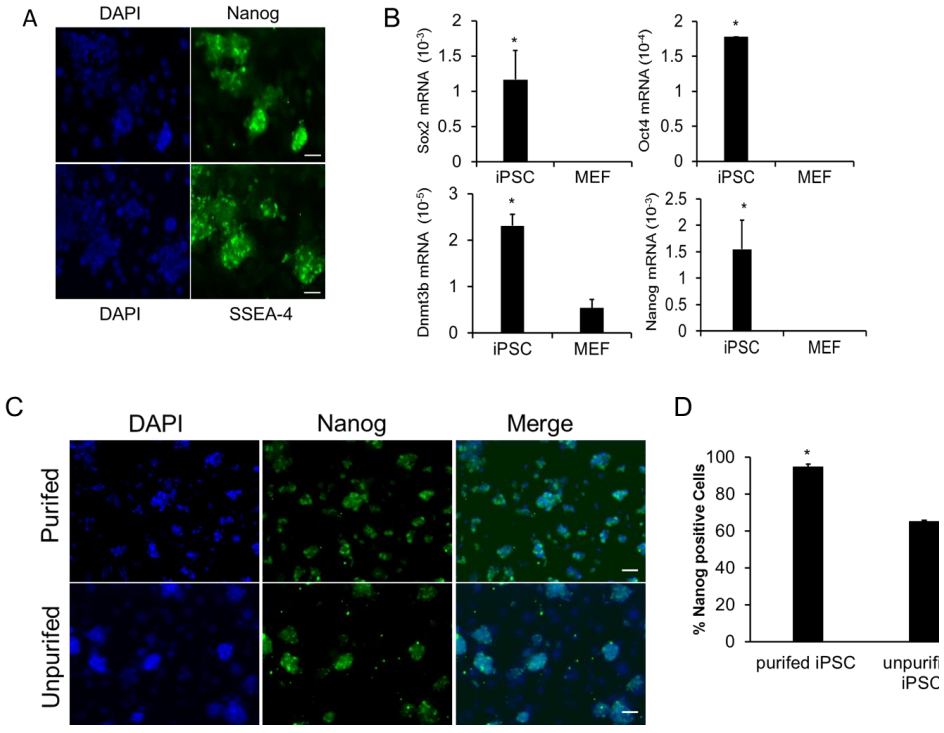

Fig. 9: Identification of mouse iPSCs by immunostaining and qRT-PCR. (A) Representative images of immunostaining for pluripotent markers (Nanog and SSEA-1) in the iPSC colonies. 4, 6-diamidino-2-phenylindole (DAPI) staining was used as a nuclear marker. Scale bar: 50 µm; (B) qRT-PCR analysis of mouse undifferentiated iPSCs compared with mouse MEF. Values for Nanog, Oct4, Dmnt3t, and Sox2 were normalized to 18S rRNA from the same cDNA sample. Results are shown as mean ± SE. *P<0.05 vs. MEF (n=3 cell preparations); (C) Purified and unpurified iPSCs were fixed and stained for Nanog. The nuclei were stained using DAPI. Scale bar: 100 µm; (D) Percentage of positive cells for Nanog. *P<0.05 vs. unpurified iPSCs (n=4).

ii. Differentiation of iPSCs to AEC II

To optimize a proper culture condition to differentiate iPSCs into AEC II with high efficiency, we first repeated the protocol developed by Roszell (78). iPSCs were seeded

on collagen IV coated 6-well plates overnight and the medium was switched to the differentiation medium with or without Activin A for 6 days and with or without FGF-2 for 5 days. We monitored mRNA expression of AEC II markers SP-C and SP-B during the differentiation process. Inclusion of activin A and FGF-2 significantly increased mRNA expression of SP-C and SP-B (Fig 10A) and decreased that of the iPSC marker, Nanog (Fig 10 B). Immunofluorescence analysis revealed that 29.19 ± 3.14% and 27.93 ± 5.86% (mean ± SE, n= 3 cell preparations) of the activin A and FGF-2-treated iPSCs were positive for AEC II markers, SP-C and ABCA3, respectively (Fig 10C-E).

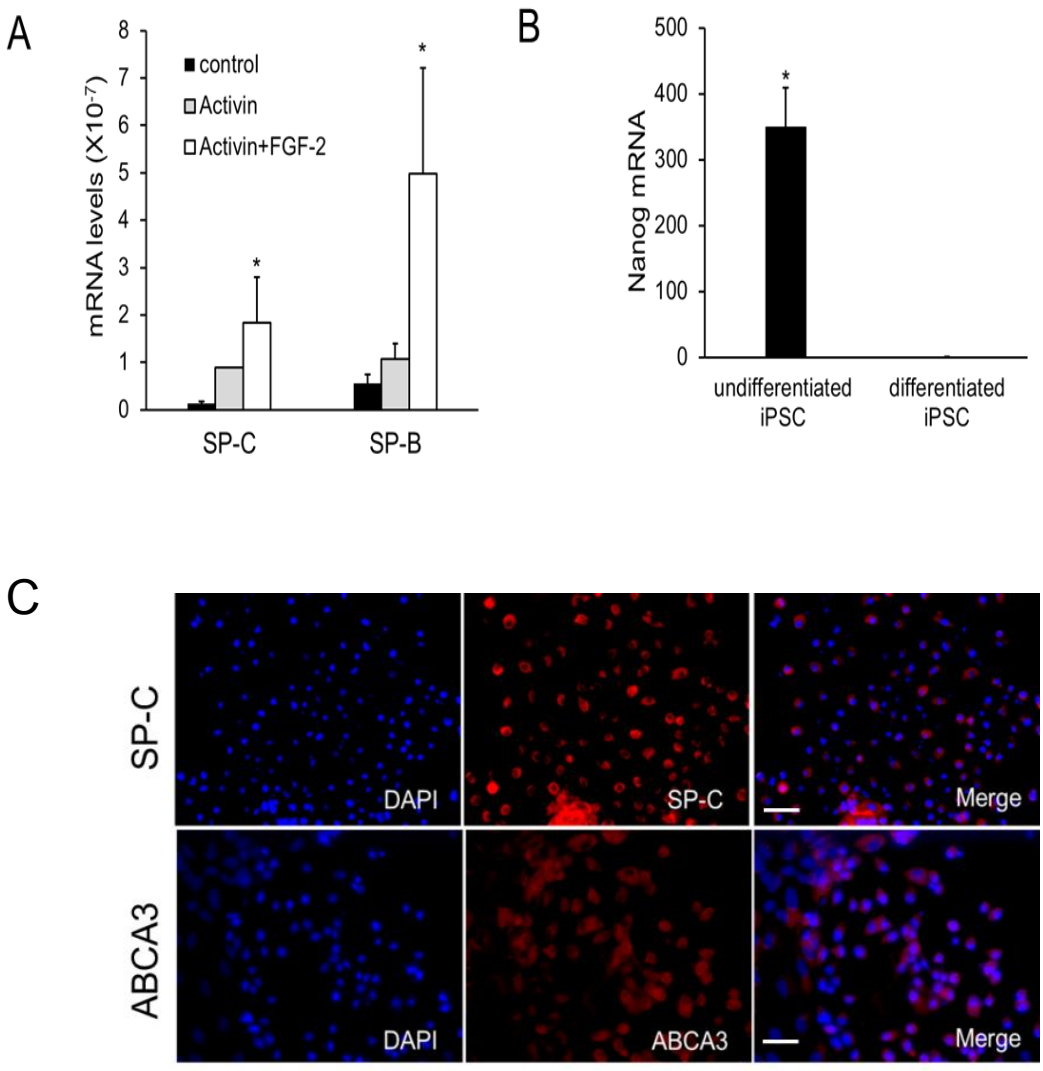

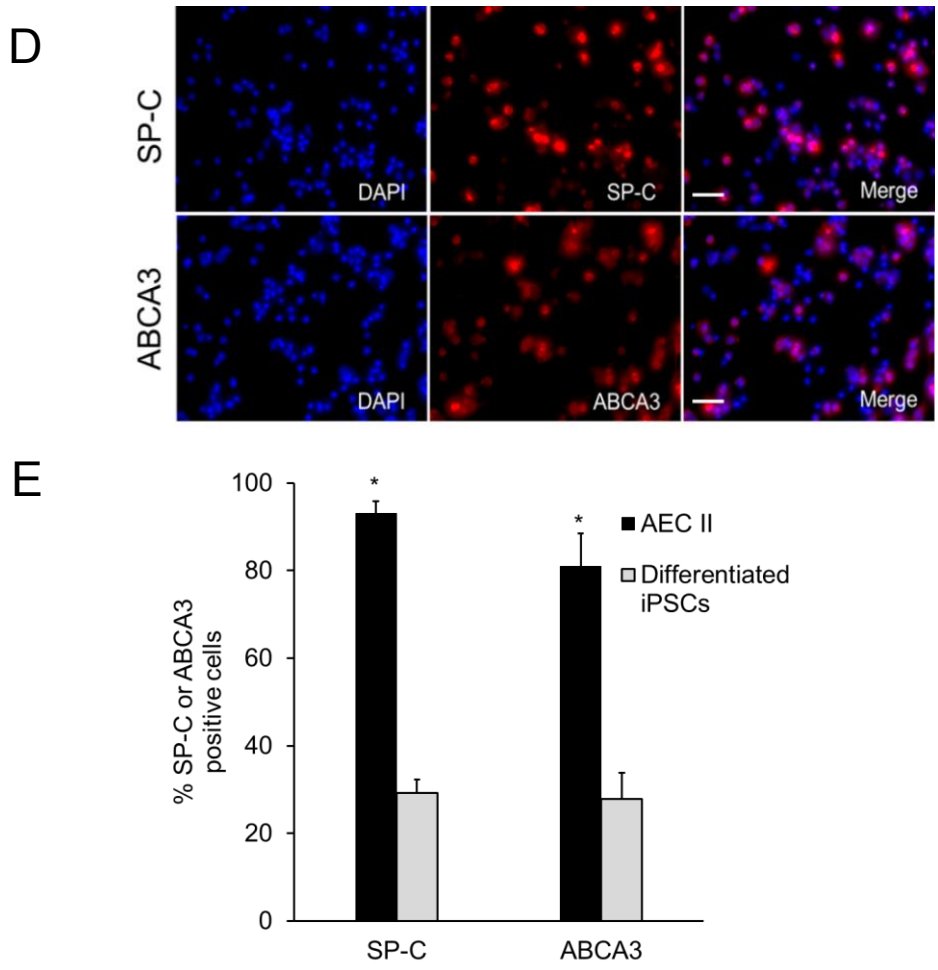

Fig. 10: Characterization of differentiated iPSCs. (A) mRNA levels of SP-B and SP-C in differentiated iPSCs as determined by real-time PCR. Control (black bar): iPSCs cultured in differentiation medium without Activin A and FGF-2 for 11 days; Activin (gray bar): iPSCs cultured in Activin A (20 ng/mL) for 6 days and cultured in differentiation medium without FGF-2 for 5 days; Activin+FGF-2 (white bar): iPSCs cultured in Activin (20 ng/mL) for 6 days and cultured in FGF-2 (50 ng/mL) for 5 days. *P<0.05 vs. control (n=3 cell preparations); (B) mRNA level of the iPSC marker Nanog in differentiated cells as determined by qRT- PCR. iPSCs were cultured in normal medium or differentiation medium with Activin A (20 ng/mL) for 6 days and with FGF-2 (50 ng/mL) for 5 days. (C-E) Immunofluorescence analysis of the AEC II markers, SP-C and ABCA3 in freshly isolated AEC II from mouse (C) and differentiated iPSCs (D). The

nuclei were stained with DAPI. Scale bar: 50 μm. (E) Quantitation of SP-C and ABCA3-positive cells. *P<0.05 vs differentiated iPSCs (n=3)

iii. Identification of miRNAs enriched in AEC II

Since miRNAs have been reported to induce the reprogramming of mouse and human somatic cells into iPSCs (15), we reasoned that certain miRNAs may be able to promote the differentiation of iPSCs into AEC II. To identify such miRNAs, we performed miRNA microarray analysis on iPSCs and AEC II to screen the miRNAs enriched in AEC II. For data analysis, the weak and bad spots were eliminated using RealSpot software according to the assigned QI. LOWESS normalization was performed for the remained spots. We found ten miRNAs (miR-19b, miR-30b, miR-451, miR-142-3p, miR-142-5p, miR-22, miR-23, miR-24, miR-29a and let-7b) are enriched in AEC II cells by by two-tailed Student's t-test analysis considering unequal variance with P<0.05. We verified all of these ten miRNAs by qRT-PCR (Fig 11).

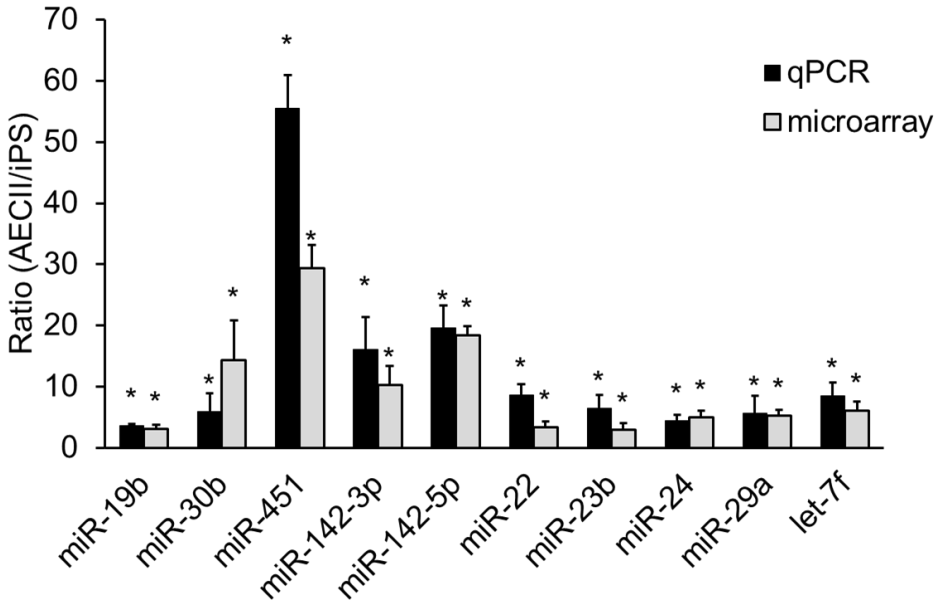

Fig. 11: Verification of AEC II-enriched miRNAs. Total RNA was extracted from AEC II cells and iPSCs. miRNA levels were determined by microarray and qRT-PCR. Each value represents a normalized ratio to iPSCs. Results are mean ± SE, *P<0.05 vs iPSCs (n=3).

iv. Effect of miRNAs on the differentiation of iPSCs to AEC II

Among these 10 miRNAs enriched in AEC II, miR-22, miR-23, miR-29a and let-7b are highly expressed in adult lungs compared to fetal lung and miR-127, miR-19 and miR-210 at the late stage of fetal lungs were used as negative miRNA controls (91). Since the differentiation of AEC II occurs at the late stages of fetal lung development and continues until adulthood, overexpressing these miRNAs may induce the differentiation of iPSCs into AECs. iPSCs seeded on collagen IV-coated plates were infected with a lentiviral virus expressing a miRNA or control vector (VC) at a MOI of 50 for 24h. The cells were serum-starved overnight and then cultured under 3 conditions for 11 days: 1) differentiation medium containing no growth factor (control); 2) differentiation medium with Activin A for the first 6 days (Activin); and 3) differentiation medium with Activin A for 6 days and then FGF-2 for 5 days (Activin + FGF-2). miR-22, miR-29a, and let-7b markedly augmented the mRNA expression of AEC II markers SP-C, SP-B, and ABCA3 (Fig 12 A-C) in the complete differentiation medium (Activin + FGF-2). However, miR-29a and let-7b reduced the mRNA levels of AEC I markers, T1α and aquaporin 5 (AQP5), while miR-22 only inhibited T1α mRNA expression (Fig 12D, E). To determine how many iPSCs were differentiated into AEC II, we immunostained the differentiated cells with antibodies for the AEC II marker, SP-C. The SP-C-positive cells were 50.55%, 51.33% and 61.06% of the total cells for miR-22, miR-29a and let-7b as compared to 29.46% in VC (Figure 12F). The trend is consistent with the changes in mRNA levels.

The mRNA expression of iPSC markers, cMyc, Klf, Nanog, and Sox was extremely low in the cells cultured in the complete differentiation media with or without miRNA overexpression compared to undifferentiated iPSCs (Figure 13).

Dexamethasone (10 nM), 8-bromoadenosine 3, 5- cyclic monophosphate (cAMP, 0.1 mM), and isobutylmethylxanthine (IBMX, 0.1 mM) (DCI) can induce the maturation of human and mouse AEC II (102). We next examined the effect of DCI on miR-29a-induced differentiation of iPSCs into AEC II. Inclusion of DCI in the differentiation media markedly increased the mRNA expression of AEC II markers. The expression levels of SP-C, SP-B and ABCA3 in these cells were 76%, 78% and 57% of freshly isolated AEC II from mouse (Fig 14A). However, these cells expressed negligible amounts of the AEC I markers, T1-α and AQP5 in comparison with AEC I trans-differentiated from AEC II (Fig 14B). At the protein level, 88.01 ± 1.7% cells are positive for SP-C in the presence of DCI compared to 51.33 ±9.4% in the absence of DCI (Fig 14C). These results indicate that DCI further enhances miR-29a-induced iPSC differentiation into AEC II.

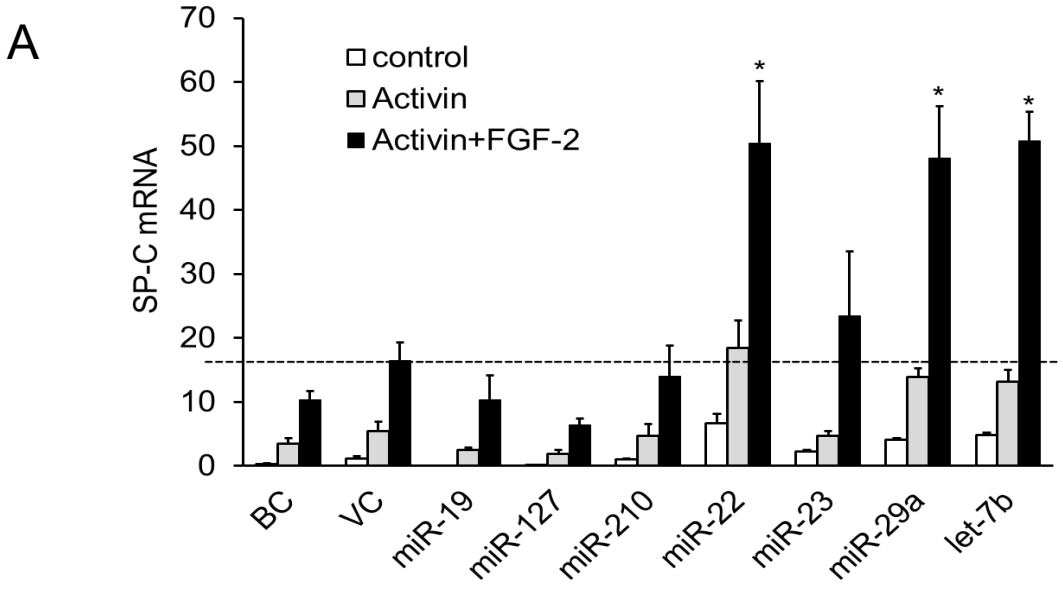

B

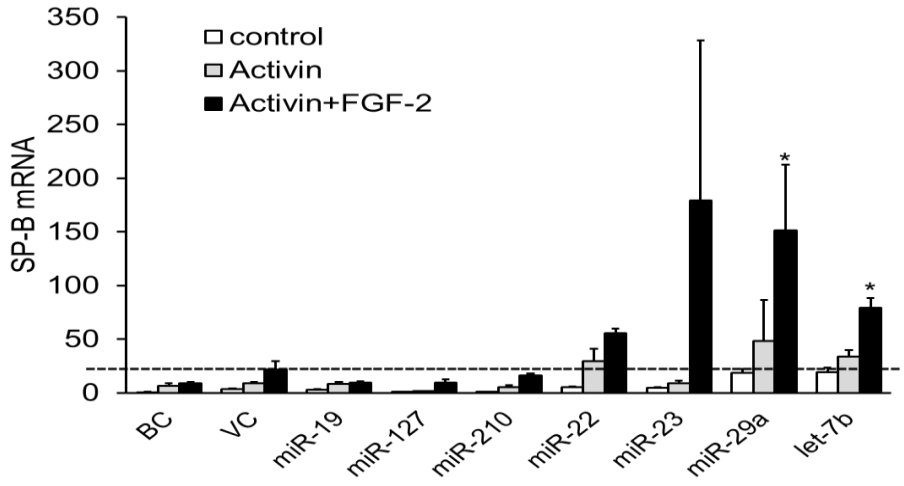
control
Activin
Activin+FGF-2
SP-B mRNA
350
300
250
200
150
100
50
0
BC
VC
miR-19
miR-127
miR-210
miR-22
miR-23
miR-29a
let-7b

C

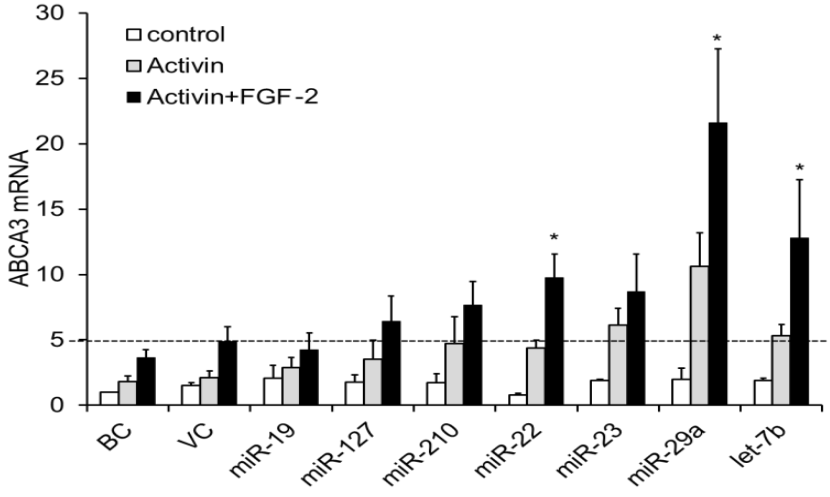
control
Activin
Activin+FGF-2
ABCA3 mRNA
30
25
20
15
10
5
0
BC
VC
miR-19
miR-127
miR-210
miR-22
miR-23
miR-29a
let-7b

D

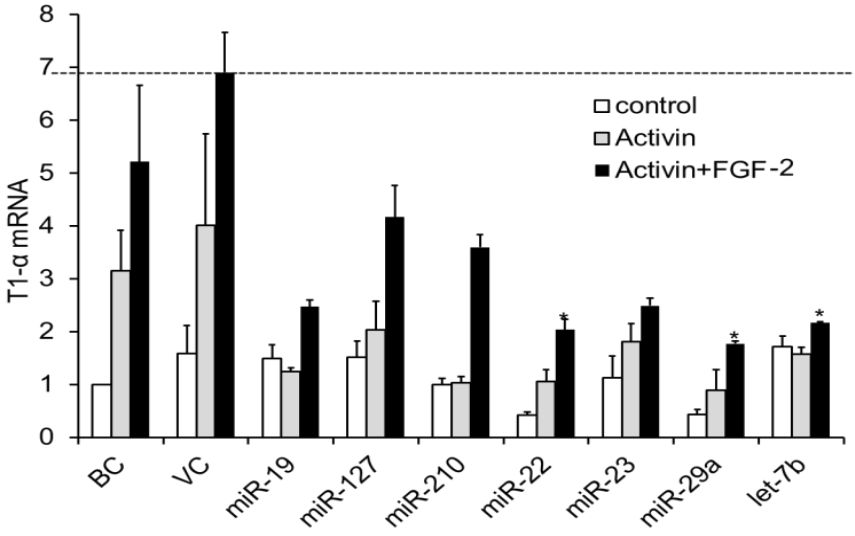
control
Activin
Activin+FGF-2
T1-α mRNA
8
7
6
5
4
3
2
1
0
BC
VC
miR-19
miR-127
miR-210
miR-22
miR-23
miR-29a
let-7b

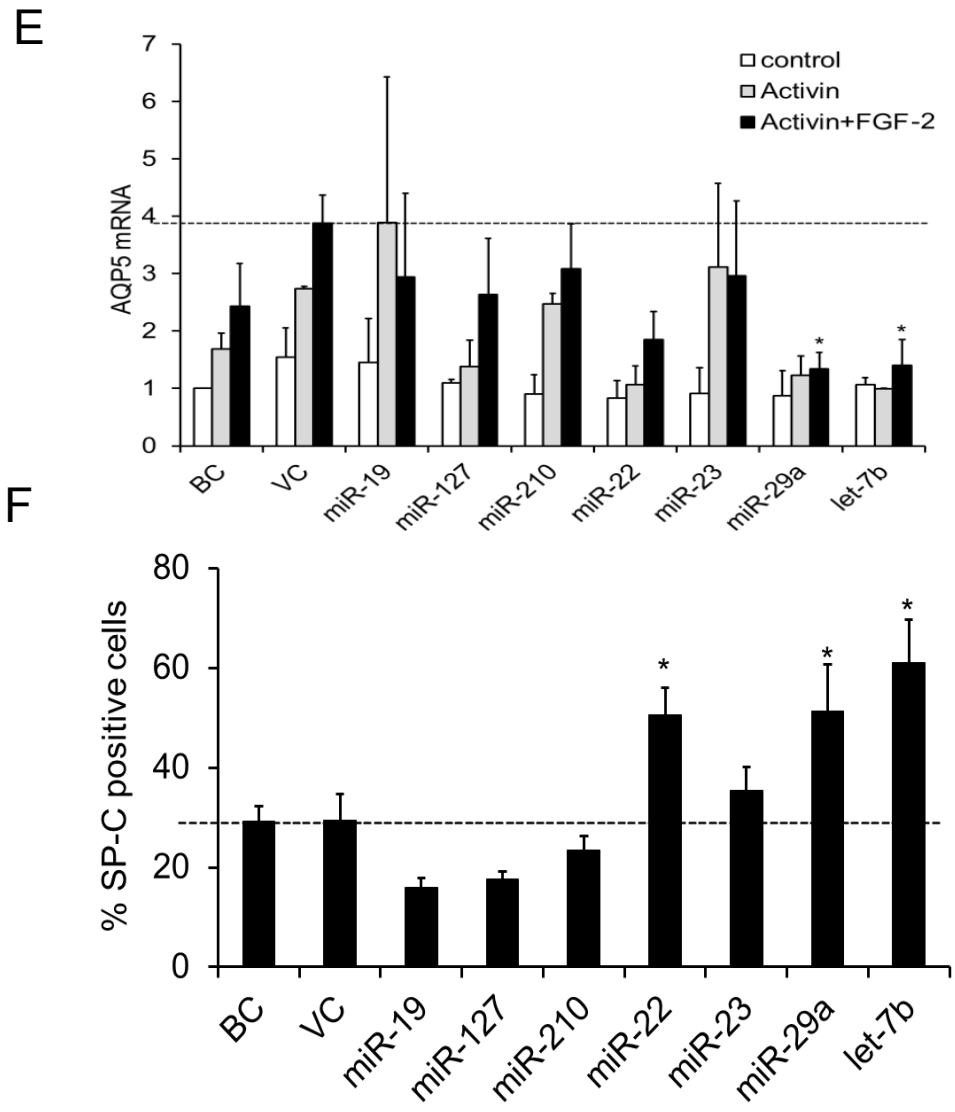

Fig. 12: AEC II and AEC I marker expression in miRNA-overexpressed differentiated iPSCs. iPSCs were infected with a lentivirus expressing a miRNA at a MOI of 50. Blank control (BC): iPSCs cultured in differentiation medium without miRNA infection. The cells were then cultured in differentiation medium with or without Activin A (20 ng/mL) for 6 days and with or without FGF-2 (50 ng/mL) for 5 days. mRNA expression levels of AEC II markers, SP-C, SP-B, and ABCA3 (A-C) and AEC I markers, T1α and AQP5 (D, E) were determined by real-time PCR

and normalized to vector control (VC). (F) SP-C-positive cells as determined by immunostaining. BC: blank control; VC: vector control. *P< 0.05 vs. VC (n=3).

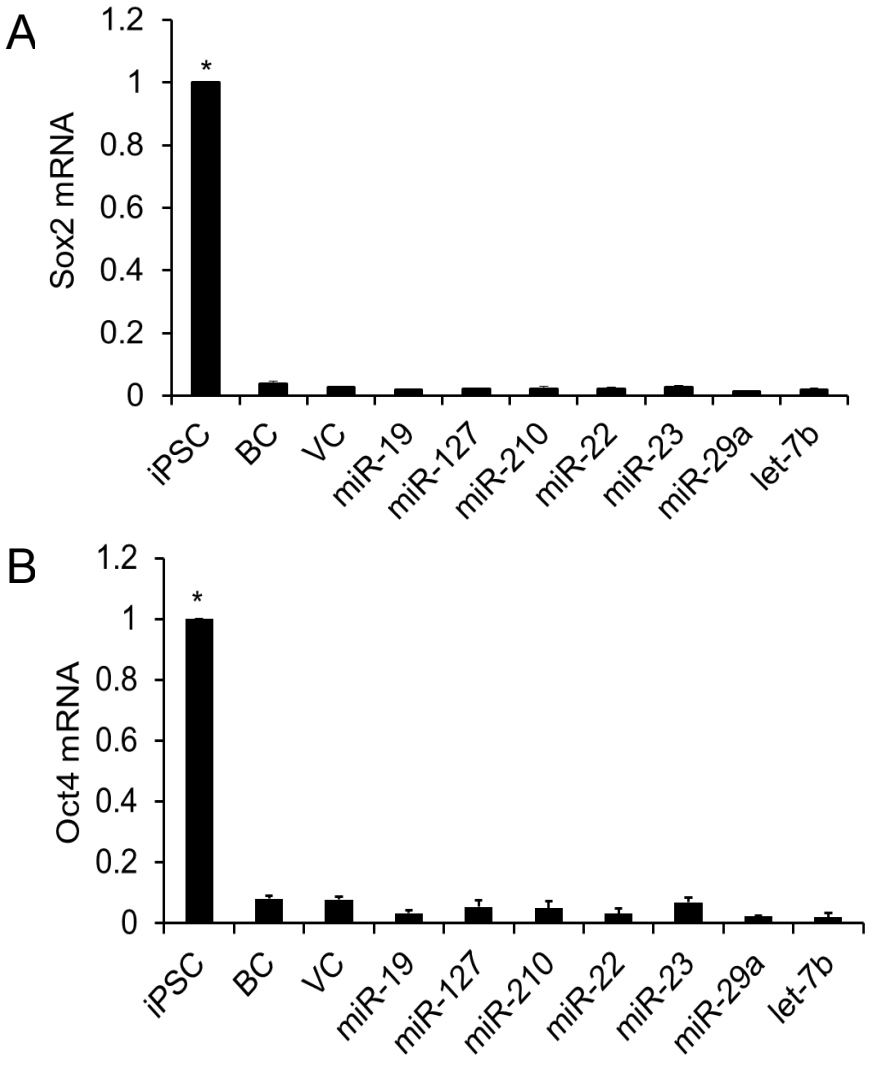

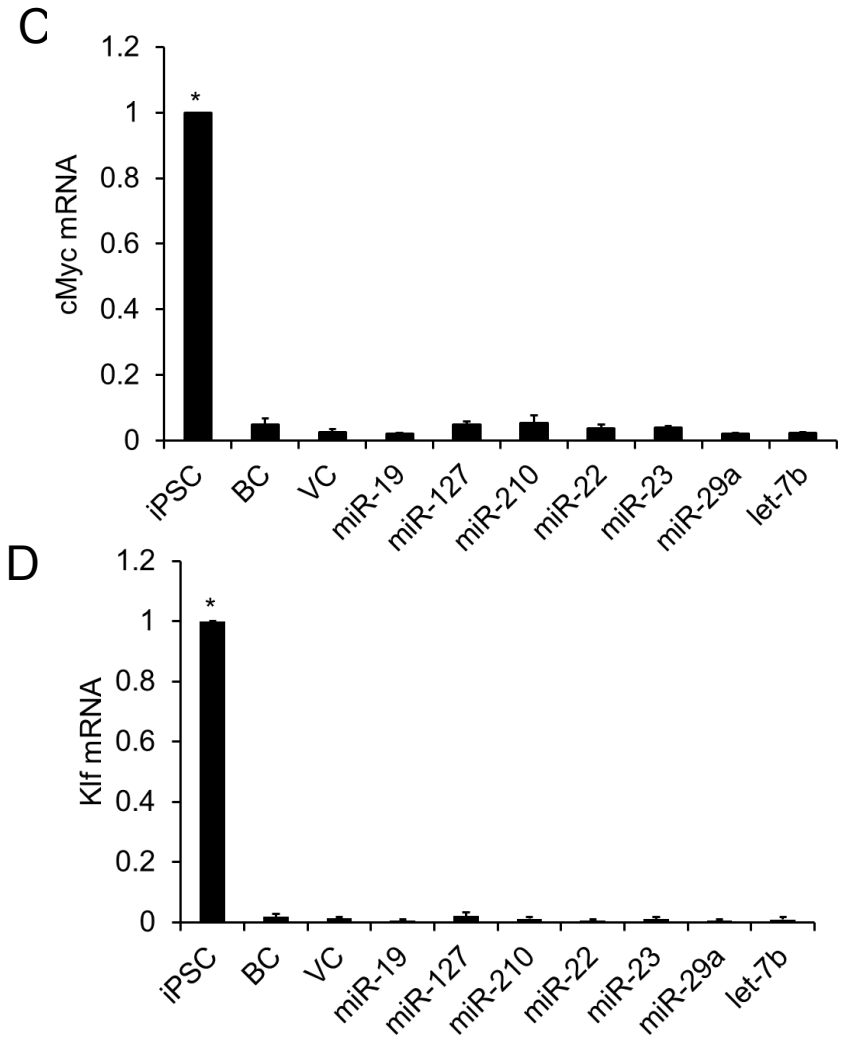

Fig. 13: mRNA expression levels of iPSC markers after differentiation. iPSCs were infected with a lentivirus expressing a miRNA at a MOI of 50. The cells were then cultured in differentiation medium with Activin A (20 ng/mL) for 6 days and with FGF-2 (50 ng/mL) for 5 days. mRNA levels of Oct4 (A), Sox2 (B), cMyc (C) and Klf (D) in undifferentiated iPSCs and differentiated cells with miRNA overexpression were determined by qRT-PCR and normalized to iPSCs. BC: blank control; VC: vector control. *P< 0.05 vs. all other groups (n=3).

A

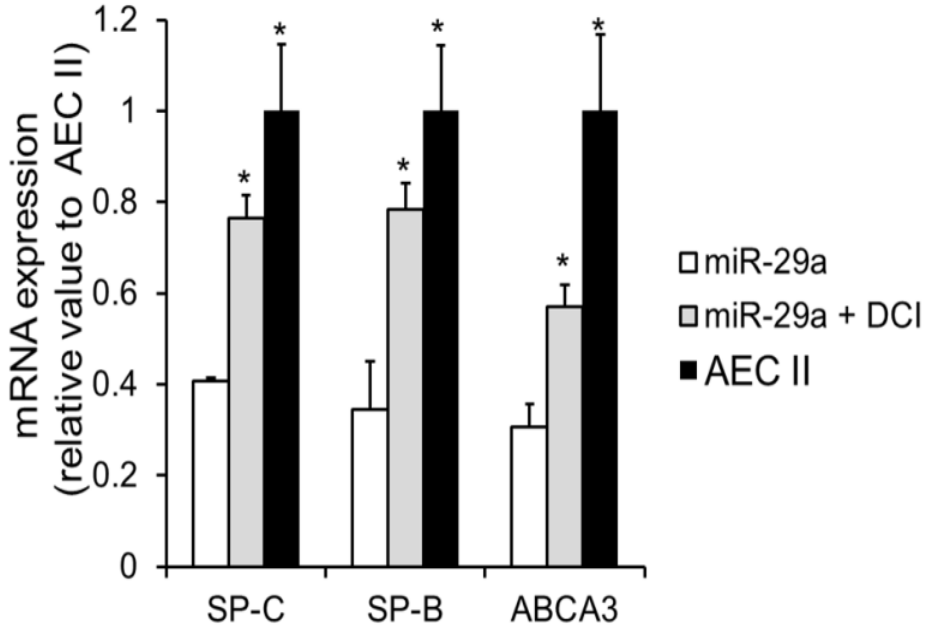
mRNA expression
(relative value to AEC II)
1.2
1
0.8
0.6
0.4
0.2
0
SP-C
SP-B
ABCA3
miR-29a
miR-29a + DCI
AEC II

B

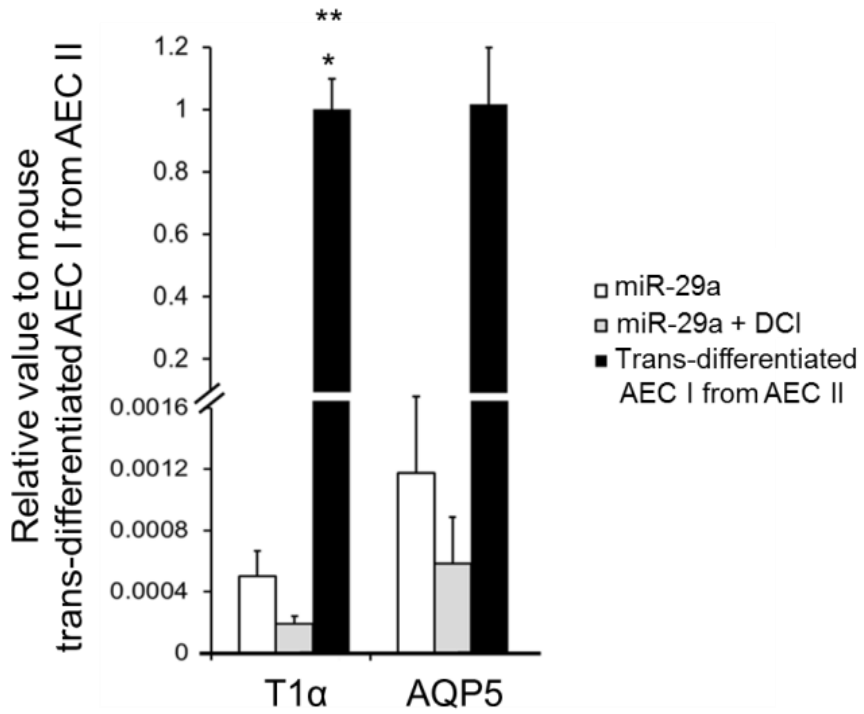
Relative value to mouse
trans-differentiated AEC I from AEC II
1.2
1
0.8
0.6
0.4
0.2
0.0016
0.0012
0.0008
0.0004
0
T1α
AQP5
miR-29a
miR-29a + DCI
Trans-differentiated
AEC I from AEC II

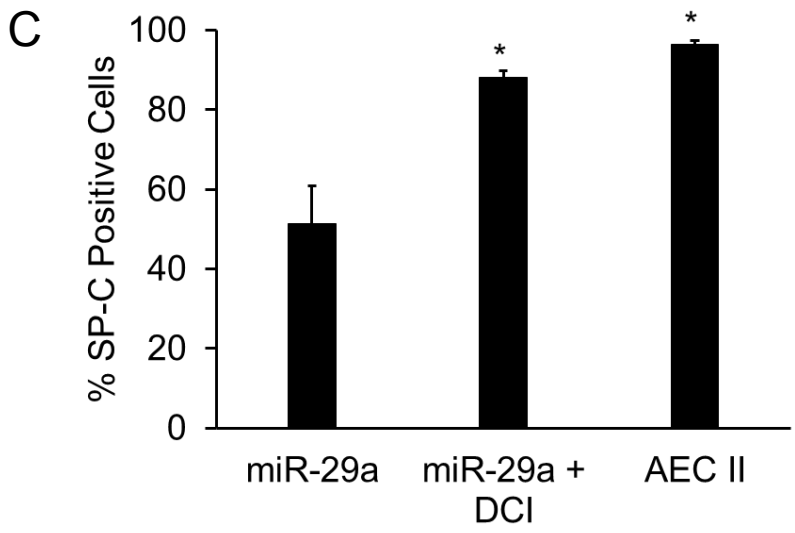

Fig.14: Effect of DCI on iPSC differentiation. iPSCs were infected with a lentivirus expressing miR-29a at a MOI of 50. The cells were then cultured in differentiation medium with or without dexamethasone (10 nM), 8-bromoadenosine 3, 5- cyclic monophosphate (cAMP, 0.1 mM), and isobutylmethylxanthine (IBMX, 0.1 mM) (DCI) with Activin A (20 ng/mL) for 6 days and with FGF-2 (50 ng/mL) for 5 days. mRNA levels of AEC II markers, SP-C, SP-B and ABCA3 (A) and AEC I markers, T1α and AQP5 (B) were determined by qRT-PCR and normalized to 18S rRNA. SP-C-positive cells were determined by immunostaining (C). Freshly isolated AEC II from mice and AEC I trans-differentiated from mouse AEC II were used as positive controls. *P< 0.05 vs. miR-29a (n=3).

v. ERK and JNK signaling pathways are up-regulated by miR-29a and let-7b

To decipher how miR-22, miR-29a and let-7b regulate the differentiation of iPSCs into AEC II, we used the web-based software PicTar to predict the pathways that miR-22, miR-29a and let-7b regulate. ERK, JNK and Wnt/β-catenin are the predicted pathways for the action of miR-22, miR-29a and let-7b (Table 5). To experimentally verify the prediction, we utilized the pathway luciferase reporter assay, in which a pathway-specific transcription factor-responsive element was

fused to the firefly luciferase reporter gene. We found that both miR-29a and let-7b up-regulated the ERK and JNK luciferase reporter activities, but had no effect on Wnt/β-catenin luciferase reporter activity (Fig 15). miR-22 also increased JNK reporter activity, but not those of ERK and Wnt/β-catenin pathways.

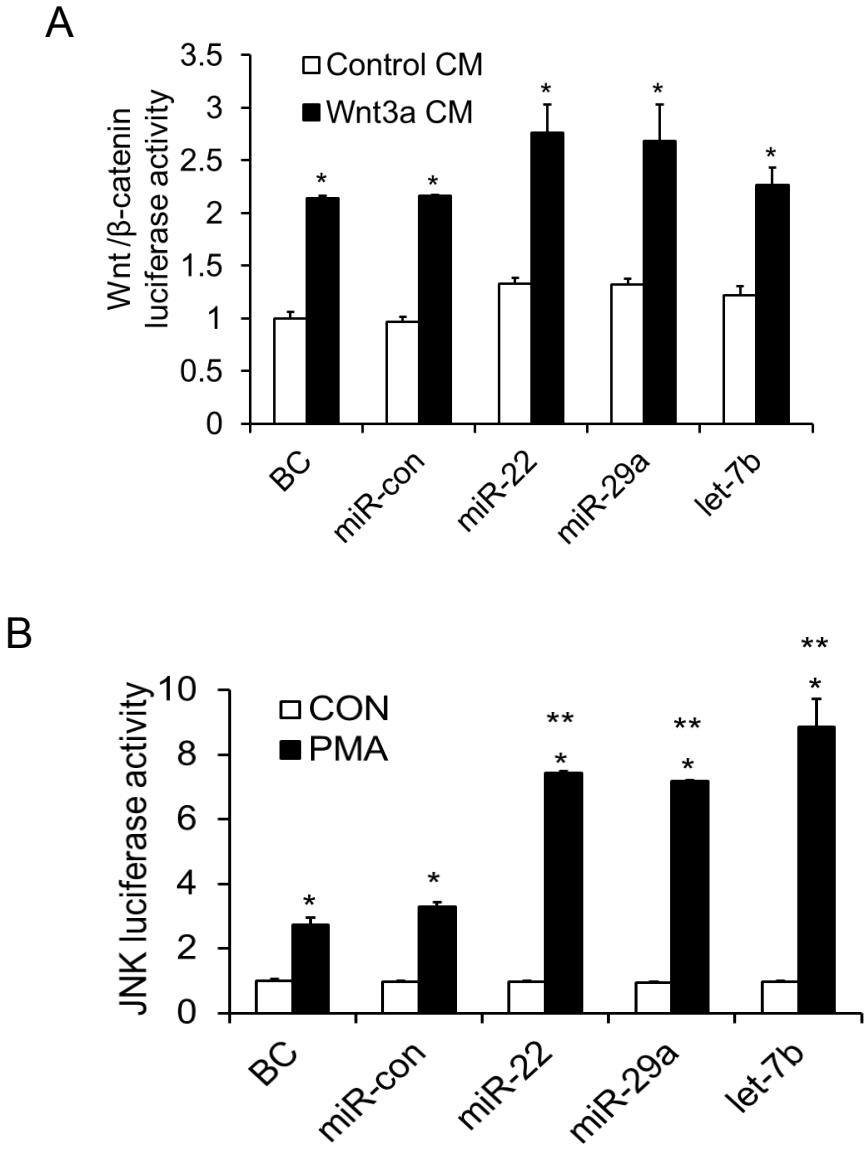

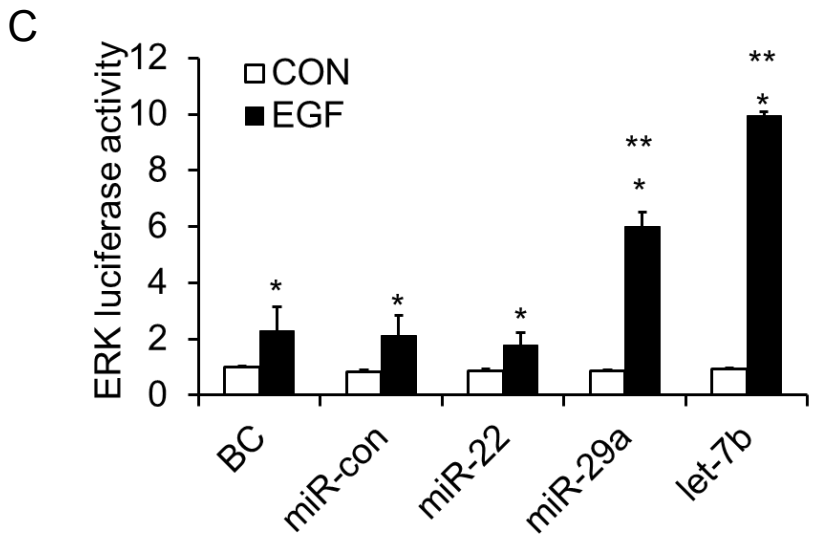

Fig. 15: miR-29a and let-7b up-regulate ERK and JNK signaling pathways but not the Wnt/β-catenin signaling pathway. iPSCs were cultured in differentiation medium with Activin A (20 ng/mL) for 6 days and with FGF-2 (50 ng/mL) for 5 days. The cells were then transfected with Wnt/β-catenin luciferase-reporter construct (A), JNK luciferase-reporter construct (B) or ERK luciferase-reporter construct (C) along with miR-22, miR-29a or let-7b for 24 h. After 18 h stimulation with Wnt 3a conditioned medium (50% v/v), PMA (1 ng/well) or EGF (10 ng/well), the dual luciferase activities were measured. Data was expressed as a ratio of firefly luciferase activity to *Renilla* luciferase activity. All experiments were carried out in triplicate. *P<0.05 vs non-stimulation. **P<0.05 vs miR-con with stimulation (n=3).

vi. DUSP2 is repressed by miR-29a

The bioinformatics tool, Targetscan, predicts many target genes of miR-29a and let-7b involved in the ERK and JNK pathways (Table 5). Since they up-regulate ERK and JNK pathways, miR-29a and let-7b must target negative regulators of these pathways. Both Akt and DUSP are known to negatively regulate MAPK pathways (103, 104). Thus, Akt3 and DUSP2,

and Akt2 and DUSP9 are the possible targets of miR-29a and let-7b for regulating MAPK pathways, respectively.

To verify these predications, iPSC-derived AEC II were co-transfected with the 3'-UTR firefly luciferase reporter vector of DUSP2, Akt3, DUSP9 or Akt2 and miR-29a or let-7b or the control vector, miR-Con. We found that miR-29a and let-7b repressed the activities of DUSP2 and DUSP9 3'-UTR reporters, respectively, but had no effects on those of Akt3 and Akt2 (Fig16A, B). When we mutated the miRNA binding site in DUSP2 and DUSP9, miR-29a or let-7b-mediated inhibition of the reporter activities were abolished.

To further confirm the results, iPSC-derived AEC II were infected with a lentivirus expressing miR-29a or let-7b. miR-29a reduced the protein levels of DUSP2, but not DUSP9 (Fig 16C). However, let-7b had no effects on DUSP2 and DUSP9 protein levels. We thus concluded that miR-29a activated ERK and JNK pathways through repressing DUSP2 (Fig 16D).

Table 5 Predicted pathways and genes for miR-22, miR29a and let-7b

miRNA	KEGG Pathway	Gene Name	Found Genes
miR22	MAPK signaling pathway	EVI1, TGFBR1, MAP2K4, TP53, SRF, ACVR1B, MAPK14, MAX, ARRB1, AKT3	10
miR22	Wnt signaling pathway	TP53, FRAT2, NFAT5, EP300, SMAD4	5
miR29a	Wnt signaling pathway	DAAM1, NFAT5, NFATC4, GSK3B, CCND2, PPP2CA, CAMK2G, CTNNBIP1	13
miR29a	MAPK signaling pathway	MAP4K4, FOS, TNFRSF1A, PDGFB, CACNG4, DUSP2, MAP2K4, MAP2K6, NFATC4, CDC42, RPS6KA3, GNG12, PDGFRB, AKT3	14
let-7b	MAPK signaling pathway	MAP4K3, MAP4K4, DUSP4, TGFBR1, MAP3K1, PDGFB, MAP3K7IP2, MAPK11, DUSP9, FASLG, CACNG4, CACNA1D, DUSP16, MAP3K3, PAK1, TP53, FGF11, AKT2, ACVR1B, PLA2G3, NLK, DUSP1, FGF5, ACVR1C, FAS, RPS6KA3, CASP3	27
let-7b	Wnt signaling pathway	NLK, CCND2, SENP2, WNT1, MAPK9, CCND1	12

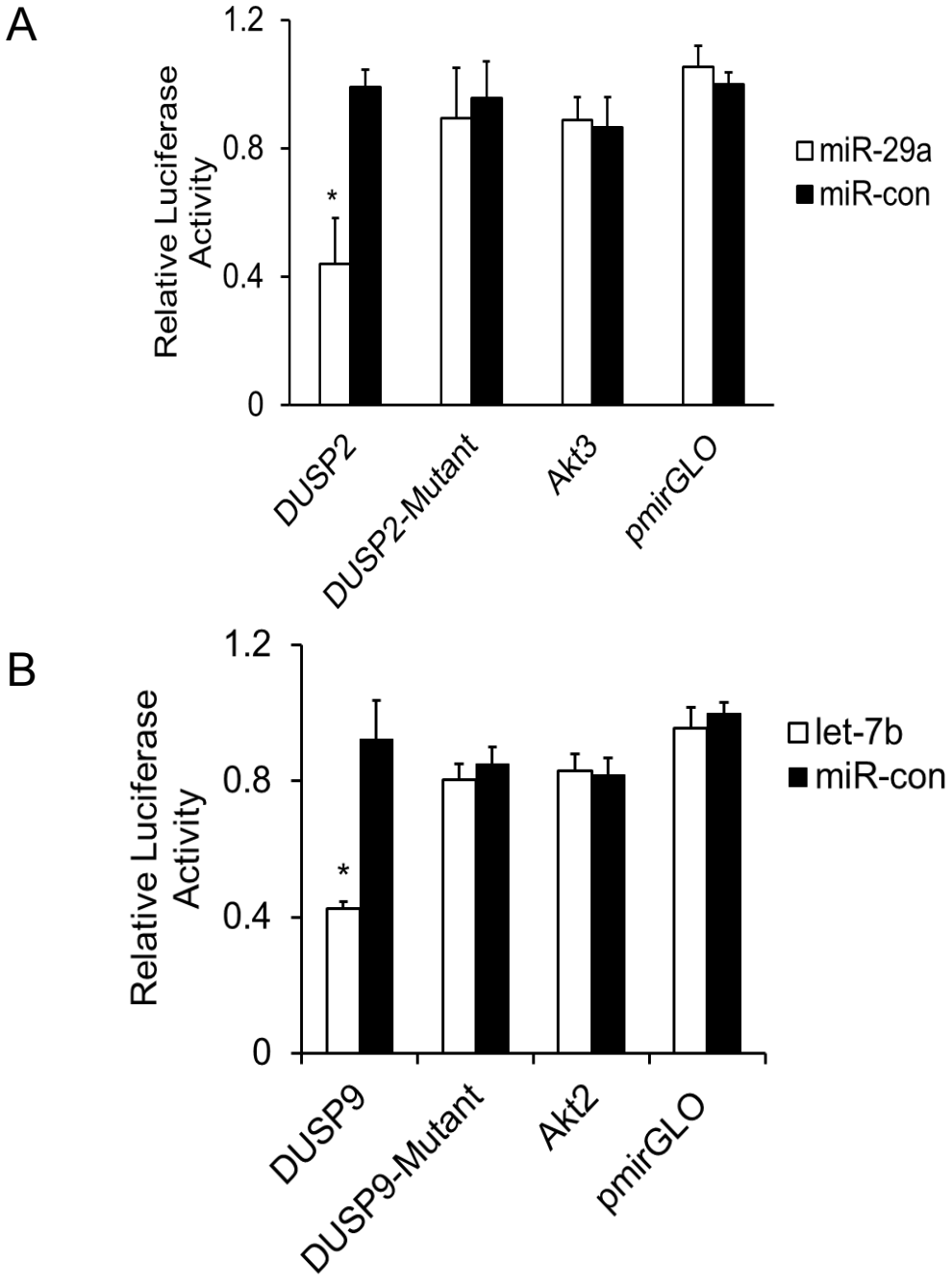
A
1.2
0.8
0.4
0
Relative Luciferase Activity
*
miR-29a
miR-con
DUSP2
DUSP2-Mutant
Akt3
pmirGLO
B
1.2
0.8
0.4
0
Relative Luciferase Activity
*
let-7b
miR-con
DUSP9
DUSP9-Mutant
Akt2
pmirGLO

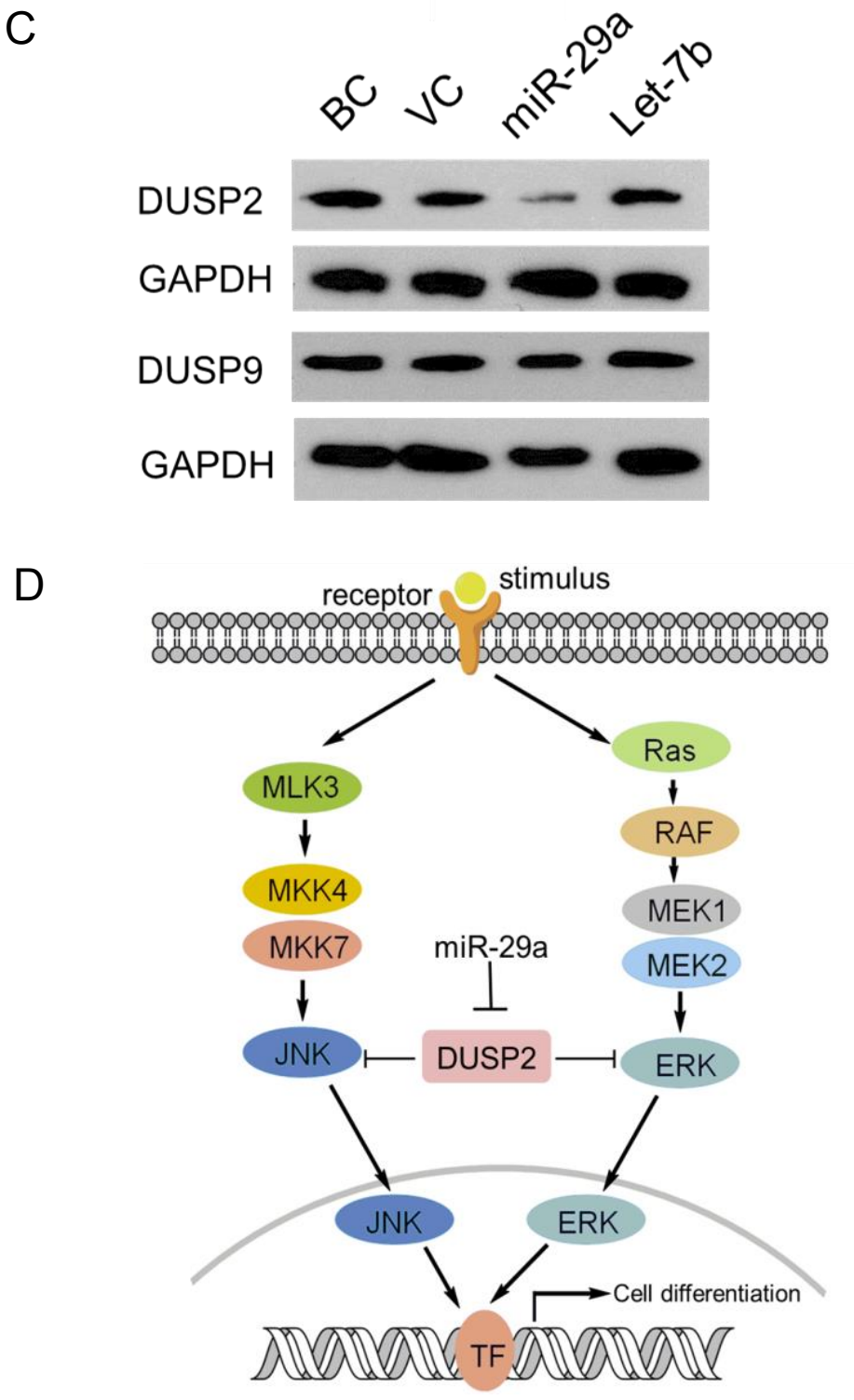

Fig. 16: DUSP2 is a target of miR-29a. HEK 293T cells were transfected with 3'-UTR luciferase reporter or its mutant for DUSP2 or Akt3 with miR-29a (A) or 3'-UTR luciferase

reporter or its mutant for DUSP9 or Akt2 with let-7b (B) for 24 h. Dual luciferase activities were measured. Firefly luciferase activity was normalized to *Renilla* luciferase activity. Data were expressed as mean ± SE. *P<0.05 vs. miR-Con (n=3). (C) Western blot analysis for DUSP2 and DUSP9. iPSCs were infected without lentivirus (BC) or with a lentivirus expressing miR-29a, let-7b or miR-con (VC) for 48 h and DUSP2 and DUSP9 protein levels were determined by Western blot. (D) A proposed mechanism of miR-29a-mediated activation of ERK and JNK pathways in iPSCs through repression of DUSP2.

vii. iPSC – derived AEC II cells are functional

AEC II proliferate and differentiate into AEC I when AEC I are damaged (102). We investigated whether the iPSC derived ACE II (iPSC-AEC II) were able to proliferate *in vitro* by BrdU assay. iPSC-AEC II did proliferate although less compared to mouse primary AEC II (Figure 17A).

When they were cultured on plastic dishes for 5-7 days, AEC II trans-differentiate into AEC I (102). To determine whether iPSC-AEC II can trans-differentiate into AEC I, iPSC-AEC II or AEC II isolated from mice were cultured in DMEM with 10% FBS on plastic dishes for 7 days and AEC I and AEC II markers were determined by qRT-PCR. The trans-differentiated AEC I from iPSC-AEC II expressed a similar level of the AEC I markers, AQP5 and T1α as the trans-differentiated AEC I from primary AEC II and expressed little of the AEC II markers, ABCA3, SP-B and SP-C (Figure 17B). While 78% of iPSC-AEC II expressed SP-C, 75% of the trans-differentiated AEC I from iPSC-AEC II expressed T1α (Figure 17C-F).

One of the major functions of AEC II is to secrete lung surfactant (105). Lung surfactant secretagogues (ATP, PMA and terbutaline) stimulated the secretion of surfactant lipids by 3.9-fold from iPSC-AEC II in comparsion with 5.5-fold from primary AEC II (Figure 18A). These lung surfactant secretagogues also increased secretion of the surfactant protein SP-C in both

iPSC-AEC II and primary AEC II (Fig 18B). These results suggest that iPSC-AEC II behave similarly to isolated mouse AEC II *in vitro*.

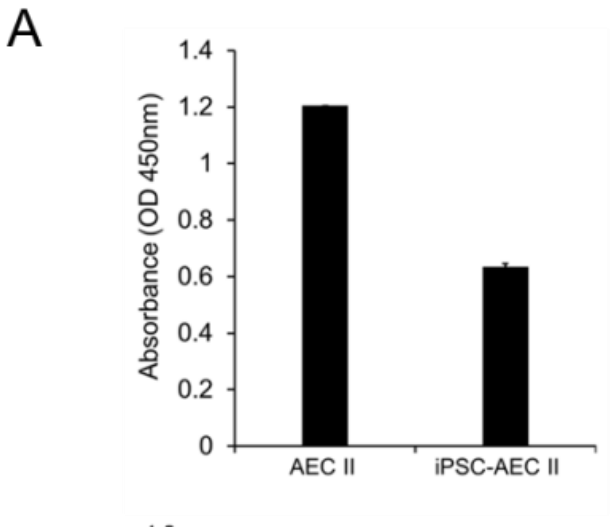

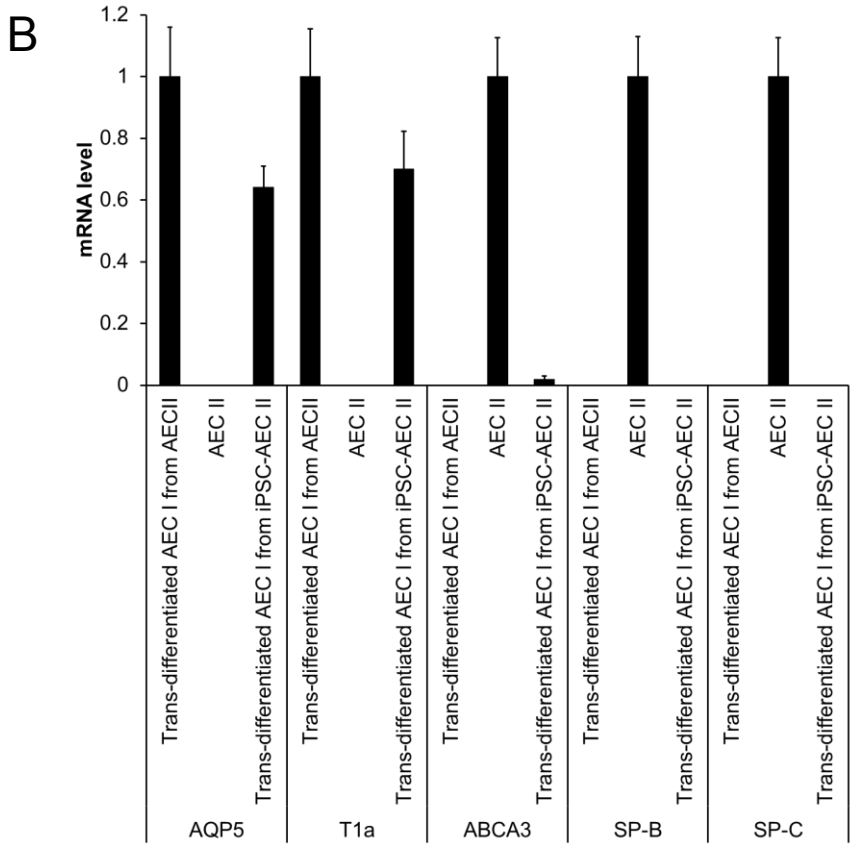

C

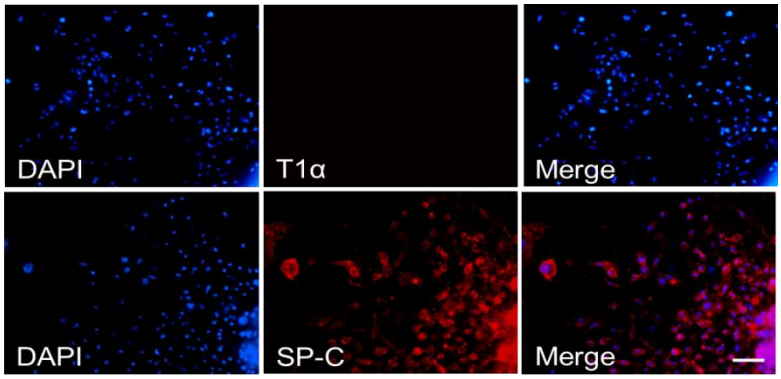
DAPI
T1α
Merge
DAPI
SP-C
Merge

D

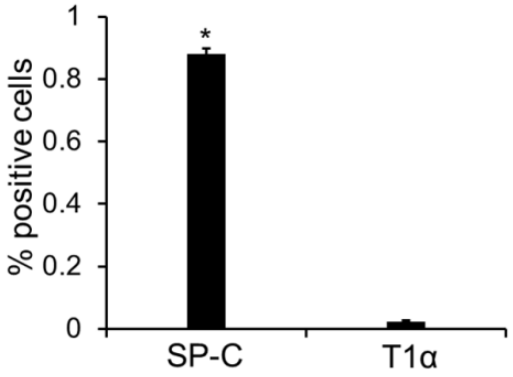
% positive cells
1
0.8
0.6
0.4
0.2
0
*
SP-C
T1α

E

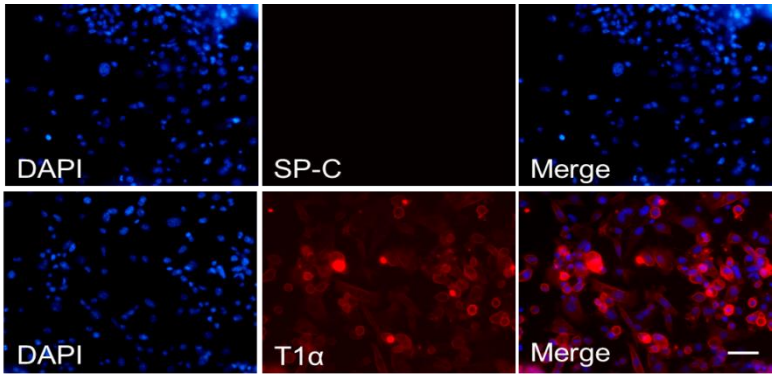
DAPI
SP-C
Merge
DAPI
T1α
Merge

F

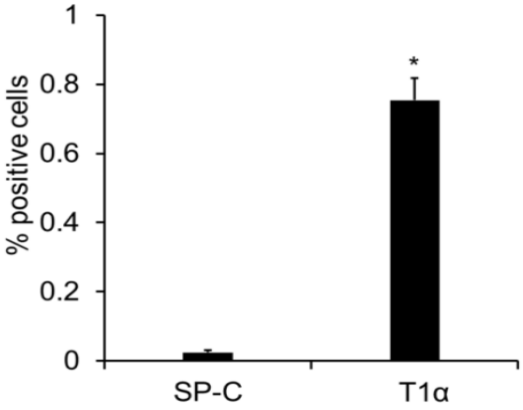
% positive cells
1
0.8
0.6
0.4
0.2
0
*
SP-C
T1α

Fig. 17: iPSC- AEC II can proliferate and transdifferentiate into AEC I. iPSCs were infected with a lentivirus expressing miR-29a at a MOI of 50. The cells were then cultured in differentiation medium in the presence of DCI with Activin A (20 ng/mL) for 6 days and with FGF-2 (50 ng/mL) for 5 days and designated as iPSC-AEC II. (A) Cell proliferation as determined by BrdU labeling in freshly isolated AEC II and iPSC-AEC II. (B-F) Freshly isolated AEC II and iPSC-AEC II were cultured on plastic plates in DMEM for 7 days. mRNA levels of AEC I and AEC II cell markers were determined by qRT-PCR and normalized to 18S rRNA (B). SP-C and T1α-positive cells were determined by immunostaining before (C, D) or after 7-day culture (E, F). *P<0.05 vs the other (n=3). Scale bar: 50μm.

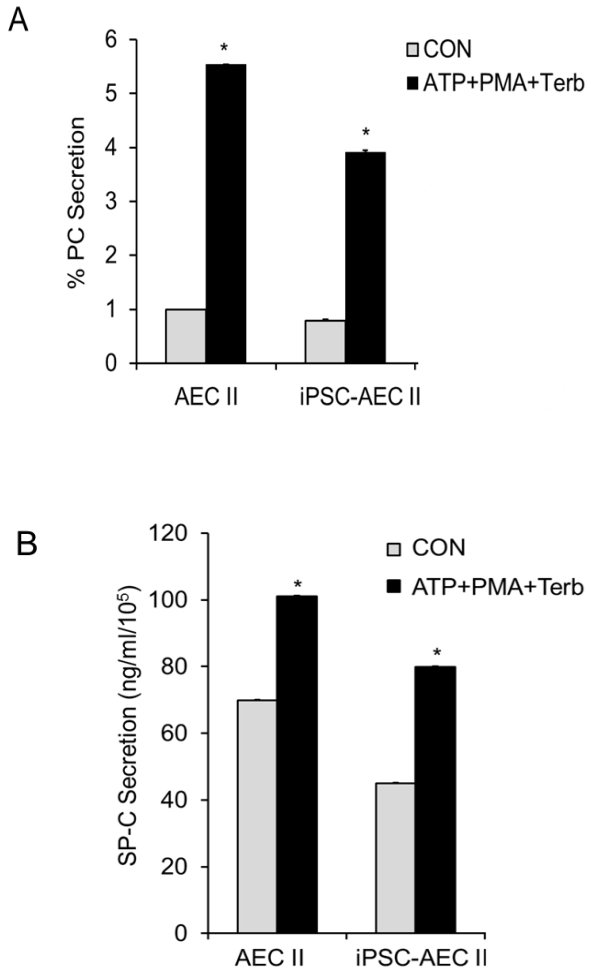

Fig. 18: iPSC-AEC II can secrete lung surfactant lipid and protein. iPSCs were infected with a lentivirus expressing miR-29a at a MOI of 50. The cells were then cultured in differentiation medium in the presence of DCI with Activin A (20 ng/mL) for 6 days and with FGF-2 (50 ng/mL) for 5 days and designated as iPSC-AEC II. Freshly isolated AEC II and iPSC- AEC II were cultured overnight and stimulated for 2 hours with lung surfactant secretagogues (100 µM ATP, 0.1 µM PMA and 10 µM terbutaline, ATP+PMA+Terb). Phosphatidylcholine (A) and SP-C (B) secretion were measured. Results are shown as mean ± SE. *P<0.05 vs. control (n=3).

IV-2-2: MSCs

i. Characterization of mouse bone marrow (BM)-MSCs

The cell surface markers of P2 BM-MSCs were determined by FACS. More than 95% of the MSC population expressed the stem-cell antigen 1 (Sca-1), tetraspanin proteins (CD9 and CD81) and β_1-integrin (CD29) (Fig. 19). And, 62% of the MSC population expressed endoglin receptor (CD44) (Fig. 19). Additionally, these cells lacked expression (<1% positive) of the leukocyte common antigen CD45 and macrophage-1 antigen CD11b (Fig. 19).

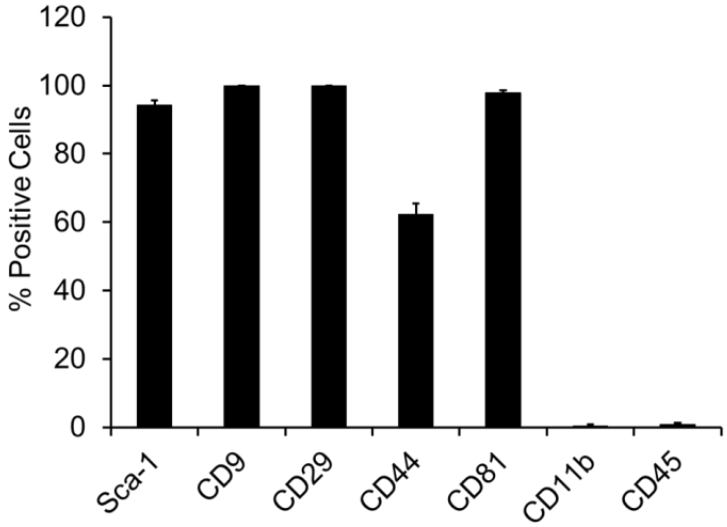

Fig. 19: Flow cytometry analysis of cell surface markers of mouse MSCs. MSCs were isolated from bone marrow of C57BL/6 mice. P2 MSCs were stained with monoclonal antibodies conjugated to FITC, PE, or PE-Cy5 against Sca-1, CD9, CD29, CD44, CD81, CD11b, or CD45. Results are shown as mean ± SE, n=3.

ii. Differentiation of MSCs to AEC II

To find the proper conditions to differentiate MSCs into AEC II, we used different matrices to drive the differentiation, including gelatin and collagen IV. We found that collagen IV but not gelatin can drive MSC differentiation into AEC II (data not shown).

P2 MSCs were seeded on mouse collagen IV-coated 6-well plates overnight. On the second day, the medium was switched to the differentiation medium, small airway growth medium (SAGM). The cells were cultured for 11 days. In the parallel group, MSCs were cultured in MSC culture medium (Control) for 11 days. We observed that approximately 25% of MSCs differentiated into AEC II based on immunostaining for the AEC II marker SP-C (Fig. 20). The result indicated that SAGM medium could drive MSCs to differentiate into AEC II, but the efficiency was low.

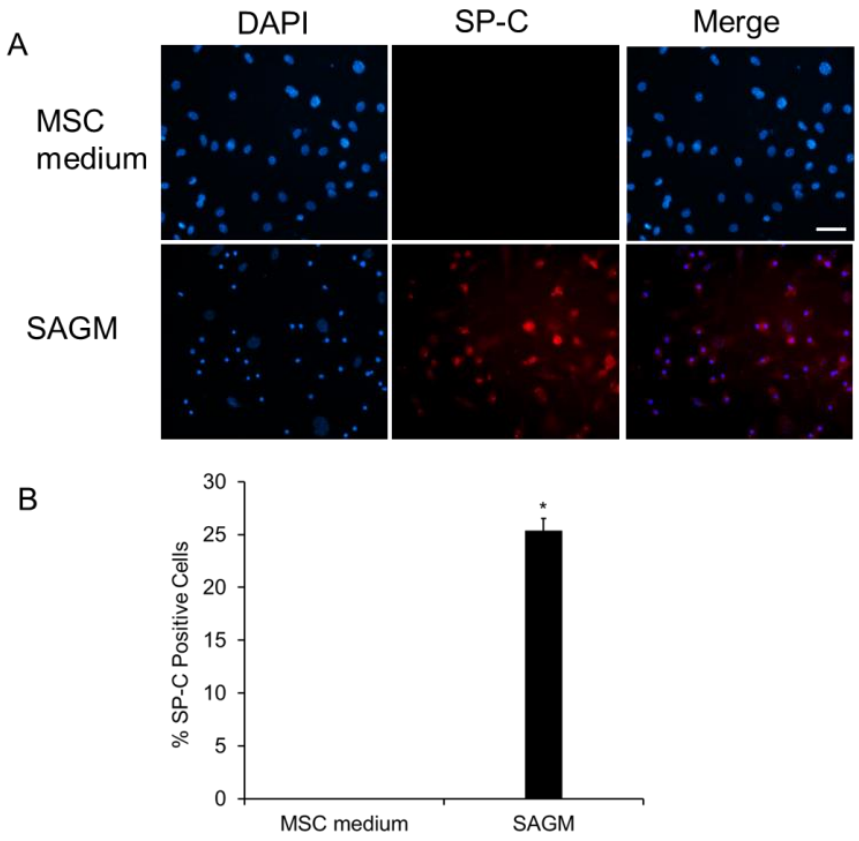

Fig. 20: SP-C protein expression in differentiated MSCs. P2 MSCs were cultured in MSC medium or SAGM for 11 days. Cells were fixed and stained for SP-C (red). DAPI staining was performed for counting cells. (A) Fluorescent images. magnification: 20X. (B) Quantitation of SP-C-positive cells. Results are shown as means ± SE. *P< 0.05 vs. MSC medium (n=3). Scale bar: 50µm

iii. miR-29a enhances differentiation of MSCs into AEC II

We have previously identified several miRNAs that are enriched in AEC II and highly expressed in adult lungs, and have shown that some of those miRNAs can promote the differentiation of iPSCs into AEC II. We next asked whether those miRNAs could enhance the differentiation of MSCs into AEC II. To test the possibility, we infected MSCs with miR-22, miR-23, miR29a, and let-7b lentivirus or control virus (VC) at a MOI of 50 and cultured them on collagen IV-coated plates in the differentiation medium for 11 days. miR-210 was used as a

negative control. The parallel blank control group (BC) was MSCs without virus infection. miR-29a markedly augmented mRNA expression of the AEC II markers, SP-C, SP-B, and ABCA3 (Fig. 21A-C). Since AEC II can spontaneously differentiate into AEC I (106), we assessed the expression of AEC I markers T1α and aquaporin-5 (AQP5) by qRT–PCR in the differentiated cells. miR-29a significantly decreased the mRNA expression level of AEC I markers, T1α and AQP5 (Fig. 21D, E).

In addition, we monitored the protein expression level of the AEC II marker, SP-C, by immunostaining in the differentiated cells. We found that approximately 55% of the miR-29a-overexpressed MSCs were SP-C-positive compared to 25% of the VC-treated MSCs. (Fig. 22 A, B). The typical characteristic organelle of AECII, lamellar bodies, were found in MSCs differentiated in the SAGM, and miR-29a increased the number of lamellar bodies (Fig. 22 C). Collectively, these results suggest that miR-29a can efficiently promotes the differentiation of MSCs into AEC II.

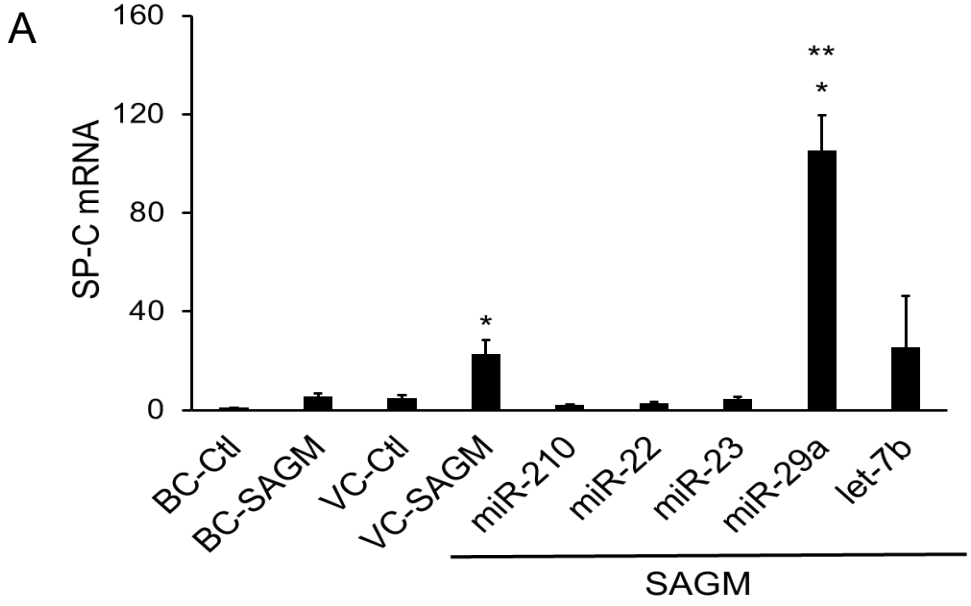

B

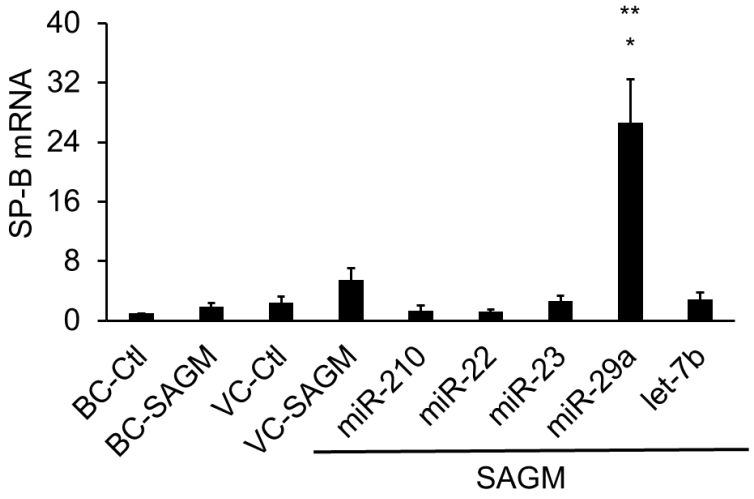
SP-B mRNA
40
32
24
16
8
0
**
*
BC-Ctl
BC-SAGM
VC-Ctl
VC-SAGM
miR-210
miR-22
miR-23
miR-29a
let-7b
SAGM

C

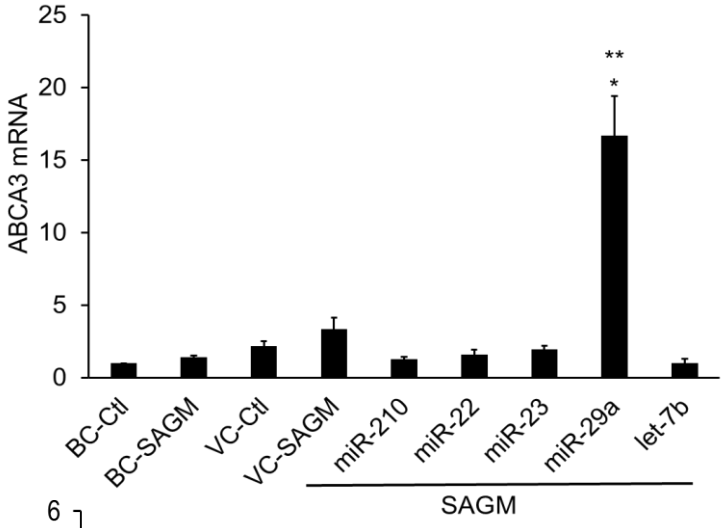
ABCA3 mRNA
25
20
15
10
5
0
**
*
BC-Ctl
BC-SAGM
VC-Ctl
VC-SAGM
miR-210
miR-22
miR-23
miR-29a
let-7b
SAGM

D

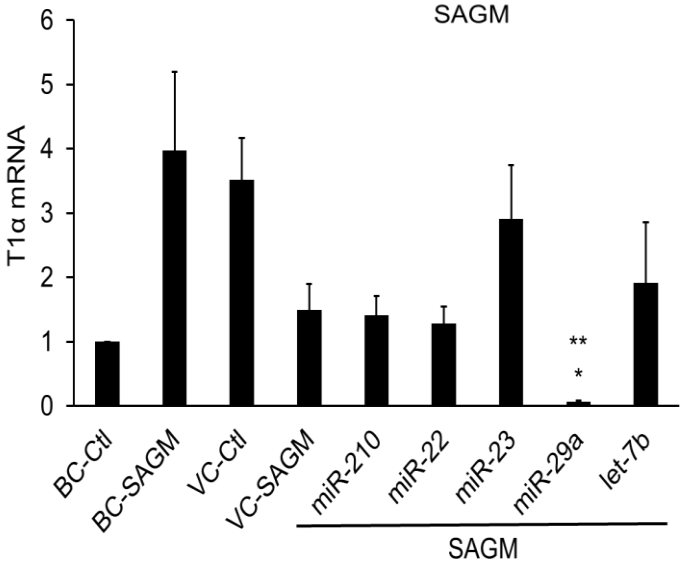
T1α mRNA
6
5
4
3
2
1
0
**
*
BC-Ctl
BC-SAGM
VC-Ctl
VC-SAGM
miR-210
miR-22
miR-23
miR-29a
let-7b
SAGM

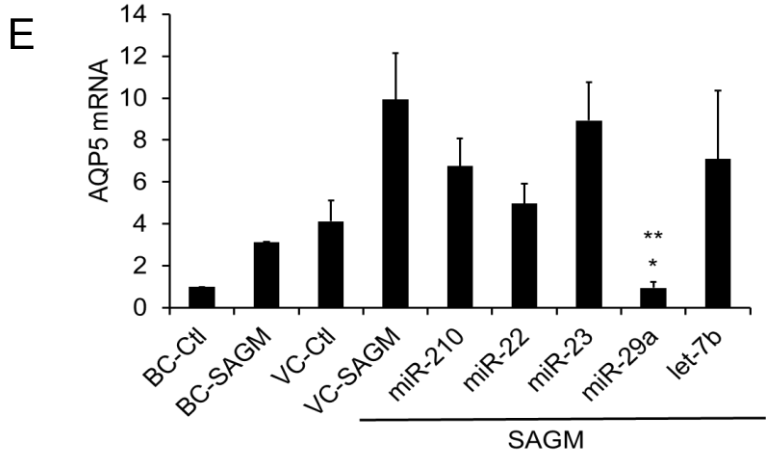

Fig. 21: mRNA levels of AEC II and AEC I cell markers in differentiated MSCs with miRNA-overexpression. P2 MSCs were infected with a lentivirus expressing a miRNA or a virus control (VC) at a MOI of 50. The cells were then cultured in SAGM medium for 11 days. Blank control (BC) and virus control (VC) cells were also cultured in MSC complete culture media as a negative control (Ctl). mRNA levels of SP-C (A), SP-B (B), ABCA3 (C), T1α (D) and AQP5 (E) were determined by q-RT-PCR and normalized to 18S rRNA. Results are shown as mean ± SE. *P<0.05 vs BC-SAGM. **P<0.05 vs VC-SAGM (n=3).

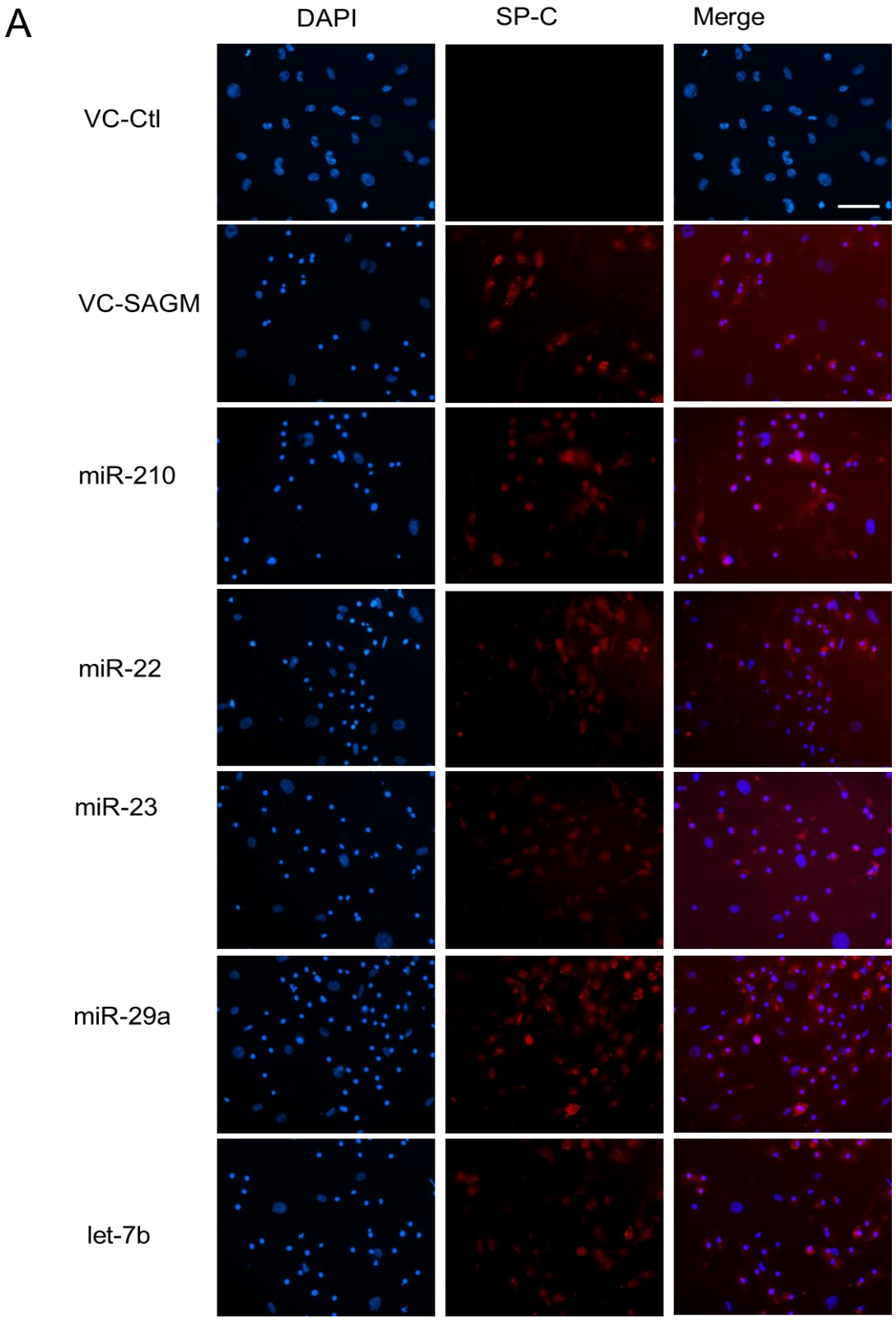
A
DAPI
SP-C
Merge
VC-Ctl
VC-SAGM
miR-210
miR-22
miR-23
miR-29a
let-7b

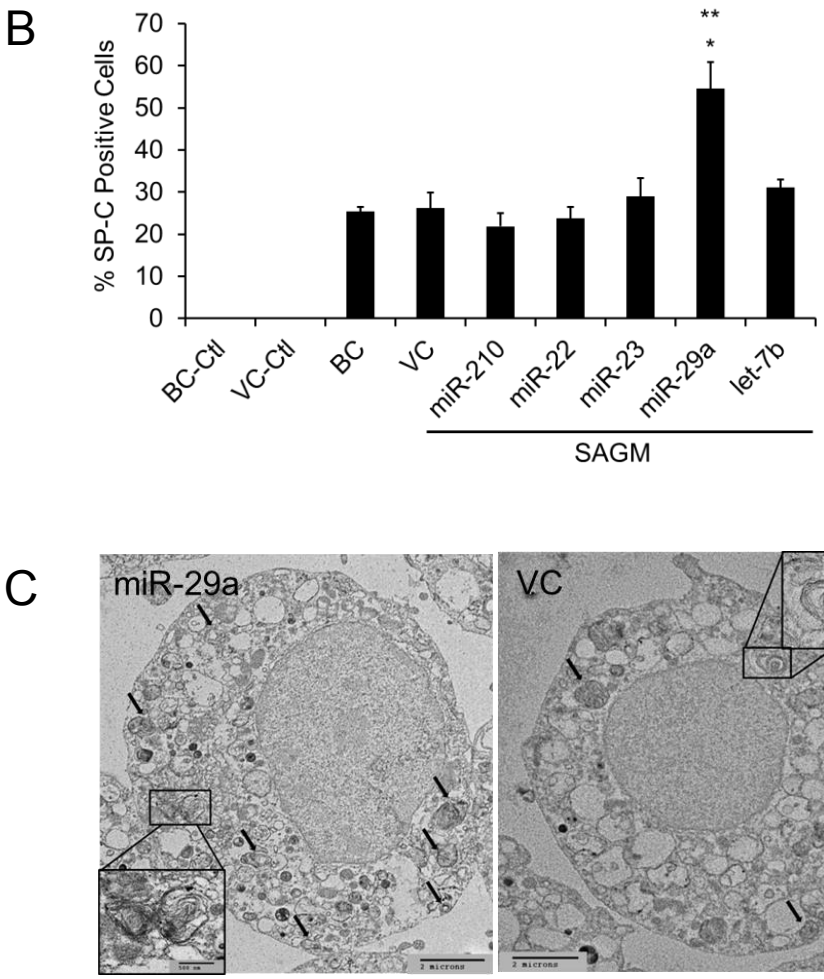

Fig. 22: SP-C protein expression and lamellar bodies in differentiated MSCs with miRNA-overexpression. P2 MSCs were infected with a lentivirus expressing a miRNA or with a virus control (VC) at a MOI of 50. The cells were then cultured in SAGM medium for 11 days. Blank control (BC) and VC control cells were also cultured in MSC complete culture media as a negative control (Ctl). SP-C protein expression was determined by immunostaining. (A) Fluorescent images. Magnification: 20X. Scale bar: 50μm (B) Quantitation of SP-C-positive cells. Results are shown as means ± SE. *P<0.05 vs BC-SAGM. **P<0.05 vs VC-SAGM (n=3). (C) Electron microscopy images of lamellar bodies (LB) in the differentiated MSC overexpressed with miR-29a and miR-con (VC) cultured in SAGM. Arrows: LB. Scale bar: 2 μm.

iv. DCI promotes miR-29a-mediated differentiation of MSCs into AEC II

Since dexamethasone (10 nM), 8-bromoadenosine 3,5- cyclic monophosphate (cAMP, 0.1 mM), and isobutylmethylxanthine (IBMX, 0.1 mM) (DCI) can induce the maturation of AEC II (102), we next examined the effect of DCI on miR-29a-mediated differentiation of MSCs into AEC II. The treatment of miR-29a and DCI strongly induced the mRNA expression levels of the AEC II cell markers (SP-C, SP-B and ABCA3) compared to miR-29a alone (Fig. 23A). The treatment with DCI appears to decrease the mRNA expression levels of AEC I markers, T1α and AQP5 although AEC I marker expression in these cells was negligable compared to AEC I (Fig. 23B).

Further characterization was done by immunostaining of SP-C and T1α. On day 11 of the differentiation, 90 ± 0.19% of the cells were positive for SP-C in the differentiated cells with miR-29a overexpression together with DCI compared to 54 ± 6.2 % in the absence of DCI Only 3 ± 0.3 % of the cells were positive for T1α (Fig. 23C, D). The differentiated cells mediated by miR-29a and DCI lost all the MSCs surface markers (2.4% Sca-1,2.1% CD9, 1.3% CD29, 1.5%, CD44, 1.4% CD81, 0.47% CD11b, 0.83% CD45). Taken together, these results suggest that DCI promotes miR-29a-mediated differentiation of MSCs into AEC II.

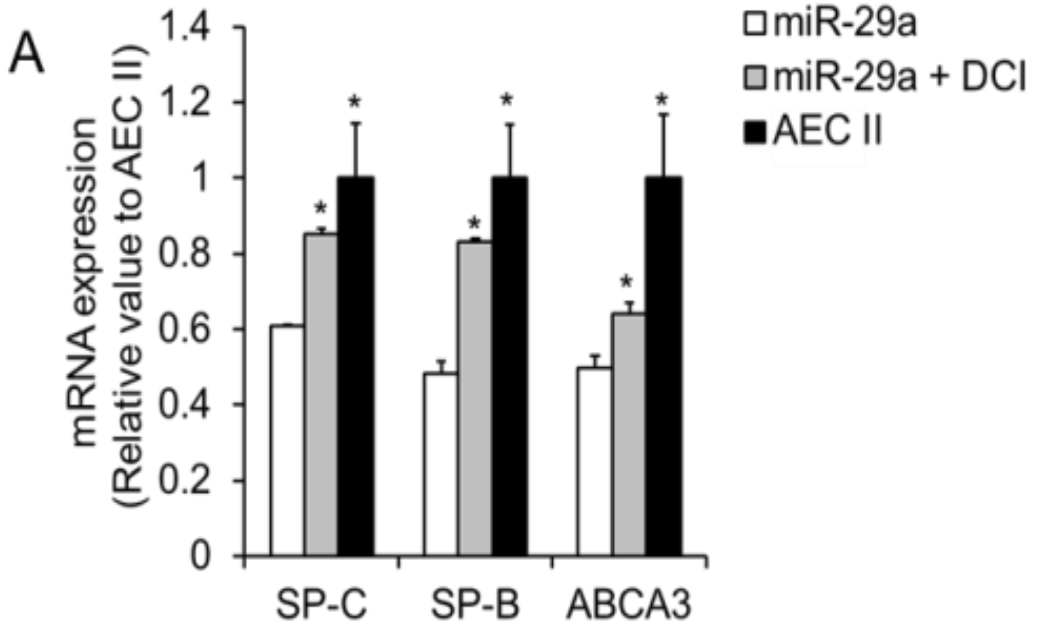
A
mRNA expression
(Relative value to AEC II)
1.4
1.2
1
0.8
0.6
0.4
0.2
0
SP-C
SP-B
ABCA3
miR-29a
miR-29a + DCI
AEC II

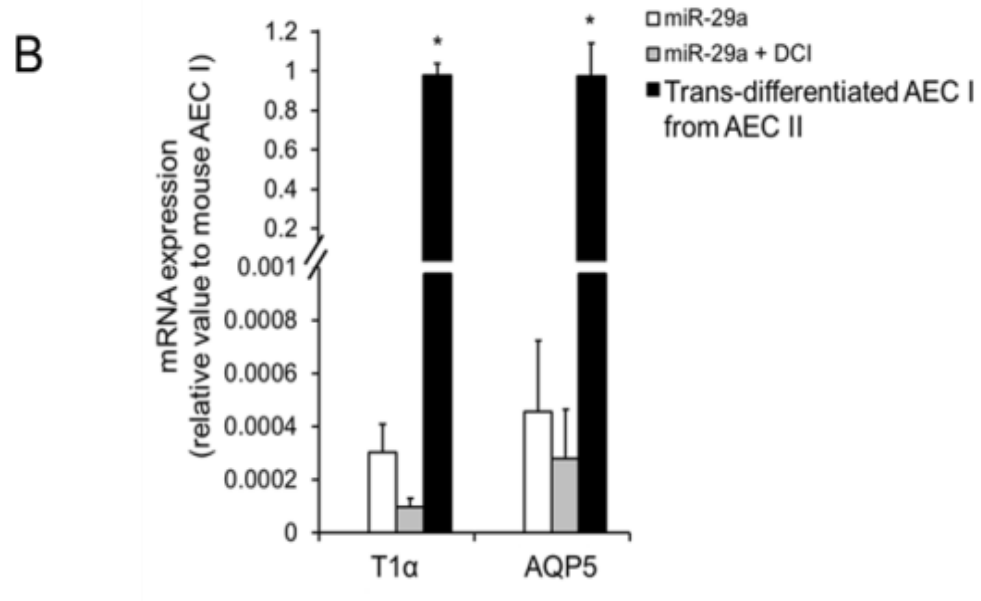
B
mRNA expression
(relative value to mouse AEC I)
1.2
1
0.8
0.6
0.4
0.2
0.001
0.0008
0.0006
0.0004
0.0002
0
T1α
AQP5
miR-29a
miR-29a + DCI
Trans-differentiated AEC I
from AEC II

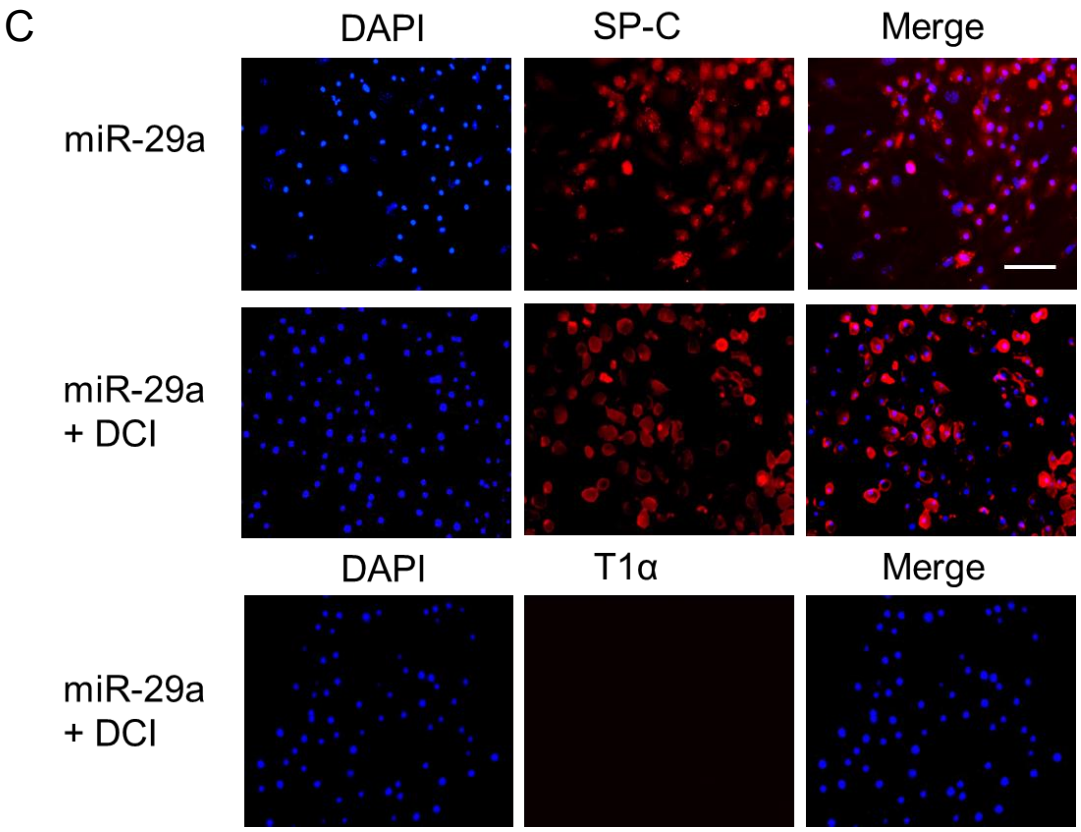
C
DAPI
SP-C
Merge
miR-29a
miR-29a
+ DCI
DAPI
T1α
Merge
miR-29a
+ DCI

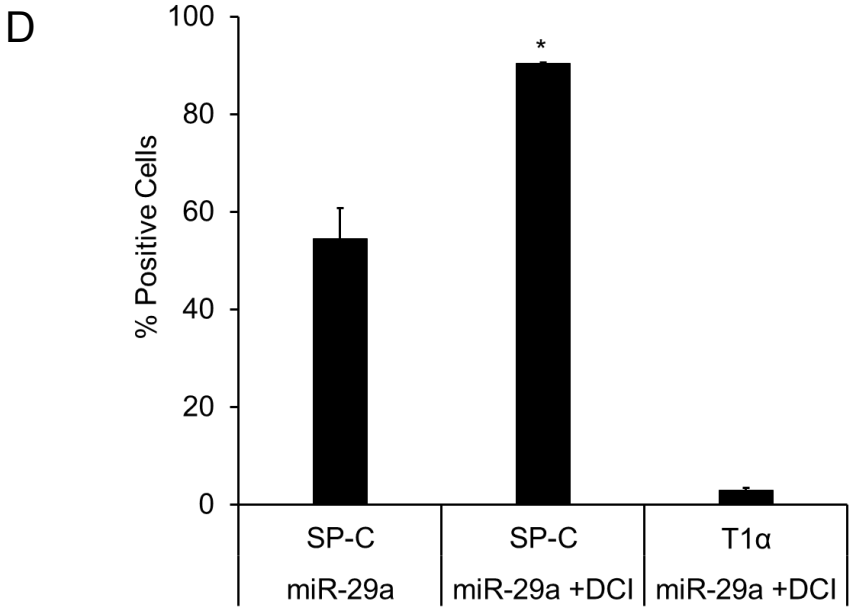
D
100
80
60
40
20
0
% Positive Cells
*
SP-C
miR-29a
SP-C
miR-29a +DCI
T1α
miR-29a +DCI

Fig. 23: Effects of DCI on miR-29a-mediated differentiation of MSCs into AEC II. miR-29a overexpressed MSCs were cultured in SAGM with or without DCI for 11 days. The mRNA expression of SP-C, SP-B, and ABCA3 (A), T1α and AQP5 (B) was measured by qRT-PCR using 18S rRNA as an endogenous control. Primary mouse AEC II was used as positive controls. (C) Immunostaining of the differentiated cells using anti-SP-C and anti-T1α antibodies. Scale bar: 50μm (D) Quantitation of SP-C-positive cells. Results are shown as means ± SE. *P<0.05 vs miR-29a (n=3).

v. DUSP2 is the target of miR-29a in MSCs

DUSP2 has been reported to have an important role in differentiation. Recently, we have demonstrated that DUSP2 is the target of miR-29a in iPSCs. To examine whether DUSP2 is also target of miR-29a in MSCs, we infected MSCs with miR-29a lentivirus and performed Western blotting to determine the DUSP2 protein levels. A decreased protein level of DUSP2 was found in the MSCs infected with a miR-29a lentivirus compared to the cells infected with the control virus or blank control without virus infection. Let-7b had no effects on DUSP2 protein expression (Fig. 24).

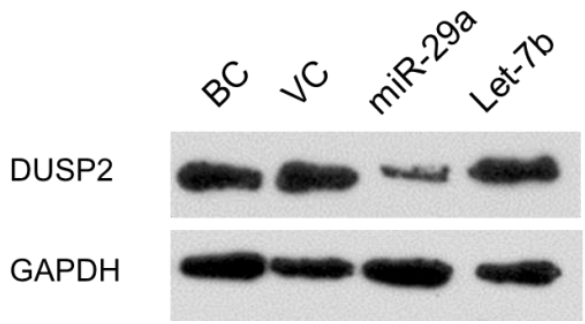

Fig. 24: miR-29a reduces DUSP2 level in MSCs. MSCs were infected with a lentivirus expressing miR-29a, let-7b or a virus control (VC). Blank control (BC) is the MSC without infection. DUSP2 protein levels were analyzed by Western blotting using GAPDH as a loading control.

vi. miR-29a enhances MAPK signaling pathway

DUSP2 is known to inhibit the MAPK signaling pathway by dephosphorylation of threonine and tyrosine residues on MAPKs (103). Therefore, we next investigated whether miR-29a can activate the MAPK signaling pathway during differentiation as we found in the differentiation of iPSCs**.**

We first used a dual luciferase reporter assay to assess the effect of miR-29a on the ERK or JNK pathway. miR-29a up-regulated the activity of both ERK and JNK luciferase reporters after stimulation compared to the control vector, miR-Con (Fig. 25A). Then, we determined the effects of the activators or inhibitors of ERK and JNK pathways on the MSC differentiation. As seen in Fig. 25B, the inclusion of ERK or JNK activator in the differentiation medium significantly increased the mRNA levels of SP-C. Additionally, the combination of ERK and JNK activators increased the SP-C mRNA level even more than any single activator (Fig. 25B). On the other hand, ERK and JNK inhibitors repressed the MSC differentiation mediated by miR-29a (Fig. 25C). These results suggest that miR-29a promoted the differentiation of MSCs into AEC II by up-regulating both ERK and JNK signaling pathways (Fig. 25D).

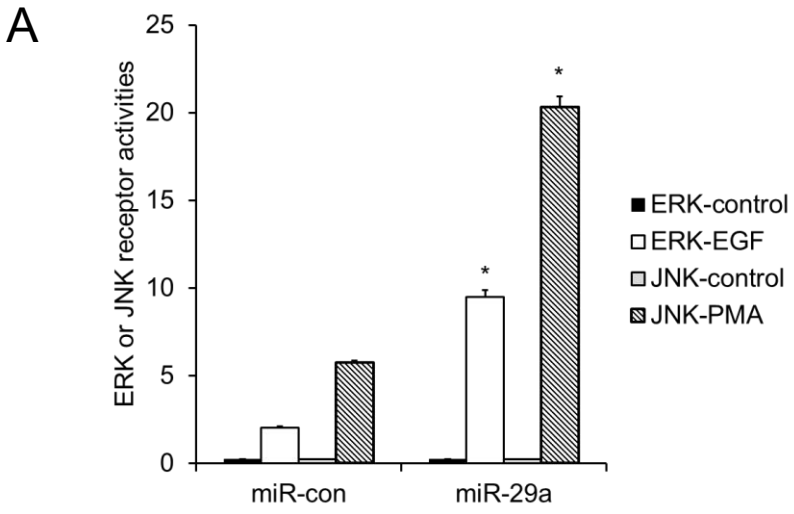

B

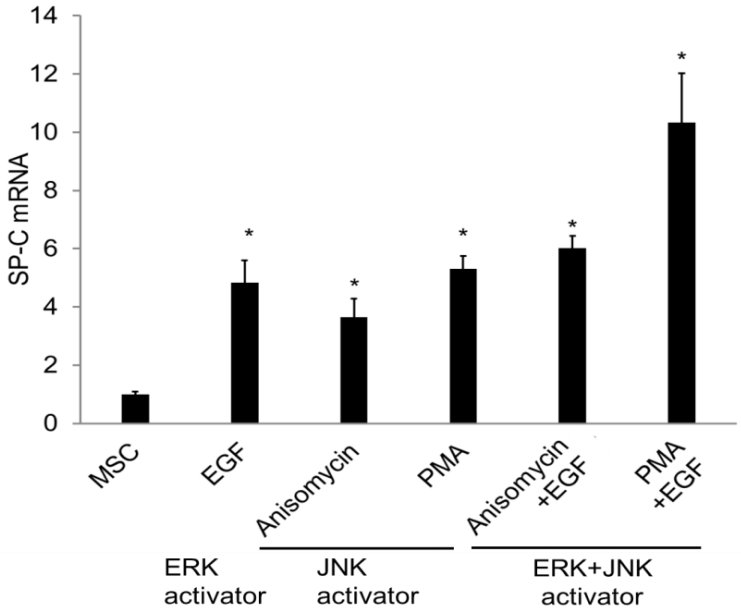
SP-C mRNA
14
12
10
8
6
4
2
0
MSC
EGF
Anisomycin
PMA
Anisomycin +EGF
PMA +EGF
ERK activator
JNK activator
ERK+JNK activator

C

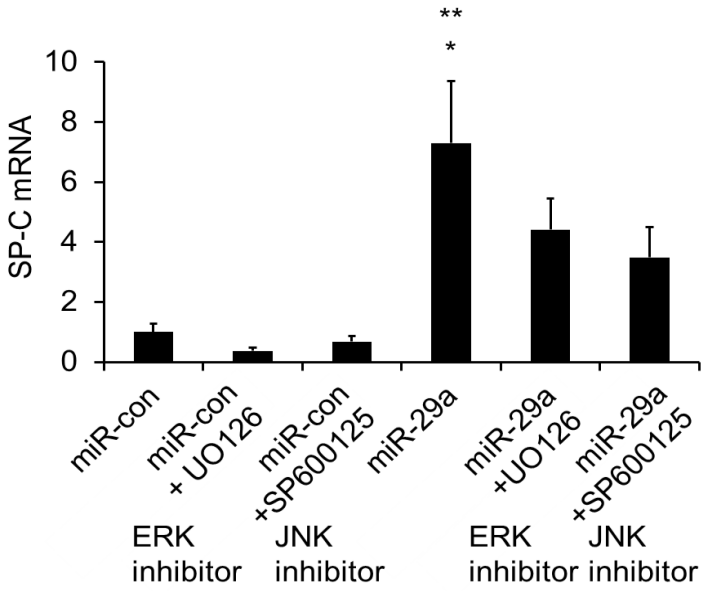
SP-C mRNA
10
8
6
4
2
0
miR-con
miR-con + UO126
miR-con +SP600125
miR-29a
miR-29a +UO126
miR-29a +SP600125
ERK inhibitor
JNK inhibitor
ERK inhibitor
JNK inhibitor

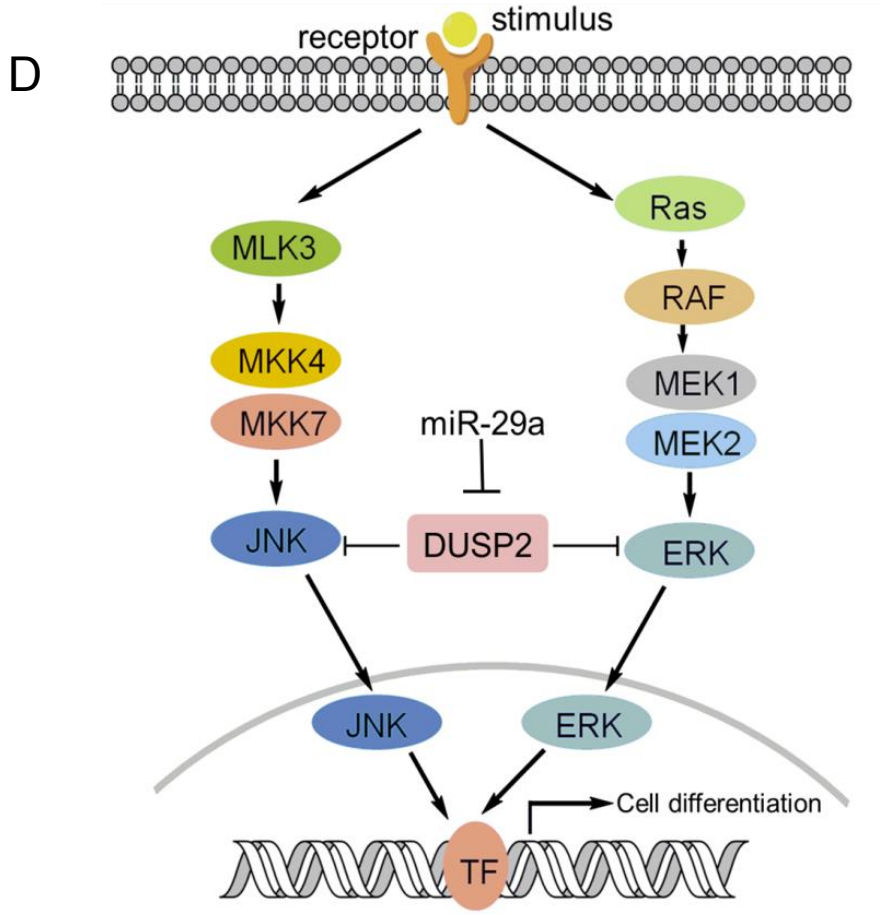

Fig. 25: Role of ERK and JNK pathways in the differentiation of MSCs into AEC II. (A) HEK 293T cells were co-transfected with ERK or JNK luciferase-reporter construct and miR-29a or a vector control (miR-Con). The cells were stimulated with EGF or PMA. The firefly luciferase activity was normalized to *Renilla* luciferase activity. Results are expressed as fold change over control. *P<0.05. Error bars represent SE. (B) Effects of ERK and JNK activators on mRNA levels of SP-C. MSCs were cultured in SAGM in the presence or absence of ERK activators (EGF) and JNK activator (Anisomycin and PMA) for 11 days and SP-C mRNA was determined by qRT-PCR. *P<0.05 vs. MSCs cultured without activators (n=3). Error bars represent SE. (C) Effect of ERK and JNK inhibitors on mRNA levels of SP-C. miR-29a-overexpressed MSCs were cultured in SAGM in the presence or absence of ERK inhibitor

(UO126) and JNK inhibitor (SP600125) for 11 days and SP-C mRNA was determined by qRT-PCR. *P<0.05vs miR-29a+UO126, **P<0.05 vs miR-29a+SP600125 (n=3). Error bars represent SE. (D) Proposed mechanism of miR-29a-mediated activation of ERK and JNK pathways.

vii. MSC–derived AEC II are functional

We first examined whether the miR-29a and DCI mediated MSC-differentiated AEC II (MSC-AEC II) were able to proliferate by BrdU assay. MSC-AEC II were able to proliferate although the proliferation rate was lower than that of the freshly isolated AEC II (Fig. 26A).

AEC II trans-differentiate into AEC I when they are cultured on plastic dishes. We next determined whether MSC-AEC II could trans-differentiate into AEC I. MSC-AEC II were cultured in DMEM with 10% FBS for 7 days on plastic dishes and were then harvested for qRT–PCR and immunostaining analyses. The mRNA expression of the AEC II markers, SP-C, SP-B and ABCA3, were significantly decreased, whereas the mRNA expression of the AEC I markers, T1α and AQP5 were significantly enhanced (Fig. 26B). Immunostaining demonstrated 86.01 % T1α positive cells and 3.8 % SP-C positive cells in the 7-day cultured MSC-AEC II (Fig. 26C, D). These results suggest that MSC-AEC II can proliferate and be trans-differentiated into AEC I.

We next examined whether MSC-AEC II can secrete lung surfactant lipids and proteins. Phosphatidylcholine (PC) and SP-C were chosen as representatives of lung surfactant lipids and proteins. Lung surfactant secretagagues (ATP, PMA and terbutaline) stimulated PC secretion by 4.6 folds in MSC-AEC II in comparsion with 5-fold from primary AEC II (Fig. 26E). ELISA measurements of SP-C protein in the cell culture supernatants indicated that lung surfactant secretagogues also increased SP-C secretion in freshly isolated AEC II and MSC-AEC II (Fig. 26F). The data suggest that MSC-ACE II are able to secrete PC and SP-C. In conclusion, MSC-AEC II behave similarly to primary AEC II.

A

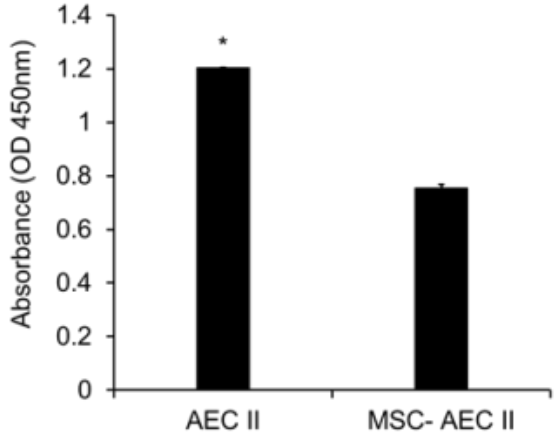
Absorbance (OD 450nm)
1.4
1.2
1
0.8
0.6
0.4
0.2
0
*
AEC II
MSC- AEC II

B

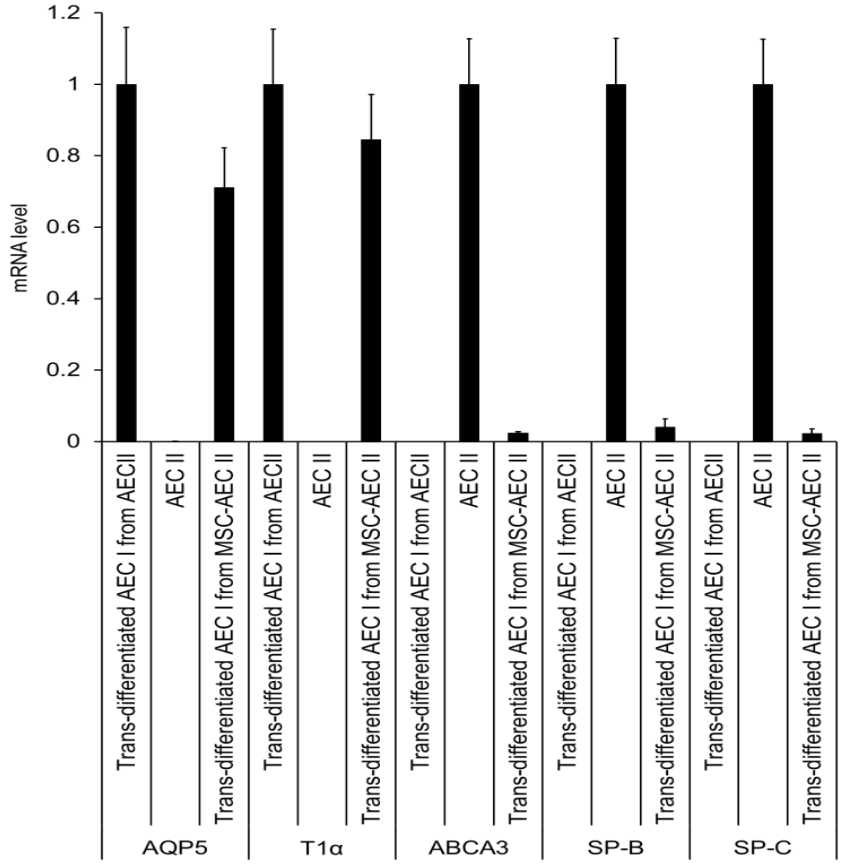
mRNA level
1.2
1
0.8
0.6
0.4
0.2
0
Trans-differentiated AEC I from AECII
AEC II
Trans-differentiated AEC I from MSC-AEC II
AQP5
T1α
ABCA3
SP-B
SP-C

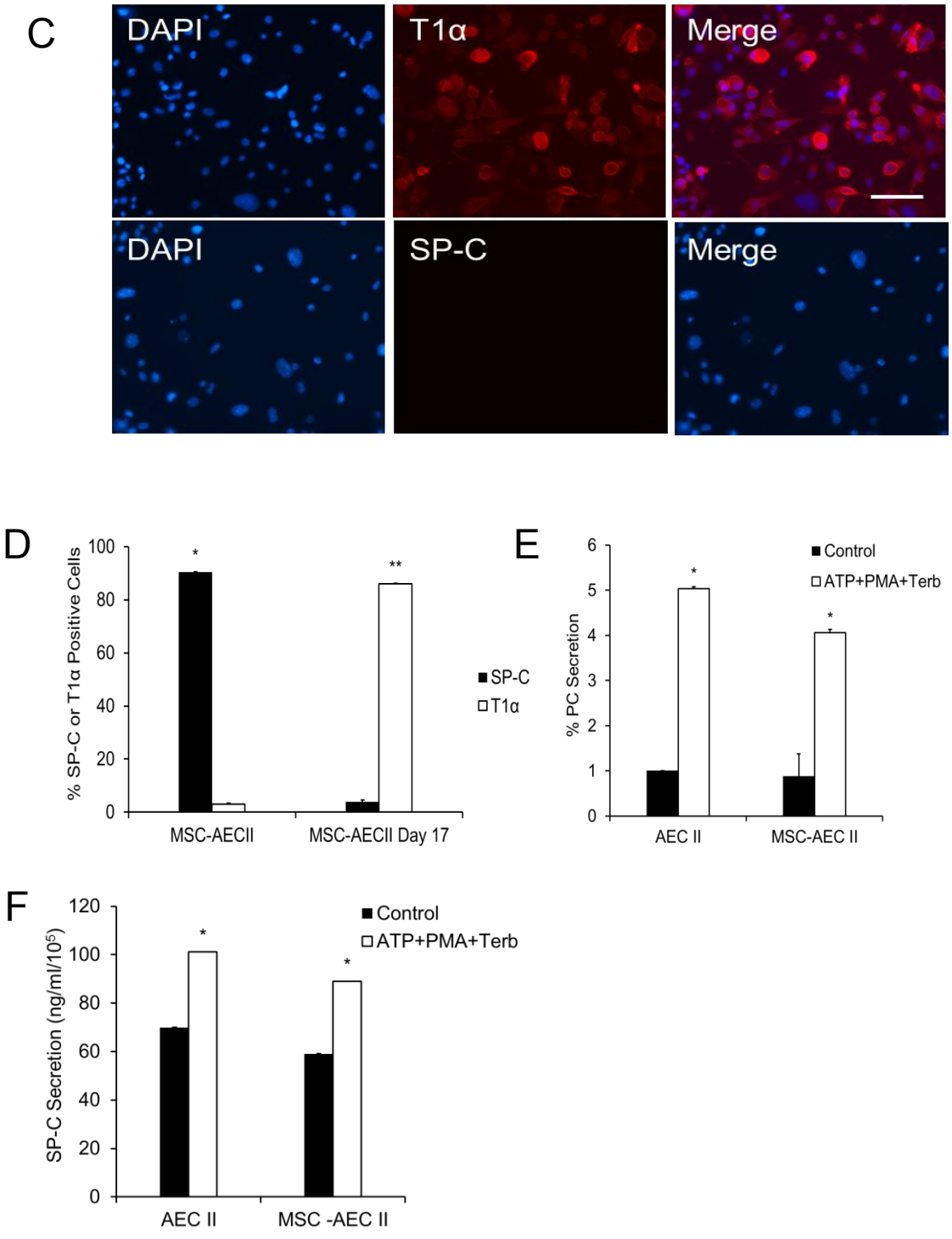

Fig. 26: Functional characterization of MSC-AEC II. MSC-AEC II were obtained by culturing miR-29a-overexpressed MSCs in SAGM in the presence of DCI for 11 days. Primary AEC II were used as a positive control. (A) Cell proliferation as determined by BrdU assay. (B, C) Trans-

differentiation. MSC–AEC II or primary AEC II were cultured in DMEM for 7 days. mRNA (B) and protein (C) levels of AEC II and AEC I markers were determined by qRT-PCR and immunofluorescent staining. Scale bar: 50μm Quantification of SP-C- or T1α-positive cells was presented in (D) *P<0.05 vs. MSC-AEC II Day 17; **P<0.05 vs MSC-AEC II (n=3). (E, F) Lung surfactant lipid and protein secretion. Primary AEC II and MSC-AEC II were stimulated for 2 hours with lung surfactant secretagogues (100 μM ATP, 0.1 μM PMA and 10 μM terbutaline; ATP+PMA+Terb) Phosphatidylcholine secretion (E) and SP-C secretion (F) were measured. Results shown are mean ± SE. *P<0.05 vs. control (n=3 cell preparations).

viii. MSC-AEC II reduces elastase-induced airspace enlargement and lung inflammation, and limits elastase-induced weight loss in mice

We next test whether MSC-AEC II function *in vivo* in the elastase-induced emphysema mouse model. Pulmonary emphysema is an important component of COPD which is characterized by reduced alveolar surface area and increased alveolar size (107). MSC-AEC II used for this study were the AEC II that were differentiated from MSCs mediated by miR-29a for 11 days in SAGM in the absence of DCI (designated as miR-29a-MSC-AEC II). The vector control was AEC II that were differentiated from MSCs mediated by miR-con for 11 days in SAGM in the absence of DCI (designated as miR-Con-MSC-AEC II). Elastase was intratrachally administrated into the lungs of C57BL/6 mice. PBS was used as a control group. After two weeks, the mice with elastase injection were randomly assigned to receive intratracheal injections of miR-29a-MSC-AEC II, miR-Con-MSC-AEC II or PBS. The non-elastase control group was received PBS injection. The lungs were collected 1 week after the cell injection.

To evaluate whether the injected male cells were retained in the female mouse lungs, we performed qRT-PCR to detect the presence of the Y chromosome. Low levels of Y-chromosome

DNA were detected in both miR-29a-MSC-AEC II and miR-Con-MSC-AEC II groups, but not in the non-elastase and elastase control groups (Fig. 27A).

Histological analysis showed that elastase injection resulted in airway enlargement. This was reflected by a significant increase in the mean linear intercept (MLI) (Fig. 27 B-F). miR-Con-MSC-AEC II reduced elastase-induced airway enlargement and miR-29a-MSC-AEC II decreased further compared to the elastase alone group.

We also determined the levels of inflammatory cytokines in the lungs. The mRNA levels of TNF-α, IL-1β, IL-6, and MCP-1 were strongly increased by elastase compared to PBS (Fig. 27 G-J). miR-29a-MSC-AEC II significantly decreased elastase-induced cytokine expression. However, miR-Con-MSC-AEC II had little effect.

In addition to damaging pulmonary structures and inducing inflammation, elastase also induced significant total body weight loss compared to PBS control groups (Fig. 9K). miR-29a-MSC-AEC II significantly limited the elastase-induced body weight loss (Fig. 9K). miR-con-MSC-AEC II also limited the elastase-induced body weight loss, but this effect did not reach the significant level (Fig. 27K).

These results support the conclusion that miR-29a-MSC-AEC II are able to ameliorate elastase-induced emphysematous changes.

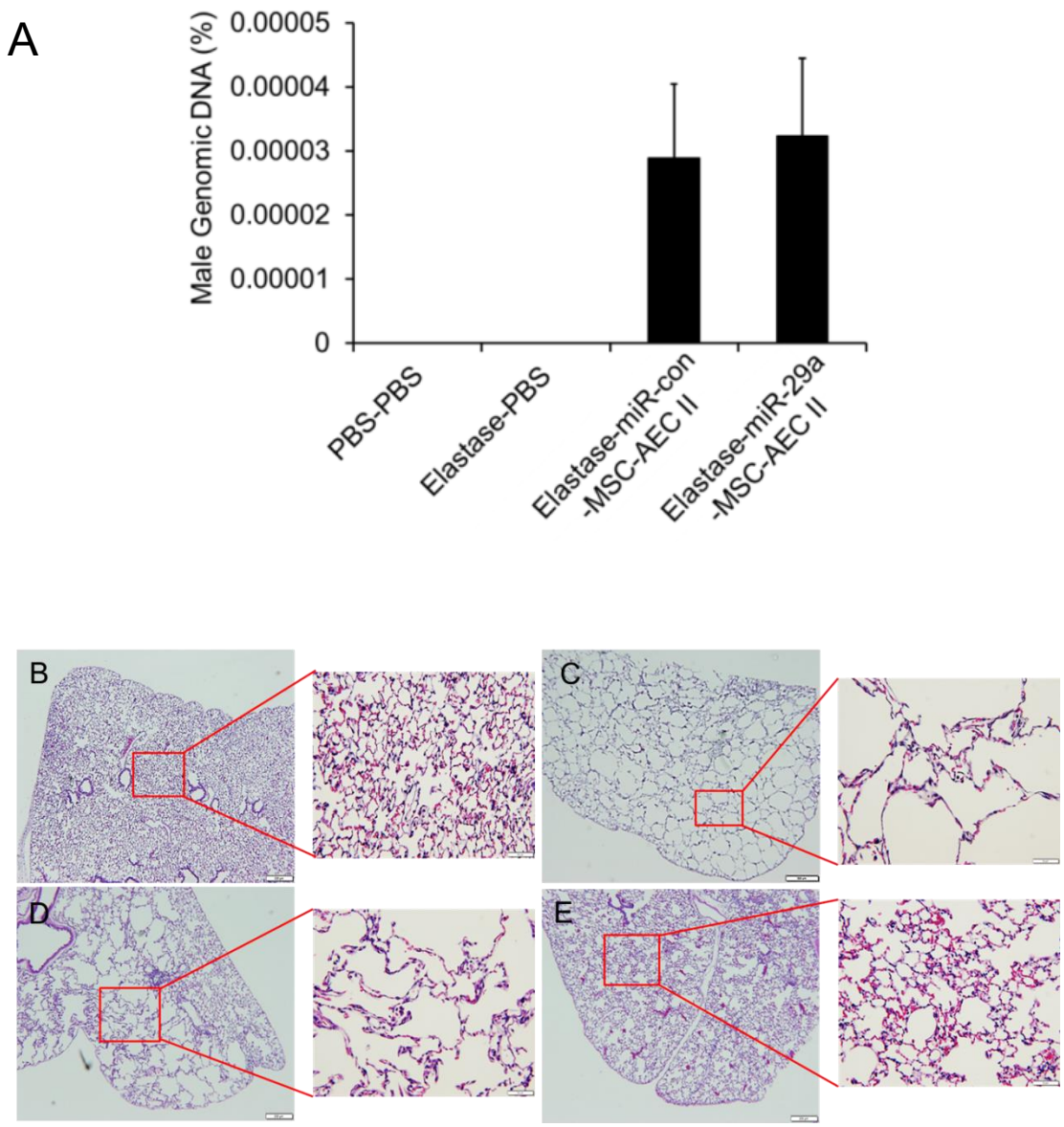
A
Male Genomic DNA (%)
0.00005
0.00004
0.00003
0.00002
0.00001
0
PBS-PBS
Elastase-PBS
Elastase-miR-con -MSC-AEC II
Elastase-miR-29a -MSC-AEC II
B
C
D
E

F

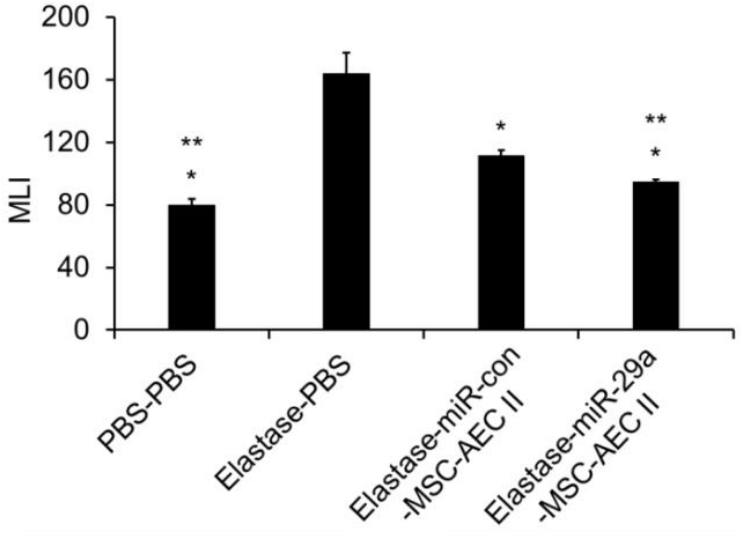
200
160
120
80
40
0
MLI
**
*
*
**
*
PBS-PBS
Elastase-PBS
Elastase-miR-con -MSC-AEC II
Elastase-miR-29a -MSC-AEC II

G

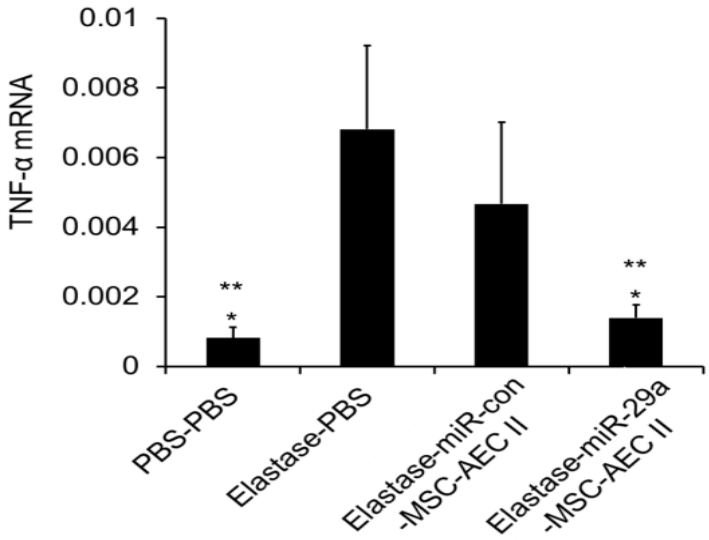
0.01
0.008
0.006
0.004
0.002
0
TNF-α mRNA
**
*
**
*
PBS-PBS
Elastase-PBS
Elastase-miR-con -MSC-AEC II
Elastase-miR-29a -MSC-AEC II

H

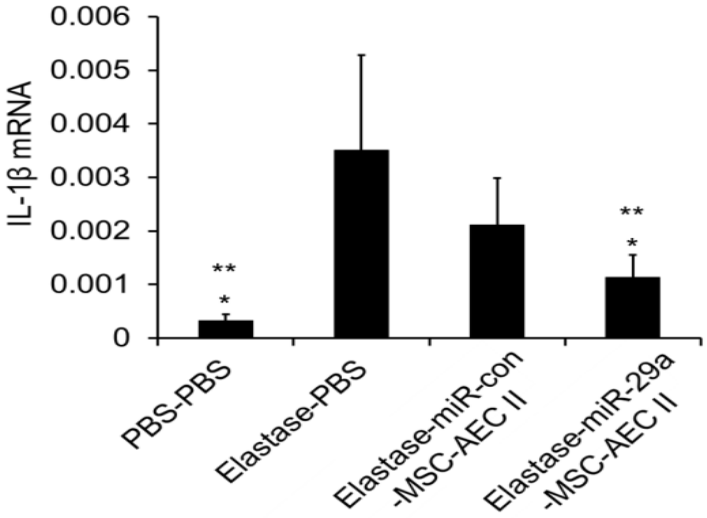
0.006
0.005
0.004
0.003
0.002
0.001
0
IL-1β mRNA
**
*
**
*
PBS-PBS
Elastase-PBS
Elastase-miR-con -MSC-AEC II
Elastase-miR-29a -MSC-AEC II

I

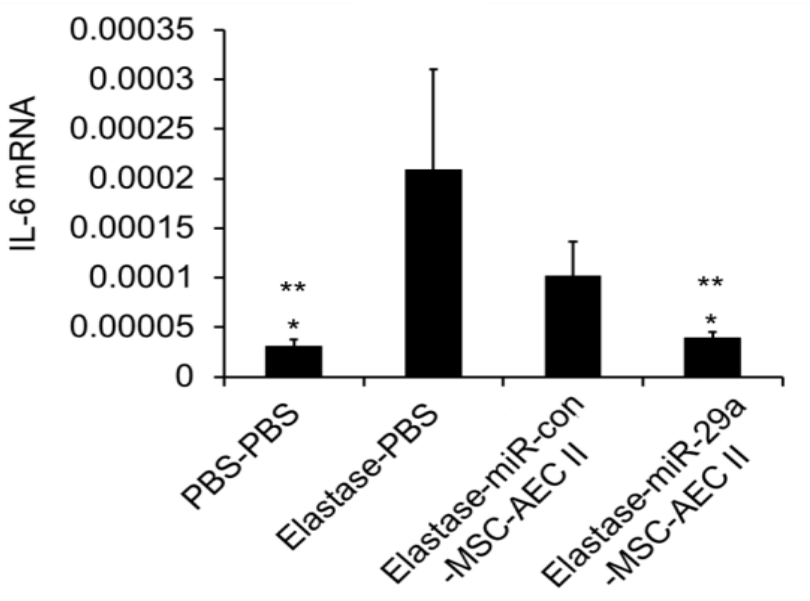
IL-6 mRNA
0.00035
0.0003
0.00025
0.0002
0.00015
0.0001
0.00005
0
**
*
**
*
PBS-PBS
Elastase-PBS
Elastase-miR-con -MSC-AEC II
Elastase-miR-29a -MSC-AEC II

J

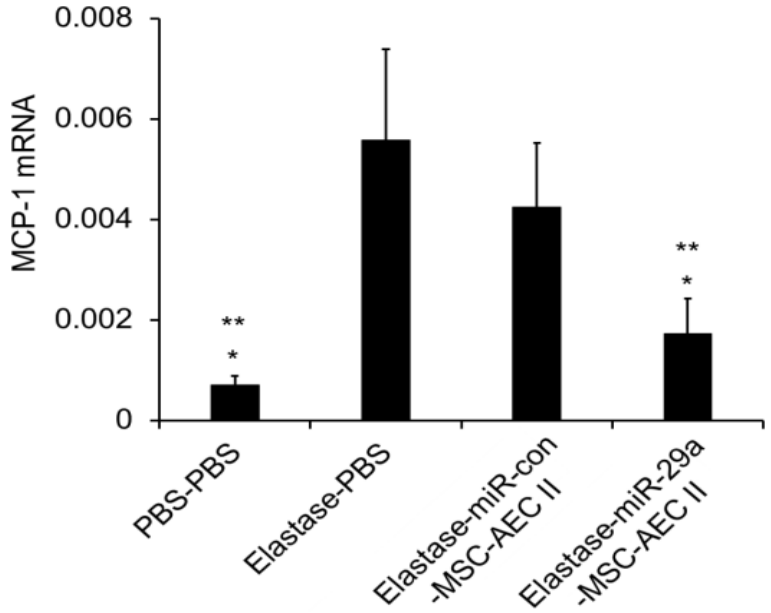
MCP-1 mRNA
0.008
0.006
0.004
0.002
0
**
*
**
*
PBS-PBS
Elastase-PBS
Elastase-miR-con -MSC-AEC II
Elastase-miR-29a -MSC-AEC II

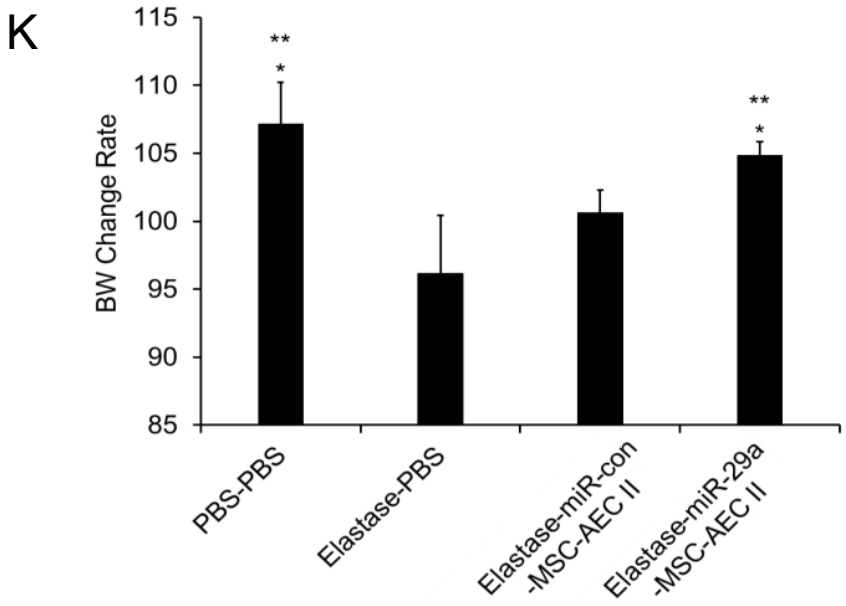

Fig. 27: Effect of MSC-AEC II treatment on elastase-induced airspace enlargement and lung inflammation. Female C57BL/6 mice were treated with elastase or PBS for 2 weeks, then intratracheally injected with PBS, miR-29a engineered male MSCs or miR-con engineered MSCs cultured in SAGM for 11 days. After 1 week treatment, the lungs were collected for analyses. (A) Percentage of male DNA within the lungs of female transplant mice after receiving an intratracheal injection of male miR-29a or miR-con MSC-AEC II. (B-E) Hematoxylin and eosin (H&E) of lung sections from mice treated by PBS (B), elastase (C), elastase plus miR-con-MSC-AEC II (D), and elastase plus miR-29a-MSC-AEC II (E). (F) Mean linear intercepts (MLI). Results shown are mean ± SE. *P<0.05 vs. elastase group (n>5); **P<0.05 vs. miR-con-MSC-AEC II group (n>5). (G-J) mRNA levels of TNF-α, IL-1β, IL-6 and MCP-1 in the lungs were determined by qRT-PCR. Results shown are means ± SE. *P<0.05 vs. elastase group (n>5); **P<0.05 vs. miR-con-MSC-AEC II group (n>5). (K) Body weight. Data was % of body weight at day 21 over that on day 0. *P<0.05 vs. elastase group (n>5); **P<0.05 vs. elastase-miR-con-MSC-AEC II group (n>5).

CHAPTER IV

DISCUSSION

IV-1: MicroRNA-26b modulates the NF-κB pathway in bovine alveolar macrophages by regulating PTEN

The expression and functions of miRNAs are cell- and tissue-specific. The role of miRNAs in the inflammatory response of bovine alveolar macrophages to LPS challenge has not been investigated in detail and certainly has not been explored in regards to BRD. In this study, LPS of *E. coli* was demonstrated to increase cytokine mRNA expression level and nitric oxide production by activating bAMs and miR-26b was found to be a LPS-responsive miRNA in bAMs that promoted bAM expression of inflammatory cytokines and nitric oxide production but not IL-6. miR-26b also enhanced NF-κB pathway activity by targeting PTEN, therefore acting upstream of the NF-κB pathway. Taken together, these data reveal that miR-26b promotes inflammatory responses in LPS-stimulated bAMs through the activation of the NF-κB pathway by inhibiting PTEN (Fig. 28). Importantly, it raises the possibility for the development of novel therapeutic strategies for decreasing the morbidity associated with BRD by regulating miR-26b activity.

Previous evidence revealed that LPS from *E. coli* caused intensive enzymatic and oxidative response of bovine neutrophils *in vitro* and destructive neutrophil response was observed during the course of BRD (4). Therefore, in our studies we concentrated on the effect of LPS from *E.coli*

on bAMs as a responsible cause of lung injury. In this study, we demonstrated that *E. coli* LPS increased cytokine mRNA expression level and nitric oxide production by bAMs.

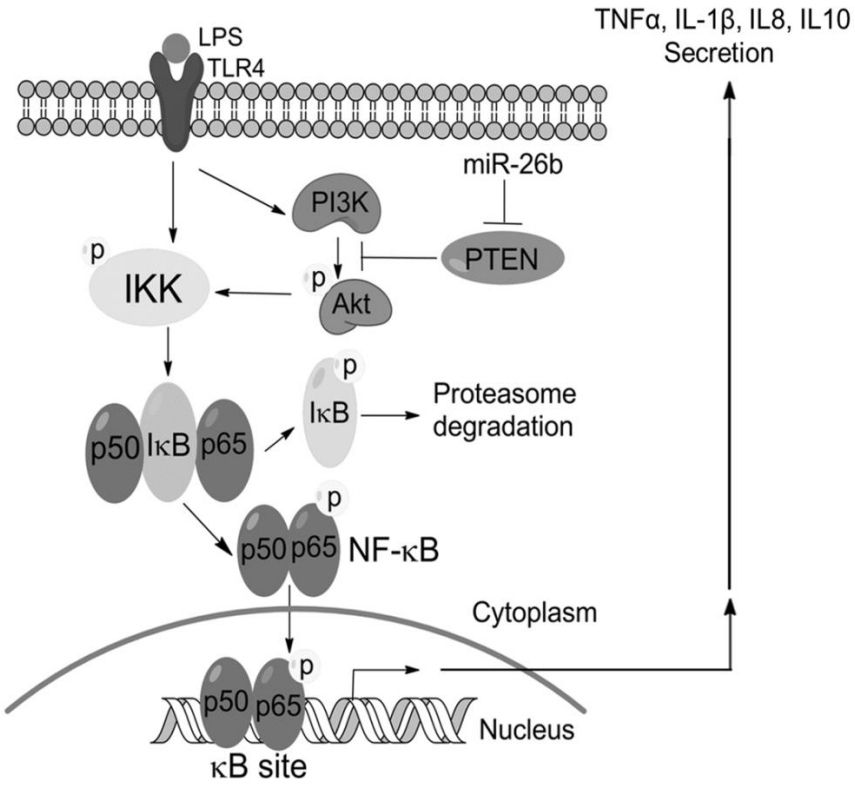

Fig. 28: Proposed mechanism of miR-26b enhancement of LPS-stimulated NF-κB pathway through down-regulation of PTEN.

Alterations in gene expression including miRNA expression can regulate cellular responses to exogenous stimulation. LPS is one potential virulence factor and is known as an inducer of inflammation that plays a significant role in the lesion severity in lung tissue (26, 108). Since BRD is a multi-factorial complex phenotype, dissecting the molecular networks involved is essential for understanding the pathogenesis of BRD. Previous study has identified up-regulated and down-regulated miRNAs and associated signaling pathways in in bovine monocyte inflammatory response network during *S. uberi* infection (109). And, many LPS-responsive

miRNAs have been identified to have a role in cytokine secretion in other species (13, 110, 111). miR-223, for example, is down-regulated in RAW264.7 cells challenged with LPS, which leads to the up-regulation of signal transducer and activator of transcription 3 (STAT3) and promotes pro-inflammatory IL-6 and IL-1β transcription in mice (110). It is unknown if miR-223 has a similar role in alveolar macrophages. This is of interest since these cells play a critical role in the innate immunity against infections of BRD. In our study, miR-26b was identified as an LPS responsive miRNA in bAMs. To our knowledge, this is the first report to study the function of LPS-responsive miRNAs in bovine alveolar macrophages and the first to report that miR-26b is an important regulator of the secretory activity of these cells.

miR-26 is involved in many biological processes. It has been suggested that miR-26 may play a significant role in tumor formation, since miR-26 expression is reportedly decreased in various kinds of tumors as tumor-suppressor but increased in glioma (112). miR-26b was found to enhance human pituitary tumor cell behavior through the direct regulation of PTEN (113). It has been observed that estrogen-repressed miR-26a regulates numerous genes associated with cell growth and proliferation in breast tumors (114). Down-regulation of miR-26b was found in carcinoma-associated fibroblasts from estrogen receptor-positive breast cancers and enhanced cell migration and invasion (115). There have been studies regarding the function of miR-26b related to inflammatory responses that down-regulation of hsa-miR-26b expression may be involved in TNF-α, leptin and resistin-induced insulin resistance and inflammatory responses (116). In spite of all these studies, there are very few functional studies of miR-26b in bovine lungs associated with inflammation. We demonstrated that miR-26b promotes pulmonary inflammation by enhancing mRNA expression levels of TNF-α, IL-8, IL-1β and IL-10 but not IL-6, supporting previous findings that IL-6 is a direct target of miR-26b (98) and is conserved in bovine inflammatory cells. Furthermore, secreted cytokine protein levels mirrored those found in the mRNA, establishing that these changes are functionally significant. Interestingly, IL-8 mRNA

level enhanced by miR-26b is strongly higher than IL-8 protein level enhanced by miR-26b in LPS-activated bAMs. It indicates that the miR-26b mediated IL-8 protein secretion is less actively translated than the miR-26b mediated high level of IL-8 mRNA in LPS-activated bAMs. This leaves us an interesting direction to study in the future. In all, these findings add to the growing body of cell- and tissue-specific functions of miR-26b.

NF-κB is a transcription factor that controls a variety of important genes encoding transcriptional factors, adhesion molecules, cytokines and growth factors involved in inflammation and the immune response. LPS is a potent activator of NF-κB in alveolar macrophages (117). Because of its importance to many biological processes, NF-κB activation and activity are tightly regulated by a battery of endogenous mechanisms. The excessive and prolonged production of pro-inflammatory mediators triggered by the NF-κB pathway, such as TNF-α and IL-6, may result in tissue damage (118). Evidence is growing rapidly that establishes an important etiologic role of miRNAs in the initiation and progression of pathological inflammation and immune responses. miRNA control of NF-κB is emerging as a significant mechanism in disease and normal homeostasis (14).

Studies have shown that the LPS-induced NF-κB pathway is completed by LPS-induced up-regulation of let-7b and down-regulation of miR-125 through decreasing κB-Ras2 expression which is an inhibitor of IKK leading to IκB stabilization in primary human macrophages. (119). miR-155 affects the production of proinflammatory cytokines through the activation of NF-κB by targeting IKKε in an epithelial cell line (120). Little is understood concerning the function of miR-26b in the regulation of NF-κB signaling and to inflammation and immune responses in bAMs challenged with LPS. In this study, we proved that miR-26b up-regulates the LPS-stimulated NF-κB signaling pathway by suppressing PTEN in bAMs, providing new insight into the regulatory role that miR-26b plays in the NF-κB pathway in alveolar macrophages.

PTEN is well known as a tumor suppressor gene and is frequently deleted or mutated in a wide variety of human cancers including lung cancers (121). PTEN encodes a protein that has sequence homology with phosphatases that dephosphorylate serine/threonine and tyrosine residues (122, 123). Specifically, PTEN dephosphorylates PIP3 to PIP2 which limits AKT ability. AKT has been demonstrated as one of the important downstream targets of PI3K (124), and IKK is one of the downstream targets of activated AKT (100). In addition, IKK is an upstream gene in the NF-κB pathway. AKT-mediated effects on target gene transcription lead to various cellular responses of cancers (121). However, it is unknown whether miRNAs acting through PTEN play any role in bovine lung inflammation and whether such an effect is mediated through the NF-κB pathway. In this study, we demonstrated that PTEN is a target of miR-26b. Additionally, we found that NF-κB signaling is up-regulated by PTEN silencing, which results in the enhancement of inflammatory cytokine mRNA expression levels including IL-6. IL-6 was increased by PTEN shRNA but it was decrease by miR-26. It indicates that IL-6 is a direct target of miR-26b. Moreover, under PTEN inhibition, the peak times of IL-8 and IL-10 shifted to 36 h compared with 1 and 6 h with miR-26b overexpression. This leaves us an interesting direction to study in the future.

In summary, our study has revealed intensive cytokine and NO responses in bAM *in vitro* to the stimulation of LPS from *E. coli*. In addition, a new LPS-responsive miRNA, miR-26b, in bAMs was identified. miR-26b enhances inflammatory responses *in vitro* through the promotion of NF-κB pathway activity by directly targeting PTEN (Fig. 8).Consequently, miR-26b has a significant mechanistic role in NF-κB activation in bAMs and may contribute to the inflammatory reaction that is important in the development of bovine lung diseases caused by gram-negative bacteria. Therefore, strategies aimed at mitigating miR-26b expression to reduce NF-κB activation in bAMs may represent a potential therapy for ameliorating disease in BRD.

For further study, to investigate whether miR-26b is a lung specific LPS-responsive miRNA, the miRNA expression profile in other organs can be detected after LPS stimulation. Furthermore, we can detect whether the levels of miR-26b at different time points paralleled by the same time points showing mRNA and protein levels of PTEN to provide more evidence for the correlation of miR-26b and PTEN.

IV-2: MicroRNA-29a Efficiently Promotes the Differentiation of Mouse Induced Pluripotent Stem Cells and Mesenchymal Stem Cells into Alveolar Epithelial Type II cells

IV-2-1: iPSCs

Cell replacement therapy requires a proper source of cells for engraftment. AEC II have become an attractive candidate for cell therapies of lung diseases since these cells have recently been identified as alveolar stem cells (125) and secrete a high level of lung surfactant in the distal alveoli. However, it is still a challenge to generate large quantities of pure AEC II. The conditions for directing iPSCs to differentiate into an alveolar epithelial lineage with homogeneity are not fully defined yet. In the present study, we found that miR-29a promoted the differentiation of mouse iPSCs into AEC II through the activation of the MAPK pathway by targeting DUSP2. Moreover, these iPSC-AEC II are capable of secreting lung surfactant, proliferating and trans-differentiating into AEC I.

The first goal of this study was to identify the optimal conditions that efficiently promote mouse iPSC differentiation into AEC II. Previous studies demonstrated that iPSCs were able to differentiate toward lung epithelium (38, 126-128). However, the efficiency was low. In our study, we demonstrated that miR-29a efficiently promoted mouse iPSC differentiation into AEC II. miR-29 has been implicated in EMT, skeletal muscle cell and osteoblast differentiation, systemic sclerosis, cardiac fibrosis and lung fibrosis (129-134). miR-29 negatively regulates several predicted targets including collagens in nasopharyngeal carcinomas and myocardial

infarction-associated cardiac fibrosis (133, 135). miR-29a also regulates TGF-β1-induced extracellular matrix synthesis through the activation of the PI3K-AKT pathway in human lung fibroblasts (136). In spite of all these studies, there is still no functional study of miR-29a in lung epithelial differentiation. Our finding that ~88% of iPSCs can be differentiated into AEC II by miR-29a suggests that this pathway may be amenable for use in large scale generation of AEC II from patient-specific iPSCs.

miRNA causes a rapid change in protein expression via inhibition of mRNA translation and stability. The ability to target different proteins can rapidly impose a dominant phenotypic change in cell destination. Our finding indicates that miR-29a expression is essential for iPSC differentiation to the lung epithelial cell lineage. Thus analysis of the regulation of mRNA targets of miR-29a may provide important information regarding both the iPSC gene network and factors whose expression is essential to efficient iPSC differentiation into lung epithelial cells. In the present study, we identified Dual-specificity phosphatase 2 (DUSP2) as a target of miR-29a and showed that DUSP2 suppression enhances differentiation of iPSCs into AEC II. DUSP-2 is a protein tyrosine phosphatase and belongs to the class I sub-family of DUSP proteins. It is a negative regulator of the mitogen-activated protein kinase (MAPK) pathway. DUSP2 de-phosphorylates the conserved TxY motif present in the activation loop of MAPK phosphatases (MKPs). DUSP2 is well known to influence metabolism in the immune system. It plays an important role in enhancing immune and inflammatory responses that are dependent on MAPK signaling (103). However, the regulatory roles of DUSPs in iPSC differentiation towards lung epithelium are unknown.

Cellular responses such as cell differentiation, immune responses, and cell survival to endogenous or exogenous stimuli are directed by MAPK signaling pathways (68, 82, 137-139). The MAPK signaling cascade includes three sequential phosphorylation steps involving MAPK kinase kinase (MAPKKK), MAPK kinase (MAPKK), and MAPK. MAPKKKs phosphorylate and

activate MAPKKs, which in turn phosphorylate and activate MAPKs (140). A variety of substrate proteins including transcription factors are phosphorylated by the activated MAPKs (140). The MAPK pathways are activated by diverse extracellular and intracellular regulators including miRNAs. Three MAPK pathways [extracellular signal-regulated kinase (ERK), c-Jun N-terminal kinase (JNK), and p38] have been characterized in detail. A recent study has reported that the activation of JNK and ERK promotes osteogenesis from mesenchymal stem cells (MSCs) by regulating cell shape (141). However, studies on the role of MAPK pathways associated with DUSP in stem cell differentiation are limited. In our study, we uncovered a novel mechanism for the activation of the MAPK signaling pathway by miR-29a through targeting DUSP2, which resulted in effective enhancement of iPSC differentiation into AEC II.

In summary, we identified miR-29a as a mouse AEC II enriched miRNA. miR-29a effectively enhances the differentiation of iPSCs into AEC II through the activation of the MAPK pathway by directly targeting DUSP2. Additionally, AEC II derived from miR-29a engineered-iPSCs are functional. Our studies represent an initial and important step towards the ultimate goal of cell-based therapy of COPD.

IV-2-2: MSCs

Chronic obstructive pulmonary disease (COPD) is a common condition primarily associated with cigarette smoking. Chronic exposure to cigarette smoke results in emphysema and pulmonary inflammation. MSCs haven been used to treat lung disease. The main observation of this study was that miR-29a effectively promoted the differentiation of MSCs into AEC II through activation of the MAPK pathway by targeting DUSP2. Furthermore, these MSC-AEC II secrete pulmonary surfactant, proliferate and trans-differentiate into AEC I. In addition, MSC-AEC II are also capable of ameliorating the pulmonary damage caused by elastase. The observed profound protective effects of MSC-AEC II in the mouse lung identify them as a potentially promising therapy for emphysema.

Previous studies have demonstrated the ability of MSCs to differentiate into several cell lineages including endothelial cells, the osteogenic lineage, and the epithelial lineage (142-144). In this study, we attempted to identify optimal conditions that efficiently promote mouse MSC differentiation into AEC II. We demonstrated that miR-29a efficiently promoted mouse MSC differentiation into AEC II. One previous study reported that epigenetic modification improved the differentiation of MSC lineage specification (145). miRNAs were also found to effectively differentiate MSCs into specific cell lineages. miR-128 regulates the differentiation of rat bone MSCs into neuron-like cells via Wnt signaling (19) . Up-regulation of miR-29a strongly inhibits chondrocyte-specific markers during *in vitro* chondrogenic differentiation of MSCs by targeting FOXO3A (18). In spite of all these studies, there are no studies on miRNAs as they relate to MSC differentiation into AEC II. Our finding that efficient differentiation of MSCs into AEC II is enhanced by miR-29a may prove to be amenable for use in large scale AEC II generation.

Phosphorylation-dephosphorylation plays an essential role in the assembly and disassembly of multiprotein complexes and determines cell fate. The mitogen-activated protein kinase (MAPK) pathway is known to activate a wide range of transcription factors involved in innate immunity, cell growth, stress responses, apoptosis, and differentiation (146). The signaling mediators of MAPK include extracellular signal-regulated kinases (ERKs), c-Jun N-terminal kinases (JNKs), and p38 MAPK (147). Notably the activation of JNK and ERK1/2 MAPK are important in the differentiation of mouse embryonic stem cells (ESCs) and rat dental follicle stem cells (148, 149). miRNAs have been reported to activate MAPK through targeting upstream or downstream regulatory proteins. miR-21 has been reported to promote proliferation and migration, and to inhibit apoptosis, in Eca109 cells by activating the ERK1/2 MAPK pathway (150). Furthermore, miR-21 has also been demonstrated to modulate the ERK–MAPK signaling pathway by regulating SPRY2 expression during human mesenchymal stem cell differentiation

(151). Our present study showed that the activation or inhibition of ERK or JNK signaling resulted in an increase or decrease of MSC-to-AEC II differentiation, pointing to the importance of MAPK signaling in this process.

The ability of miRNAs to simultaneously target many mRNAs involved in cellular signaling increases the complexity underlying the mechanisms of miRNA actions. Correlative analysis of changed signaling pathways and mRNA targets of miR-29a underscores the role of DUSP2 in MSC-to-AEC II differentiation. The miR-29a-mediated reduction of DUSP2 protein is likely responsible for enhancing MSC-to-AEC II differentiation. DUSP2 is a protein tyrosine phosphatase that inhibits MAPK pathways. DUSP2 serves as mitogen- and stress-inducible nuclear MAPK phosphatase (103). However, whether DUSP2 is involved in MSC-to-AEC II differentiation remains unclear. In this study, we demonstrated that DUSP2 was a target of miR-29a and miR-29a-mediated DUSP2 suppression resulted in the enhancement of the differentiation of MSCs into AEC II.

Remarkably, our current studies demonstrated that MSC–AEC II are functional. First, MSC–AEC II are able to secrete SP-C and PC after stimulation. Second, MSC-AEC II can proliferate and trans-differentiate into AEC I. This ability of MSC-AEC II cells to behave like native AEC II increases their potential to protect the lung from the damage caused by elastase. A previous study has demonstrated that adipose stem cell (ASC) can attenuate the pulmonary damage such as airspace enlargement and lung inflammation, and reverse body weight loss caused by elastase in an emphysema mouse model (65). Our MSC–AEC II are also capable of attenuating elastase-induced lung inflammation and airspace enlargement. The protective effects of MSC-AEC II in the mouse lung of elastase model suggest a potentially promising intervention for emphysema.

Future studies include investigation of multiple mechanisms engaged in the therapeutic effects of MSC-AEC II in lung diseases, such as secretion of antiapoptotic factors, paracrine

protective action on neighboring resident lung cells, activation of endogenous progenitor cell cycling and differentiation, repair of the lung endothelial barrier, and rescue and recruitment of circulating cells for pulmonary repair *in vivo*.

In summary, miR-29a effectively enhances MSC differentiation into AEC II *in vitro* through the activation of the MAPK pathway by directly targeting DUSP2. miR-29a engineered MSC-AEC II are able to secrete lung surfactant, proliferate and trans-differentiate into AEC I. Furthermore, miR-29a engineered MSC-AEC II exerts protective effects against elastase-induced airway enlargement and pulmonary inflammation. miR-29a engineered MSC-AEC II may be a viable therapeutic option for cell therapy of COPD.

For future deeper study, to calculate how many miR-29a-MSC-AEC II cells could be delivered *in vivo*, the miR-29a-MSC-AEC II cells can be labeled with a fluorescent cell tracker dye, such as CMTX cell tracker (green), for intratracheal instillation into C57/B6 mice.

REFERENCES

1. Bartel, D. P. 2004. MicroRNAs: genomics, biogenesis, mechanism, and function. In *Cell*. 281-297.
2. Bushati, N., and S. M. Cohen. 2007. microRNA functions. In *Annual review of cell and developmental biology*. 175-205.
3. Eulalio, A., E. Huntzinger, and E. Izaurralde. 2008. Getting to the root of miRNA-mediated gene silencing. *Cell* 132: 9-14.
4. Filipowicz, W., S. N. Bhattacharyya, and N. Sonenberg. 2008. Mechanisms of post-transcriptional regulation by microRNAs: are the answers in sight? *Nature reviews. Genetics* 9: 102-114.
5. Fabian, M. R., N. Sonenberg, and W. Filipowicz. 2010. Regulation of mRNA translation and stability by microRNAs. *Annual review of biochemistry* 79: 351-379.
6. Vasudevan, S., Y. C. Tong, and J. A. Steitz. 2007. Switching from repression to activation: MicroRNAs can up-regulate translation. *Science* 318: 1931-1934.
7. Wu, L., and J. G. Belasco. 2008. Let me count the ways: mechanisms of gene regulation by miRNAs and siRNAs. *Molecular cell* 29: 1-7.
8. Lodish, H. F., B. Zhou, G. Liu, and C. Z. Chen. 2008. Micromanagement of the immune system by microRNAs. *Nature reviews. Immunology* 8: 120-130.
9. Stadler, B. M., and H. Ruohola-Baker. 2008. Small RNAs: keeping stem cells in line. *Cell* 132: 563-566.
10. Stefani, G., and F. J. Slack. 2008. Small non-coding RNAs in animal development. *Nature reviews. Molecular cell biology* 9: 219-230.
11. Coutinho, L. L., L. K. Matukumalli, T. S. Sonstegard, C. P. Van Tassell, L. C. Gasbarre, A. V. Capuco, and T. P. L. Smith. 2007. Discovery and profiling of bovine microRNAs from immune-related and embryonic tissues. *Physiol Genomics* 29: 35-43.
12. O'Connell, R. M., D. S. Rao, A. A. Chaudhuri, and D. Baltimore. 2010. Physiological and pathological roles for microRNAs in the immune system. *Nature reviews. Immunology* 10: 111-122.
13. Taganov, K. D., M. P. Boldin, K. J. Chang, and D. Baltimore. 2006. NF-kappaB-dependent induction of microRNA miR-146, an inhibitor targeted to signaling proteins of innate immune responses. *Proceedings of the National Academy of Sciences of the United States of America* 103: 12481-12486.
14. Ma, X., L. E. Becker Buscaglia, J. R. Barker, and Y. Li. 2011. MicroRNAs in NF-kappaB signaling. *Journal of molecular cell biology* 3: 159-166.

15. Anokye-Danso, F., C. M. Trivedi, D. Juhr, M. Gupta, Z. Cui, Y. Tian, Y. Zhang, W. Yang, P. J. Gruber, J. A. Epstein, and E. E. Morrisey. 2011. Highly efficient miRNA-mediated reprogramming of mouse and human somatic cells to pluripotency. *Cell Stem Cell* 8: 376-388.
16. Yang, C. S., Z. Li, and T. M. Rana. 2011. microRNAs modulate iPS cell generation. *RNA* 17: 1451-1460.
17. Judson, R. L., J. E. Babiarz, M. Venere, and R. Blelloch. 2009. Embryonic stem cell-specific microRNAs promote induced pluripotency. *Nat Biotechnol* 27: 459-461.
18. Guerit, D., J. M. Brondello, P. Chuchana, D. Philipot, K. Toupet, C. Bony, C. Jorgensen, and D. Noel. 2014. FOXO3A regulation by miRNA-29a Controls chondrogenic differentiation of mesenchymal stem cells and cartilage formation. *Stem Cells Dev* 23: 1195-1205.
19. Wu, R., Y. Tang, W. Zang, Y. Wang, M. Li, Y. Du, G. Zhao, and Y. Xu. 2014. MicroRNA-128 regulates the differentiation of rat bone mesenchymal stem cells into neuron-like cells by Wnt signaling. *Mol Cell Biochem* 387: 151-158.
20. Huang, J., L. Zhao, L. Xing, and D. Chen. 2010. MicroRNA-204 regulates Runx2 protein expression and mesenchymal progenitor cell differentiation. *Stem Cells* 28: 357-364.
21. Cerrada, A., P. de la Torre, J. Grande, T. Haller, A. I. Flores, and J. Perez-Gil. 2014. Human decidua-derived mesenchymal stem cells differentiate into functional alveolar type II-like cells that synthesize and secrete pulmonary surfactant complexes. *PLoS One* 9: e110195.
22. Griffin, D., M. M. Chengappa, J. Kuszak, and D. S. McVey. 2010. Bacterial pathogens of the bovine respiratory disease complex. *The Veterinary clinics of North America. Food animal practice* 26: 381-394.
23. Rehmtulla, A. J., and R. G. Thomson. 1981. A review of the lesions in shipping fever of cattle. *The Canadian veterinary journal. La revue veterinaire canadienne* 22: 1-8.
24. Fulton, R. W., B. J. Cook, D. L. Step, A. W. Confer, J. T. Saliki, M. E. Payton, L. J. Burge, R. D. Welsh, and K. S. Blood. 2002. Evaluation of health status of calves and the impact on feedlot performance: assessment of a retained ownership program for postweaning calves. *Canadian journal of veterinary research = Revue canadienne de recherche veterinaire* 66: 173-180.
25. Czuprynski, C. J., F. Leite, M. Sylte, C. Kuckleburg, R. Schultz, T. Inzana, E. Behling-Kelly, and L. Corbeil. 2004. Complexities of the pathogenesis of Mannheimia haemolytica and Haemophilus somnus infections: challenges and potential opportunities for prevention? *Animal health research reviews / Conference of Research Workers in Animal Diseases* 5: 277-282.
26. Wessely-Szponder, J., R. Urban-Chmiel, A. Wernicki, and R. Bobowiec. 2005. Effect of leukotoxin of Mannheimia haemolytica and LPS of E. coli on secretory response of bovine neutrophils in vitro. *Polish journal of veterinary sciences* 8: 99-105.
27. Highlander, S. K. 2001. Molecular genetic analysis of virulence in Mannheimia (pasteurella) haemolytica. *Frontiers in bioscience : a journal and virtual library* 6: D1128-1150.

28. Jeyaseelan, S., M. S. Kannan, R. E. Briggs, P. Thumbikat, and S. K. Maheswaran. 2001. Mannheimia haemolytica leukotoxin activates a nonreceptor tyrosine kinase signaling cascade in bovine leukocytes, which induces biological effects. *Infection and immunity* 69: 6131-6139.
29. Smale, S. T. 2012. Transcriptional regulation in the innate immune system. *Current opinion in immunology* 24: 51-57.
30. Mullen, J. B., J. L. Wright, B. R. Wiggs, P. D. Pare, and J. C. Hogg. 1985. Reassessment of inflammation of airways in chronic bronchitis. *British medical journal* 291: 1235-1239.
31. O'Shaughnessy, T. C., T. W. Ansari, N. C. Barnes, and P. K. Jeffery. 1997. Inflammation in bronchial biopsies of subjects with chronic bronchitis: inverse relationship of CD8+ T lymphocytes with FEV1. *American journal of respiratory and critical care medicine* 155: 852-857.
32. Saetta, M., A. Di Stefano, P. Maestrelli, A. Ferraresso, R. Drigo, A. Potena, A. Ciaccia, and L. M. Fabbri. 1993. Activated T-lymphocytes and macrophages in bronchial mucosa of subjects with chronic bronchitis. *The American review of respiratory disease* 147: 301-306.
33. Saetta, M., A. Di Stefano, G. Turato, F. M. Facchini, L. Corbino, C. E. Mapp, P. Maestrelli, A. Ciaccia, and L. M. Fabbri. 1998. CD8+ T-lymphocytes in peripheral airways of smokers with chronic obstructive pulmonary disease. *American journal of respiratory and critical care medicine* 157: 822-826.
34. Leopold, J. G., and J. Gough. 1957. The centrilobular form of hypertrophic emphysema and its relation to chronic bronchitis. *Thorax* 12: 219-235.
35. Peinado, V. I., J. A. Barbera, P. Abate, J. Ramirez, J. Roca, S. Santos, and R. Rodriguez-Roisin. 1999. Inflammatory reaction in pulmonary muscular arteries of patients with mild chronic obstructive pulmonary disease. *American journal of respiratory and critical care medicine* 159: 1605-1611.
36. Wright, J. L., L. Lawson, P. D. Pare, R. O. Hooper, D. I. Peretz, J. M. Nelems, M. Schulzer, and J. C. Hogg. 1983. The structure and function of the pulmonary vasculature in mild chronic obstructive pulmonary disease. The effect of oxygen and exercise. *The American review of respiratory disease* 128: 702-707.
37. MacNee, W. 1994. Pathophysiology of cor pulmonale in chronic obstructive pulmonary disease. Part two. *American journal of respiratory and critical care medicine* 150: 1158-1168.
38. Wang, D., D. L. Haviland, A. R. Burns, E. Zsigmond, and R. A. Wetsel. 2007. A pure population of lung alveolar epithelial type II cells derived from human embryonic stem cells. *Proc Natl Acad Sci U S A* 104: 4449-4454.
39. Alison, M. R., R. Poulsom, S. Forbes, and N. A. Wright. 2002. An introduction to stem cells. *The Journal of pathology* 197: 419-423.
40. Fuchs, E., and J. A. Segre. 2000. Stem cells: a new lease on life. *Cell* 100: 143-155.
41. Bonfield, T. L., and A. I. Caplan. 2010. Adult mesenchymal stem cells: an innovative therapeutic for lung diseases. *Discov Med* 9: 337-345.
42. Kocher, A. A., M. D. Schuster, M. J. Szabolcs, S. Takuma, D. Burkhoff, J. Wang, S. Homma, N. M. Edwards, and S. Itescu. 2001. Neovascularization of ischemic myocardium by human bone-marrow-derived angioblasts prevents cardiomyocyte

apoptosis, reduces remodeling and improves cardiac function. *Nat Med* 7: 430-436.
43. Matthay, M. A., A. Goolaerts, J. P. Howard, and J. W. Lee. 2010. Mesenchymal stem cells for acute lung injury: preclinical evidence. *Crit Care Med* 38: S569-573.
44. Orlic, D., J. Kajstura, S. Chimenti, F. Limana, I. Jakoniuk, F. Quaini, B. Nadal-Ginard, D. M. Bodine, A. Leri, and P. Anversa. 2001. Mobilized bone marrow cells repair the infarcted heart, improving function and survival. *Proc Natl Acad Sci U S A* 98: 10344-10349.
45. Zhao, D. C., J. X. Lei, R. Chen, W. H. Yu, X. M. Zhang, S. N. Li, and P. Xiang. 2005. Bone marrow-derived mesenchymal stem cells protect against experimental liver fibrosis in rats. *World J Gastroenterol* 11: 3431-3440.
46. Cruz, F. F., M. A. Antunes, S. C. Abreu, L. C. Fujisaki, J. D. Silva, D. G. Xisto, T. Maron-Gutierrez, D. S. Ornellas, V. K. Sa, N. N. Rocha, V. L. Capelozzi, M. M. Morales, and P. R. Rocco. 2012. Protective effects of bone marrow mononuclear cell therapy on lung and heart in an elastase-induced emphysema model. *Respir Physiol Neurobiol* 182: 26-36.
47. Huh, J. W., S. Y. Kim, J. H. Lee, J. S. Lee, Q. Van Ta, M. Kim, Y. M. Oh, Y. S. Lee, and S. D. Lee. 2011. Bone marrow cells repair cigarette smoke-induced emphysema in rats. *Am J Physiol Lung Cell Mol Physiol* 301: L255-266.
48. Longhini-Dos-Santos, N., V. A. Barbosa-de-Oliveira, R. H. Kozma, C. A. Faria, T. Stessuk, F. Frei, and J. T. Ribeiro-Paes. 2013. Cell therapy with bone marrow mononuclear cells in elastase-induced pulmonary emphysema. *Stem Cell Rev* 9: 210-218.
49. Takahashi, K., and S. Yamanaka. 2006. Induction of pluripotent stem cells from mouse embryonic and adult fibroblast cultures by defined factors. *Cell* 126: 663-676.
50. Wetsel, R. A., D. Wang, and D. G. Calame. 2011. Therapeutic potential of lung epithelial progenitor cells derived from embryonic and induced pluripotent stem cells. *Annual review of medicine* 62: 95-105.
51. Geoghegan, E., and L. Byrnes. 2008. Mouse induced pluripotent stem cells. *Int J Dev Biol* 52: 1015-1022.
52. Garcia, O., G. Carraro, S. Navarro, I. Bertoncello, J. McQualter, B. Driscoll, E. Jesudason, and D. Warburton. 2012. Cell-based therapies for lung disease. *Br Med Bull* 101: 147-161.
53. Rock, J. R., S. H. Randell, and B. L. Hogan. 2010. Airway basal stem cells: a perspective on their roles in epithelial homeostasis and remodeling. *Disease models & mechanisms* 3: 545-556.
54. Fadini, G. P., M. Schiavon, M. Cantini, I. Baesso, M. Facco, M. Miorin, M. Tassinato, S. V. de Kreutzenberg, A. Avogaro, and C. Agostini. 2006. Circulating progenitor cells are reduced in patients with severe lung disease. *Stem Cells* 24: 1806-1813.
55. Kubo, H. 2012. Concise review: clinical prospects for treating chronic obstructive pulmonary disease with regenerative approaches. *Stem Cells Transl Med* 1: 627-631.

56. Nishikawa, S., R. A. Goldstein, and C. R. Nierras. 2008. The promise of human induced pluripotent stem cells for research and therapy. *Nature reviews. Molecular cell biology* 9: 725-729.
57. Yamanaka, S. 2007. Strategies and new developments in the generation of patient-specific pluripotent stem cells. *Cell stem cell* 1: 39-49.
58. Ghaedi, M., E. A. Calle, J. J. Mendez, A. L. Gard, J. Balestrini, A. Booth, P. F. Bove, L. Gui, E. S. White, and L. E. Niklason. 2013. Human iPS cell-derived alveolar epithelium repopulates lung extracellular matrix. *J Clin Invest* 123: 4950-4962.
59. Ishizawa, K., H. Kubo, M. Yamada, S. Kobayashi, M. Numasaki, S. Ueda, T. Suzuki, and H. Sasaki. 2004. Bone marrow-derived cells contribute to lung regeneration after elastase-induced pulmonary emphysema. *FEBS Lett* 556: 249-252.
60. Shigemura, N., M. Okumura, S. Mizuno, Y. Imanishi, T. Nakamura, and Y. Sawa. 2006. Autologous transplantation of adipose tissue-derived stromal cells ameliorates pulmonary emphysema. *Am J Transplant* 6: 2592-2600.
61. Herzog, E. L., L. Chai, and D. S. Krause. 2003. Plasticity of marrow-derived stem cells. *Blood* 102: 3483-3493.
62. Romanov, Y. A., A. N. Darevskaya, N. V. Merzlikina, and L. B. Buravkova. 2005. Mesenchymal stem cells from human bone marrow and adipose tissue: isolation, characterization, and differentiation potentialities. *Bulletin of experimental biology and medicine* 140: 138-143.
63. Tuan, R. S., G. Boland, and R. Tuli. 2003. Adult mesenchymal stem cells and cell-based tissue engineering. *Arthritis research & therapy* 5: 32-45.
64. Park, K. S., Y. S. Kim, J. H. Kim, B. Choi, S. H. Kim, A. H. Tan, M. S. Lee, M. K. Lee, C. H. Kwon, J. W. Joh, S. J. Kim, and K. W. Kim. 2010. Trophic molecules derived from human mesenchymal stem cells enhance survival, function, and angiogenesis of isolated islets after transplantation. *Transplantation* 89: 509-517.
65. Schweitzer, K. S., B. H. Johnstone, J. Garrison, N. I. Rush, S. Cooper, D. O. Traktuev, D. Feng, J. J. Adamowicz, M. Van Demark, A. J. Fisher, K. Kamocki, M. B. Brown, R. G. Presson, Jr., H. E. Broxmeyer, K. L. March, and I. Petrache. 2011. Adipose stem cell treatment in mice attenuates lung and systemic injury induced by cigarette smoking. *Am J Respir Crit Care Med* 183: 215-225.
66. Nicholas, T. E., J. H. Power, and H. A. Barr. 1982. The pulmonary consequences of a deep breath. *Respiration physiology* 49: 315-324.
67. Nicholas, T. E., J. H. Power, and H. A. Barr. 1982. Surfactant homeostasis in the rat lung during swimming exercise. *Journal of applied physiology: respiratory, environmental and exercise physiology* 53: 1521-1528.
68. Asselin-Labat, M. L., and C. E. Filby. 2012. Adult lung stem cells and their contribution to lung tumourigenesis. *Open Biol* 2: 120094.
69. Fehrenbach, H. 2001. Alveolar epithelial type II cell: defender of the alveolus revisited. *Respir Res* 2: 33-46.
70. Fujino, N., H. Kubo, T. Suzuki, C. Ota, A. E. Hegab, M. He, S. Suzuki, T. Suzuki, M. Yamada, T. Kondo, H. Kato, and M. Yamaya. 2011. Isolation of alveolar epithelial type II progenitor cells from adult human lungs. *Lab Invest* 91: 363-378.

71. Kannan, S., H. Huang, D. Seeger, A. Audet, Y. Chen, C. Huang, H. Gao, S. Li, and M. Wu. 2009. Alveolar epithelial type II cells activate alveolar macrophages and mitigate P. Aeruginosa infection. *PloS one* 4: e4891.
72. Saxena, R. K., M. I. Gilmour, and M. D. Hays. 2008. Isolation and quantitative estimation of diesel exhaust and carbon black particles ingested by lung epithelial cells and alveolar macrophages in vitro. *BioTechniques* 44: 799-805.
73. Van Leer, C., M. Stutz, A. Haeberli, and T. Geiser. 2005. Urokinase plasminogen activator released by alveolar epithelial cells modulates alveolar epithelial repair in vitro. *Thrombosis and haemostasis* 94: 1257-1264.
74. Wu, W., J. L. Booth, E. S. Duggan, K. B. Patel, K. M. Coggeshall, and J. P. Metcalf. 2010. Human lung innate immune cytokine response to adenovirus type 7. *The Journal of general virology* 91: 1155-1163.
75. Raghu, G., H. R. Collard, J. J. Egan, F. J. Martinez, J. Behr, K. K. Brown, T. V. Colby, J. F. Cordier, K. R. Flaherty, J. A. Lasky, D. A. Lynch, J. H. Ryu, J. J. Swigris, A. U. Wells, J. Ancochea, D. Bouros, C. Carvalho, U. Costabel, M. Ebina, D. M. Hansell, T. Johkoh, D. S. Kim, T. E. King, Jr., Y. Kondoh, J. Myers, N. L. Muller, A. G. Nicholson, L. Richeldi, M. Selman, R. F. Dudden, B. S. Griss, S. L. Protzko, H. J. Schunemann, and A. E. J. A. C. o. I. P. Fibrosis. 2011. An official ATS/ERS/JRS/ALAT statement: idiopathic pulmonary fibrosis: evidence-based guidelines for diagnosis and management. *American journal of respiratory and critical care medicine* 183: 788-824.
76. Aoshiba, K., and A. Nagai. 2009. Senescence hypothesis for the pathogenetic mechanism of chronic obstructive pulmonary disease. *Proceedings of the American Thoracic Society* 6: 596-601.
77. Tsuji, T., K. Aoshiba, and A. Nagai. 2006. Alveolar cell senescence in patients with pulmonary emphysema. *American journal of respiratory and critical care medicine* 174: 886-893.
78. Roszell, B., M. J. Mondrinos, A. Seaton, D. M. Simons, S. H. Koutzaki, G. H. Fong, P. I. Lelkes, and C. M. Finck. 2009. Efficient derivation of alveolar type II cells from embryonic stem cells for in vivo application. *Tissue Eng Part A* 15: 3351-3365.
79. Serrano-Mollar, A., M. Nacher, G. Gay-Jordi, D. Closa, A. Xaubet, and O. Bulbena. 2007. Intratracheal transplantation of alveolar type II cells reverses bleomycin-induced lung fibrosis. *American journal of respiratory and critical care medicine* 176: 1261-1268.
80. Wang, Y., T. T. Weng, D. M. Gou, Z. M. Chen, N. R. Chintagari, and L. Liu. 2007. Identification of rat lung-specific microRNAs by micoRNA microarray: valuable discoveries for the facilitation of lung research. *Bmc Genomics* 8.
81. Zhao, C., C. Huang, T. Weng, X. Xiao, H. Ma, and L. Liu. 2012. Computational prediction of MicroRNAs targeting GABA receptors and experimental verification of miR-181, miR-216 and miR-203 targets in GABA-A receptor. *BMC Res Notes* 5: 91.
82. Torii, S., T. Yamamoto, Y. Tsuchiya, and E. Nishida. 2006. ERK MAP kinase in G cell cycle progression and cancer. *Cancer Sci* 97: 697-702.

83. Friedman, R. C., K. K. Farh, C. B. Burge, and D. P. Bartel. 2009. Most mammalian mRNAs are conserved targets of microRNAs. *Genome Res* 19: 92-105.
84. Krek, A., D. Grun, M. N. Poy, R. Wolf, L. Rosenberg, E. J. Epstein, P. MacMenamin, I. da Piedade, K. C. Gunsalus, M. Stoffel, and N. Rajewsky. 2005. Combinatorial microRNA target predictions. *Nat Genet* 37: 495-500.
85. Grimson, A., K. K. Farh, W. K. Johnston, P. Garrett-Engele, L. P. Lim, and D. P. Bartel. 2007. MicroRNA targeting specificity in mammals: determinants beyond seed pairing. *Mol Cell* 27: 91-105.
86. Tsai, S. H., S. Y. Lin-Shiau, and J. K. Lin. 1999. Suppression of nitric oxide synthase and the down-regulation of the activation of NFkappaB in macrophages by resveratrol. *British journal of pharmacology* 126: 673-680.
87. Samadikuchaksaraei, A., and A. E. Bishop. 2006. Derivation and characterization of alveolar epithelial cells from murine embryonic stem cells in vitro. *Methods Mol Biol* 330: 233-248.
88. Samadikuchaksaraei, A., and A. E. Bishop. 2007. Effects of growth factors on the differentiation of murine ESC into type II pneumocytes. *Cloning Stem Cells* 9: 407-416.
89. Sueblinvong, V., R. Loi, P. L. Eisenhauer, I. M. Bernstein, B. T. Suratt, J. L. Spees, and D. J. Weiss. 2008. Derivation of lung epithelium from human cord blood-derived mesenchymal stem cells. *Am J Respir Crit Care Med* 177: 701-711.
90. Chen, Z., and L. Liu. 2005. RealSpot: software validating results from DNA microarray data analysis with spot images. *Physiol Genomics* 21: 284-291.
91. Bhaskaran, M., Y. Wang, H. Zhang, T. Weng, P. Baviskar, Y. Guo, D. Gou, and L. Liu. 2009. MicroRNA-127 modulates fetal lung development. *Physiol Genomics* 37: 268-278.
92. McBride, C., D. Gaupp, and D. G. Phinney. 2003. Quantifying levels of transplanted murine and human mesenchymal stem cells in vivo by real-time PCR. *Cytotherapy* 5: 7-18.
93. Jeyaseelan, S., H. W. Chu, S. K. Young, and G. S. Worthen. 2004. Transcriptional profiling of lipopolysaccharide-induced acute lung injury. *Infection and immunity* 72: 7247-7256.
94. Yoo, H. S., M. S. Rutherford, S. K. Maheswaran, S. Srinand, and T. R. Ames. 1996. Induction of nitric oxide production by bovine alveolar macrophages in response to Pasteurella haemolytica A1. *Microbial pathogenesis* 20: 361-375.
95. Chakravortty, D., and M. Hensel. 2003. Inducible nitric oxide synthase and control of intracellular bacterial pathogens. *Microbes Infect* 5: 621-627.
96. Baker, B. J., K. W. Park, H. Qin, X. Ma, and E. N. Benveniste. 2010. IL-27 inhibits OSM-mediated TNF-alpha and iNOS gene expression in microglia. *Glia* 58: 1082-1093.
97. Shimizu, M., K. Ogura, I. Mizoguchi, Y. Chiba, K. Higuchi, H. Ohtsuka, J. Mizuguchi, and T. Yoshimoto. 2013. IL-27 promotes nitric oxide production induced by LPS through STAT1, NF-kappaB and MAPKs. *Immunobiology* 218: 628-634.

98. Jones, M. R., L. J. Quinton, M. T. Blahna, J. R. Neilson, S. Fu, A. R. Ivanov, D. A. Wolf, and J. P. Mizgerd. 2009. Zcchc11-dependent uridylation of microRNA directs cytokine expression. *Nature cell biology* 11: 1157-1163.
99. Oeckinghaus, A., M. S. Hayden, and S. Ghosh. 2011. Crosstalk in NF-kappaB signaling pathways. *Nature immunology* 12: 695-708.
100. Dan, H. C., M. J. Cooper, P. C. Cogswell, J. A. Duncan, J. P. Ting, and A. S. Baldwin. 2008. Akt-dependent regulation of NF-{kappa}B is controlled by mTOR and Raptor in association with IKK. *Genes & development* 22: 1490-1500.
101. Wan, X., and L. J. Helman. 2003. Levels of PTEN protein modulate Akt phosphorylation on serine 473, but not on threonine 308, in IGF-II-overexpressing rhabdomyosarcomas cells. *Oncogene* 22: 8205-8211.
102. Bates, S. R., L. W. Gonzales, J. Q. Tao, P. Rueckert, P. L. Ballard, and A. B. Fisher. 2002. Recovery of rat type II cell surfactant components during primary cell culture. *Am J Physiol Lung Cell Mol Physiol* 282: L267-276.
103. Jeffrey, K. L., M. Camps, C. Rommel, and C. R. Mackay. 2007. Targeting dual-specificity phosphatases: manipulating MAP kinase signalling and immune responses. *Nat Rev Drug Discov* 6: 391-403.
104. Wu, M., A. Katta, M. K. Gadde, H. Liu, S. K. Kakarla, J. Fannin, S. Paturi, R. K. Arvapalli, K. M. Rice, Y. Wang, and E. R. Blough. 2009. Aging-associated dysfunction of Akt/protein kinase B: S-nitrosylation and acetaminophen intervention. *PLoS One* 4: e6430.
105. Chuquimia, O. D., D. H. Petursdottir, N. Periolo, and C. Fernandez. 2013. Alveolar epithelial cells are critical in protection of the respiratory tract by secretion of factors able to modulate the activity of pulmonary macrophages and directly control bacterial growth. *Infect Immun* 81: 381-389.
106. Bhaskaran, M., N. Kolliputi, Y. Wang, D. Gou, N. R. Chintagari, and L. Liu. 2007. Trans-differentiation of alveolar epithelial type II cells to type I cells involves autocrine signaling by transforming growth factor beta 1 through the Smad pathway. *J Biol Chem* 282: 3968-3976.
107. Baraldo, S., G. Turato, and M. Saetta. 2012. Pathophysiology of the small airways in chronic obstructive pulmonary disease. *Respiration* 84: 89-97.
108. Confer, A. W. 2009. Update on bacterial pathogenesis in BRD. *Animal health research reviews / Conference of Research Workers in Animal Diseases* 10: 145-148.
109. Lawless, N., T. A. Reinhardt, K. Bryan, M. Baker, B. Pesch, D. Zimmerman, K. Zuelke, T. Sonstegard, C. O'Farrelly, J. D. Lippolis, and D. J. Lynn. 2014. MicroRNA regulation of bovine monocyte inflammatory and metabolic networks in an in vivo infection model. *G3* 4: 957-971.
110. Chen, Q., H. Wang, Y. Liu, Y. Song, L. Lai, Q. Han, X. Cao, and Q. Wang. 2012. Inducible microRNA-223 down-regulation promotes TLR-triggered IL-6 and IL-1beta production in macrophages by targeting STAT3. *PloS one* 7: e42971.
111. Sheedy, F. J., E. Palsson-McDermott, E. J. Hennessy, C. Martin, J. J. O'Leary, Q. Ruan, D. S. Johnson, Y. Chen, and L. A. O'Neill. 2010. Negative regulation of TLR4 via targeting of the proinflammatory tumor suppressor PDCD4 by the microRNA miR-21. *Nature immunology* 11: 141-147.

112. Gao, J., and Q. G. Liu. 2011. The role of miR-26 in tumors and normal tissues (Review). *Oncology letters* 2: 1019-1023.
113. Palumbo, T., F. R. Faucz, M. Azevedo, P. Xekouki, D. Iliopoulos, and C. A. Stratakis. 2013. Functional screen analysis reveals miR-26b and miR-128 as central regulators of pituitary somatomammotrophic tumor growth through activation of the PTEN-AKT pathway. *Oncogene* 32: 1651-1659.
114. Maillot, G., M. Lacroix-Triki, S. Pierredon, L. Gratadou, S. Schmidt, V. Benes, H. Roche, F. Dalenc, D. Auboeuf, S. Millevoi, and S. Vagner. 2009. Widespread estrogen-dependent repression of micrornas involved in breast tumor cell growth. *Cancer research* 69: 8332-8340.
115. Verghese, E. T., R. Drury, C. A. Green, D. L. Holliday, X. Lu, C. Nash, V. Speirs, J. L. Thorne, H. H. Thygesen, A. Zougman, M. A. Hull, A. M. Hanby, and T. A. Hughes. 2013. MiR-26b is down-regulated in carcinoma-associated fibroblasts from ER-positive breast cancers leading to enhanced cell migration and invasion. *The Journal of pathology* 231: 388-399.
116. Xu, G., C. Ji, C. Shi, H. Fu, L. Zhu, L. Zhu, L. Xu, L. Chen, Y. Feng, Y. Zhao, and X. Guo. 2013. Modulation of hsa-miR-26b levels following adipokine stimulation. *Molecular biology reports* 40: 3577-3582.
117. Li, Y. H., Z. Q. Yan, A. Brauner, and K. Tullus. 2002. Activation of macrophage nuclear factor-kappa B and induct ion of inducible nitric oxide synthase by LPS. *Respir Res* 3.
118. Hayden, M. S., A. P. West, and S. Ghosh. 2006. NF-kappaB and the immune response. *Oncogene* 25: 6758-6780.
119. Murphy, A. J., P. M. Guyre, and P. A. Pioli. 2010. Estradiol suppresses NF-kappa B activation through coordinated regulation of let-7a and miR-125b in primary human macrophages. *Journal of immunology* 184: 5029-5037.
120. Xiao, B., Z. Liu, B. S. Li, B. Tang, W. Li, G. Guo, Y. Shi, F. Wang, Y. Wu, W. D. Tong, H. Guo, X. H. Mao, and Q. M. Zou. 2009. Induction of microRNA-155 during Helicobacter pylori infection and its negative regulatory role in the inflammatory response. *The Journal of infectious diseases* 200: 916-925.
121. Akca, H., A. Demiray, O. Tokgun, and J. Yokota. 2011. Invasiveness and anchorage independent growth ability augmented by PTEN inactivation through the PI3K/AKT/NFkB pathway in lung cancer cells. *Lung cancer* 73: 302-309.
122. Li, J., C. Yen, D. Liaw, K. Podsypanina, S. Bose, S. I. Wang, J. Puc, C. Miliaresis, L. Rodgers, R. McCombie, S. H. Bigner, B. C. Giovanella, M. Ittmann, B. Tycko, H. Hibshoosh, M. H. Wigler, and R. Parsons. 1997. PTEN, a putative protein tyrosine phosphatase gene mutated in human brain, breast, and prostate cancer. *Science* 275: 1943-1947.
123. Steck, P. A., M. A. Pershouse, S. A. Jasser, W. K. Yung, H. Lin, A. H. Ligon, L. A. Langford, M. L. Baumgard, T. Hattier, T. Davis, C. Frye, R. Hu, B. Swedlund, D. H. Teng, and S. V. Tavtigian. 1997. Identification of a candidate tumour suppressor gene, MMAC1, at chromosome 10q23.3 that is mutated in multiple advanced cancers. *Nature genetics* 15: 356-362.
124. Dudek, H., S. R. Datta, T. F. Franke, M. J. Birnbaum, R. Yao, G. M. Cooper, R. A. Segal, D. R. Kaplan, and M. E. Greenberg. 1997. Regulation of neuronal survival by the serine-threonine protein kinase Akt. *Science* 275: 661-665.

125. Barkauskas, C. E., M. J. Cronce, C. R. Rackley, E. J. Bowie, D. R. Keene, B. R. Stripp, S. H. Randell, P. W. Noble, and B. L. Hogan. 2013. Type 2 alveolar cells are stem cells in adult lung. *J Clin Invest* 123: 3025-3036.
126. Green, M. D., A. Chen, M. C. Nostro, S. L. d'Souza, C. Schaniel, I. R. Lemischka, V. Gouon-Evans, G. Keller, and H. W. Snoeck. 2011. Generation of anterior foregut endoderm from human embryonic and induced pluripotent stem cells. *Nat Biotechnol* 29: 267-272.
127. Mou, H., R. Zhao, R. Sherwood, T. Ahfeldt, A. Lapey, J. Wain, L. Sicilian, K. Izvolsky, K. Musunuru, C. Cowan, and J. Rajagopal. 2012. Generation of multipotent lung and airway progenitors from mouse ESCs and patient-specific cystic fibrosis iPSCs. *Cell Stem Cell* 10: 385-397.
128. Van Haute, L., G. De Block, I. Liebaers, K. Sermon, and M. De Rycke. 2009. Generation of lung epithelial-like tissue from human embryonic stem cells. *Respir Res* 10: 105.
129. Cushing, L., P. P. Kuang, J. Qian, F. Shao, J. Wu, F. Little, V. J. Thannickal, W. V. Cardoso, and J. Lu. 2011. miR-29 is a major regulator of genes associated with pulmonary fibrosis. *Am J Respir Cell Mol Biol* 45: 287-294.
130. Gebeshuber, C. A., K. Zatloukal, and J. Martinez. 2009. miR-29a suppresses tristetraprolin, which is a regulator of epithelial polarity and metastasis. *EMBO Rep* 10: 400-405.
131. Kapinas, K., C. B. Kessler, and A. M. Delany. 2009. miR-29 suppression of osteonectin in osteoblasts: regulation during differentiation and by canonical Wnt signaling. *J Cell Biochem* 108: 216-224.
132. Maurer, B., J. Stanczyk, A. Jungel, A. Akhmetshina, M. Trenkmann, M. Brock, O. Kowal-Bielecka, R. E. Gay, B. A. Michel, J. H. Distler, S. Gay, and O. Distler. 2010. MicroRNA-29, a key regulator of collagen expression in systemic sclerosis. *Arthritis Rheum* 62: 1733-1743.
133. van Rooij, E., L. B. Sutherland, J. E. Thatcher, J. M. DiMaio, R. H. Naseem, W. S. Marshall, J. A. Hill, and E. N. Olson. 2008. Dysregulation of microRNAs after myocardial infarction reveals a role of miR-29 in cardiac fibrosis. *Proc Natl Acad Sci U S A* 105: 13027-13032.
134. Wang, H., R. Garzon, H. Sun, K. J. Ladner, R. Singh, J. Dahlman, A. Cheng, B. M. Hall, S. J. Qualman, D. S. Chandler, C. M. Croce, and D. C. Guttridge. 2008. NF-kappaB-YY1-miR-29 regulatory circuitry in skeletal myogenesis and rhabdomyosarcoma. *Cancer Cell* 14: 369-381.
135. Sengupta, S., J. A. den Boon, I. H. Chen, M. A. Newton, S. A. Stanhope, Y. J. Cheng, C. J. Chen, A. Hildesheim, B. Sugden, and P. Ahlquist. 2008. MicroRNA 29c is down-regulated in nasopharyngeal carcinomas, up-regulating mRNAs encoding extracellular matrix proteins. *Proc Natl Acad Sci U S A* 105: 5874-5878.
136. Yang, T., Y. Liang, Q. Lin, J. Liu, F. Luo, X. Li, H. Zhou, S. Zhuang, and H. Zhang. 2013. miR-29 mediates TGFbeta1-induced extracellular matrix synthesis through activation of PI3K-AKT pathway in human lung fibroblasts. *J Cell Biochem* 114: 1336-1342.
137. Dhillon, A. S., S. Hagan, O. Rath, and W. Kolch. 2007. MAP kinase signalling pathways in cancer. *Oncogene* 26: 3279-3290.

138. McCubrey, J. A., M. M. Lahair, and R. A. Franklin. 2006. Reactive oxygen species-induced activation of the MAP kinase signaling pathways. *Antioxid Redox Signal* 8: 1775-1789.
139. Runchel, C., A. Matsuzawa, and H. Ichijo. 2011. Mitogen-activated protein kinases in mammalian oxidative stress responses. *Antioxid Redox Signal* 15: 205-218.
140. Kim, E. K., and E. J. Choi. 2010. Pathological roles of MAPK signaling pathways in human diseases. *Biochim Biophys Acta* 1802: 396-405.
141. Kilian, K. A., B. Bugarija, B. T. Lahn, and M. Mrksich. 2010. Geometric cues for directing the differentiation of mesenchymal stem cells. *Proc Natl Acad Sci U S A* 107: 4872-4877.
142. Eskildsen, T., H. Taipaleenmaki, J. Stenvang, B. M. Abdallah, N. Ditzel, A. Y. Nossent, M. Bak, S. Kauppinen, and M. Kassem. 2011. MicroRNA-138 regulates osteogenic differentiation of human stromal (mesenchymal) stem cells in vivo. *Proc Natl Acad Sci U S A* 108: 6139-6144.
143. Oswald, J., S. Boxberger, B. Jorgensen, S. Feldmann, G. Ehninger, M. Bornhauser, and C. Werner. 2004. Mesenchymal stem cells can be differentiated into endothelial cells in vitro. *Stem Cells* 22: 377-384.
144. Paunescu, V., E. Deak, D. Herman, I. R. Siska, G. Tanasie, C. Bunu, S. Anghel, C. A. Tatu, T. I. Oprea, R. Henschler, B. Ruster, R. Bistrian, and E. Seifried. 2007. In vitro differentiation of human mesenchymal stem cells to epithelial lineage. *J Cell Mol Med* 11: 502-508.
145. Hemming, S., D. Cakouros, S. Isenmann, L. Cooper, D. Menicanin, A. Zannettino, and S. Gronthos. 2014. EZH2 and KDM6A act as an epigenetic switch to regulate mesenchymal stem cell lineage specification. *Stem Cells* 32: 802-815.
146. Suganuma, T., and J. L. Workman. 2012. MAP kinases and histone modification. *J Mol Cell Biol* 4: 348-350.
147. Keshet, Y., and R. Seger. 2010. The MAP kinase signaling cascades: a system of hundreds of components regulates a diverse array of physiological functions. *Methods Mol Biol* 661: 3-38.
148. Li, C., X. Yang, Y. He, G. Ye, X. Li, X. Zhang, L. Zhou, and F. Deng. 2012. Bone morphogenetic protein-9 induces osteogenic differentiation of rat dental follicle stem cells in P38 and ERK1/2 MAPK dependent manner. *Int J Med Sci* 9: 862-871.
149. Wang, J., and Y. Xia. 2012. Assessing developmental roles of MKK4 and MKK7 in vitro. *Commun Integr Biol* 5: 319-324.
150. Liu, F., S. Zheng, T. Liu, Q. Liu, M. Liang, X. Li, I. Sheyhidin, X. Lu, and W. Liu. 2013. MicroRNA-21 promotes the proliferation and inhibits apoptosis in Eca109 via activating ERK1/2/MAPK pathway. *Mol Cell Biochem* 381: 115-125.
151. Mei, Y., C. Bian, J. Li, Z. Du, H. Zhou, Z. Yang, and R. C. Zhao. 2013. miR-21 modulates the ERK-MAPK signaling pathway by regulating SPRY2 expression during human mesenchymal stem cell differentiation. *J Cell Biochem* 114: 1374-1384.

APPENDICES

PERMISSION GRANTED FOR THE PURPOSE INDICATED.

VITA

Li Zhang

Candidate for the Degree of

Doctor of Philosophy

Thesis: ROLE OF MIRNAS IN LUNG ASSOCIATED DISEASES

Major Field: Physiological Sciences

Biographical:

Education:

Completed the requirements for the Doctor of Philosophy in Physiological Sciences at Oklahoma State University, Stillwater, Oklahoma in May, 2015.

Completed the requirements for the Master of Science in Biochemistry and Molecular Biology at Oklahoma State University, Stillwater, Oklahoma in May, 2010.

Completed the requirements for the Master of Science in Microbiology at Sichuan University, Chengdu, Sichuan, China in July, 2007.

Completed the requirements for the Bachelor of Science in Biotechnology at Sichuan University, Chengdu, Sichuan, China in July, 2004.

Experience:

Graduate Research Assistant (Sep, 2004- Jul, 2007)
Graduate Research Assistant (Aug, 2007- May, 2010)
Graduate Research Associate (Aug, 2010- May, 2015)

Professional Memberships:

ASIP (American Society for Investigative Pathology)
AAAS (American Association for the Advancement of Science)